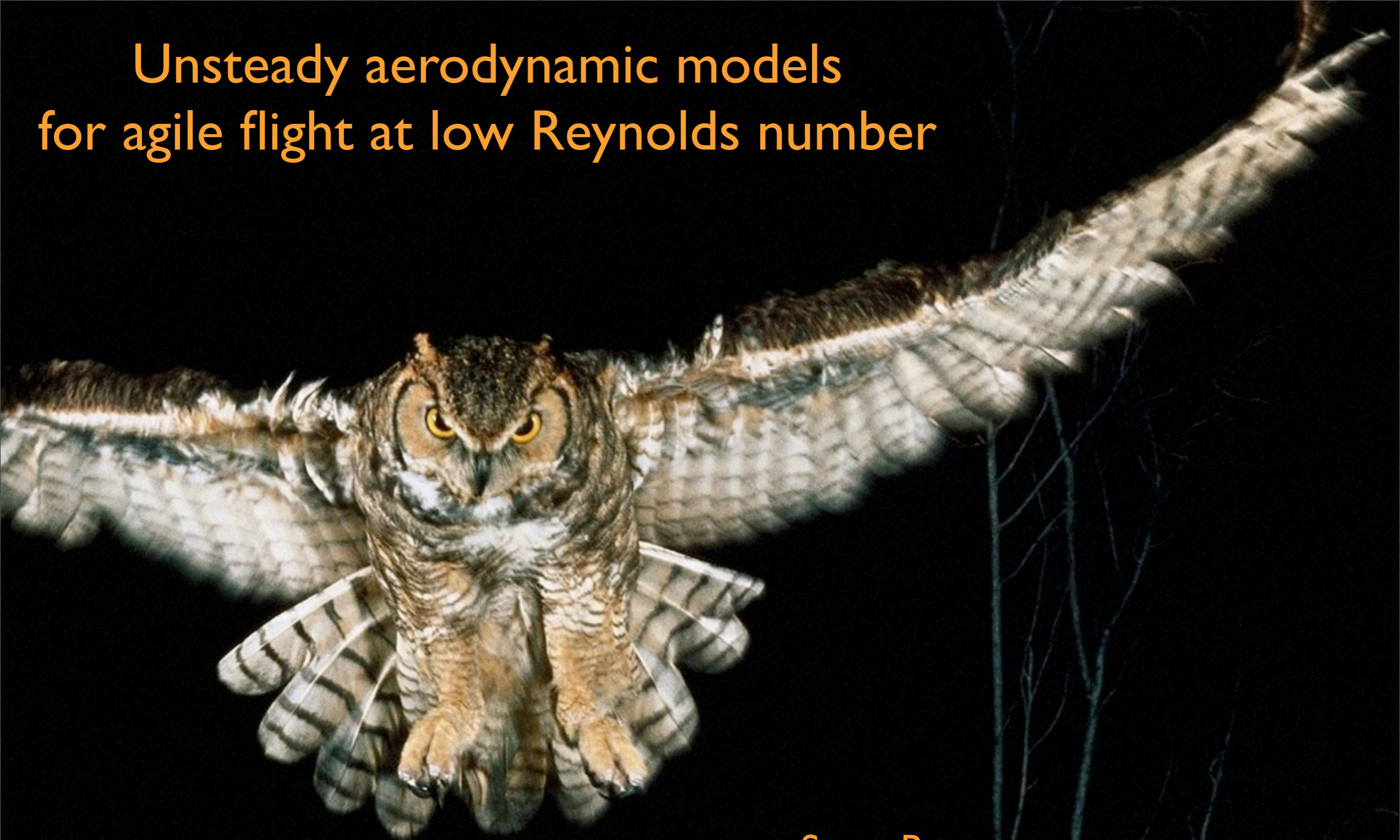


Unsteady aerodynamic models for agile flight at low Reynolds number

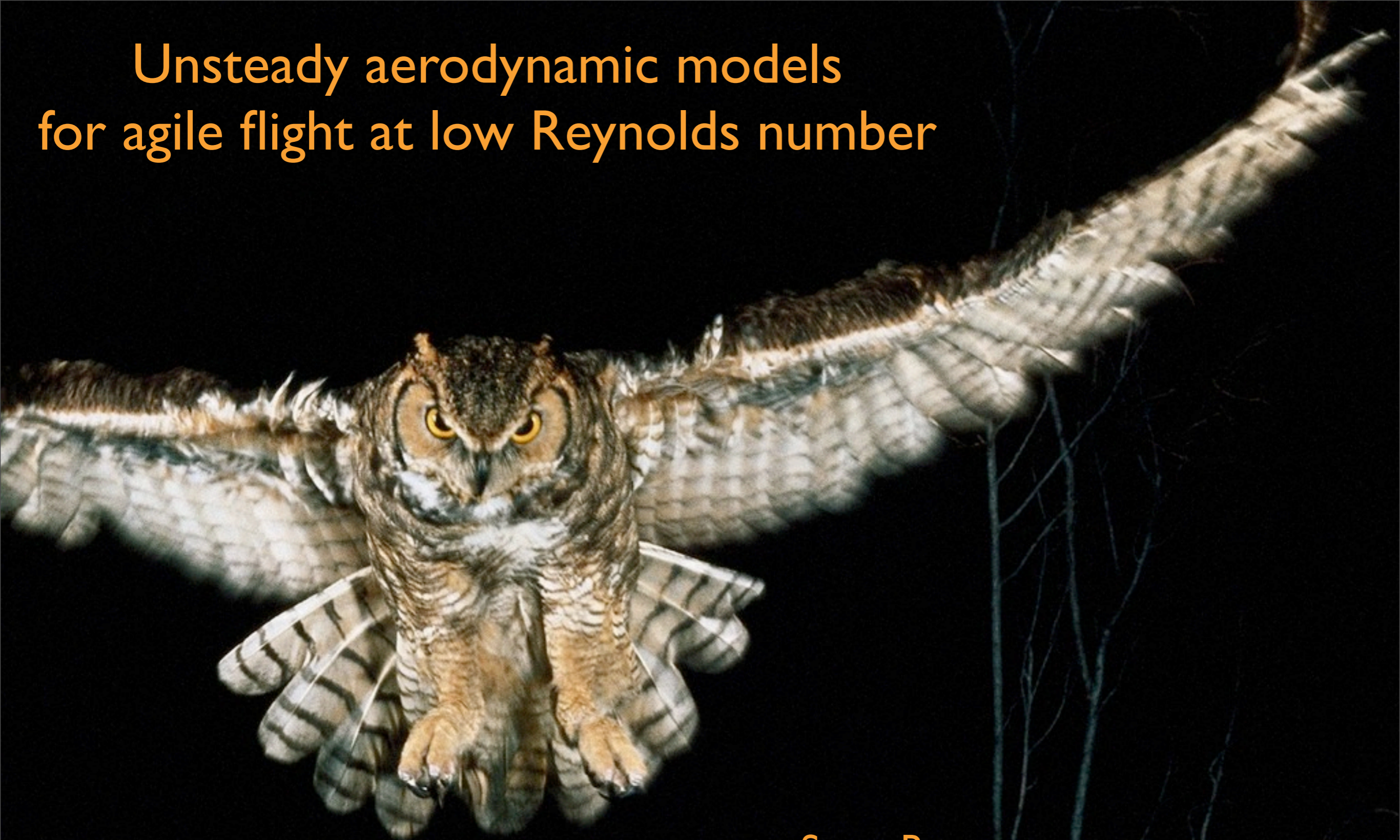


Steve Brunton

Princeton University

FPO - March 13, 2012

Unsteady aerodynamic models for agile flight at low Reynolds number



$$\text{Re} = \frac{LV}{\nu}$$

L = Length

V = Velocity

ν = Viscosity

Steve Brunton

Princeton University

FPO - March 13, 2012



Motivation



Applications of Unsteady Models

Conventional UAVs (performance/robustness)

Micro air vehicles (MAVs)

Flow control, flight dynamic control

Autopilots / Flight simulators

Gust disturbance mitigation

Understand bird/insect flight

Need for State-Space Models

Need models suitable for control

Combining with flight models

FLYIT Simulators, Inc.



Predator (General Atomics)



Bio-locomotion



**Flexible Wing
(University of Florida)**



Flow Control (expert)



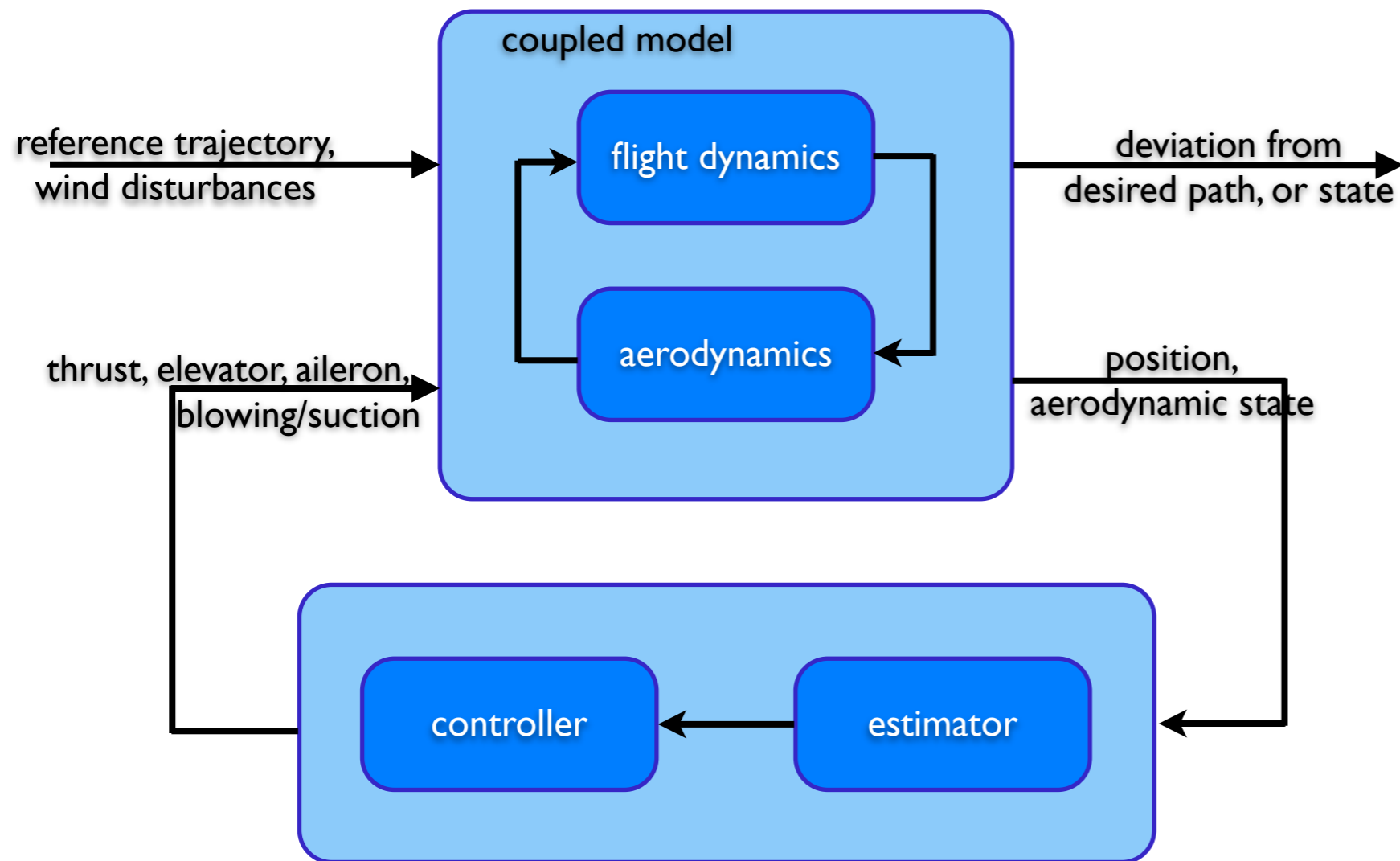


Flow Control (expert)





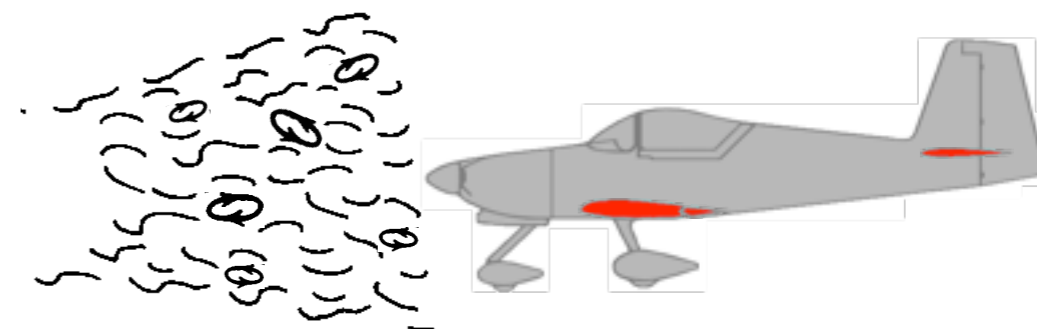
Flight Dynamic Control



Performance



Disturbance rejection Noise attenuation



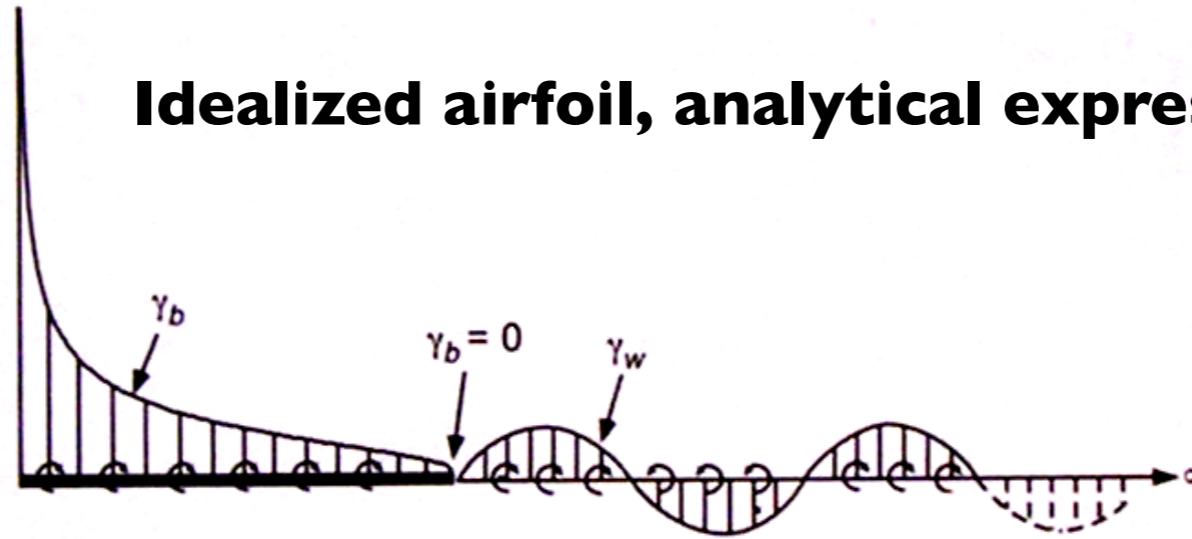
In general, feedback control benefits from more accurate aerodynamic models.



Three Aerodynamic Models



Idealized airfoil, analytical expression



Direct numerical simulations, $Re=100$

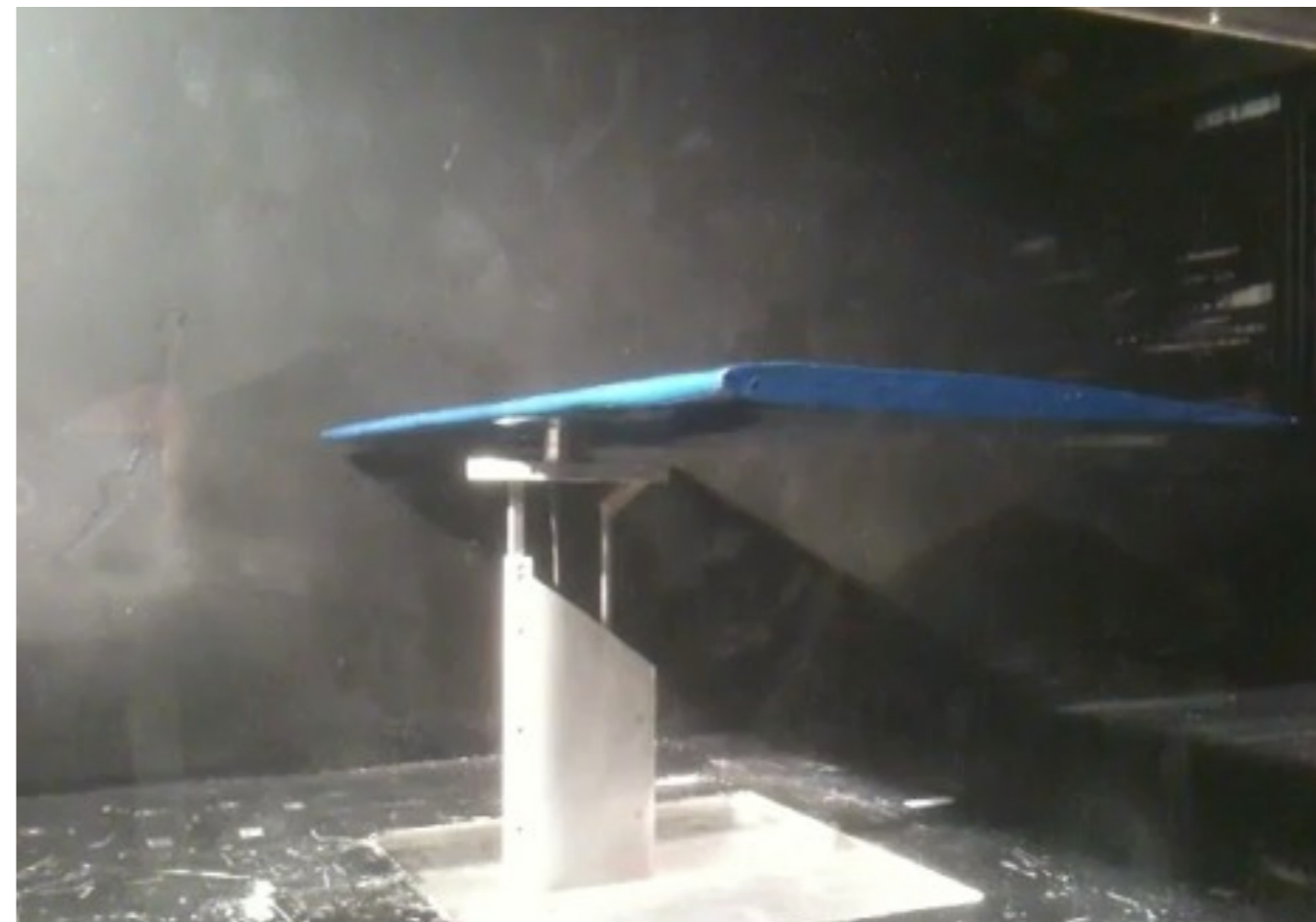


Pitch



Plunge

Wind tunnel experiment, $Re=65,000$





2D Incompressible Flow, (Re=100)



Stationary, AoA = 25



Pitch



Stationary, AoA = 35



Plunge

Immersed boundary method

Multi-domain approach

Boundary forces computed as Lagrange-multipliers to enforce no slip

Colonus & Taira, 2008.

2D Incompressible Navier-Stokes:

$$\frac{\partial \mathbf{u}}{\partial t} + (\mathbf{u} \cdot \nabla) \mathbf{u} = -\nabla p + \frac{1}{\text{Re}} \nabla^2 \mathbf{u} + \int_s \mathbf{f}(\xi(s, t)) \delta(\xi - \mathbf{x}) ds$$

$$\nabla \cdot \mathbf{u} = 0$$

$$\mathbf{u}(\xi(s, t)) = \int_{\mathbf{x}} \mathbf{u}(\mathbf{x}) \delta(\mathbf{x} - \xi) d\mathbf{x} = \mathbf{u}_B(\xi(s, t))$$



Unsteady Base Flow



Idea: Instead of moving body, move base flow!



Base flow velocity:

$$u(x, y, t) = \|\mathbf{V}\| \cos(\alpha) - \dot{\theta}(y - y_C)$$

$$v(x, y, t) = \|\mathbf{V}\| \sin(\alpha) + \dot{\theta}(x - x_C)$$

Vorticity:

$$\nabla \times (u, v) = v_x - u_y = \dot{\theta} + \dot{\theta} = 2\dot{\theta}$$

where (x_C, y_C) is the center of mass.

Unsteady Base Flow

Faster simulations (Cholesky decomposition)
allows more aggressive maneuvers and gusts

24X faster, more accurate

Immersed Boundary Method

T. Colonius and K. Taira, 2008

A fast immersed boundary method using a nullspace approach and multi-domain far-field boundary conditions.



Unsteady Base Flow



Idea: Instead of moving body, move base flow!



Base flow velocity:

$$u(x, y, t) = \|\mathbf{V}\| \cos(\alpha) - \dot{\theta}(y - y_C)$$

$$v(x, y, t) = \|\mathbf{V}\| \sin(\alpha) + \dot{\theta}(x - x_C)$$

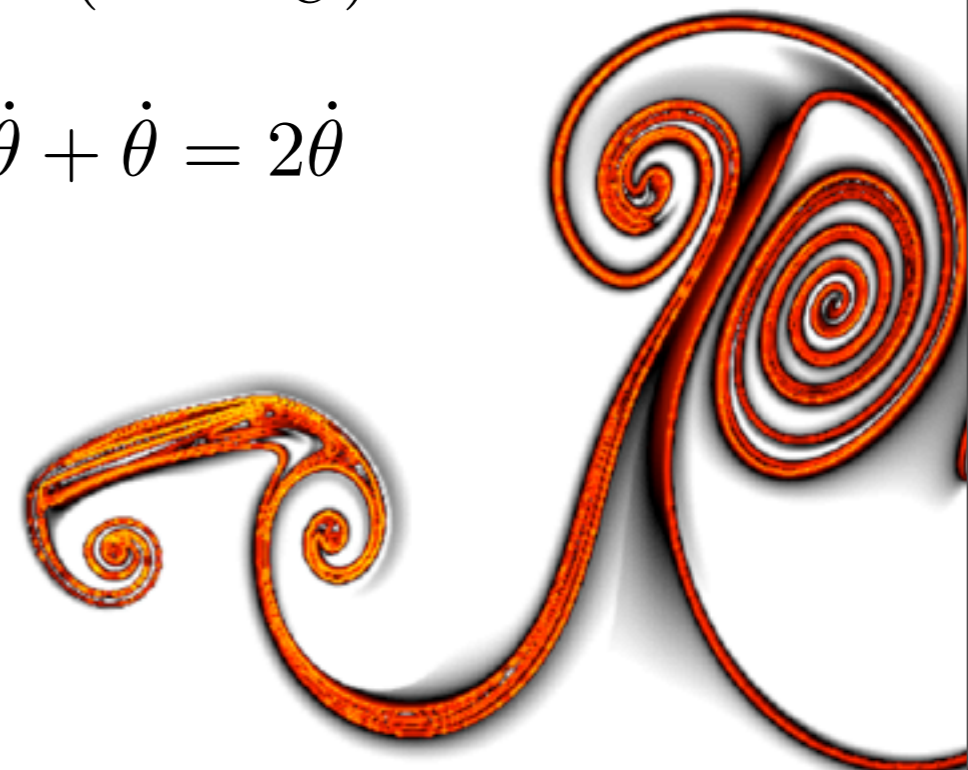
Vorticity:

$$\nabla \times (u, v) = v_x - u_y = \dot{\theta} + \dot{\theta} = 2\dot{\theta}$$

Unsteady Base Flow

Faster simulations (Cholesky decomposition)
 allows more aggressive maneuvers and gusts

24X faster, more accurate





Finite Time Lyapunov Exponents



Finite Time Lyapunov Exponents (FTLE)

Measure of stretching between neighboring particles

σ is time-dependent for unsteady flows

$$\sigma(\Phi_0^T; \mathbf{x}_0) = \frac{1}{|T|} \log \sqrt{\lambda_{\max}(\Delta(\mathbf{x}_0))}$$

where $\Delta = (\mathbf{D}\Phi_0^T)^* \mathbf{D}\Phi_0^T$

Lagrangian Coherent Structures (LCS)

LCS are hyperbolic ridges in the FTLE field

Generalize invariant manifolds for time varying flows

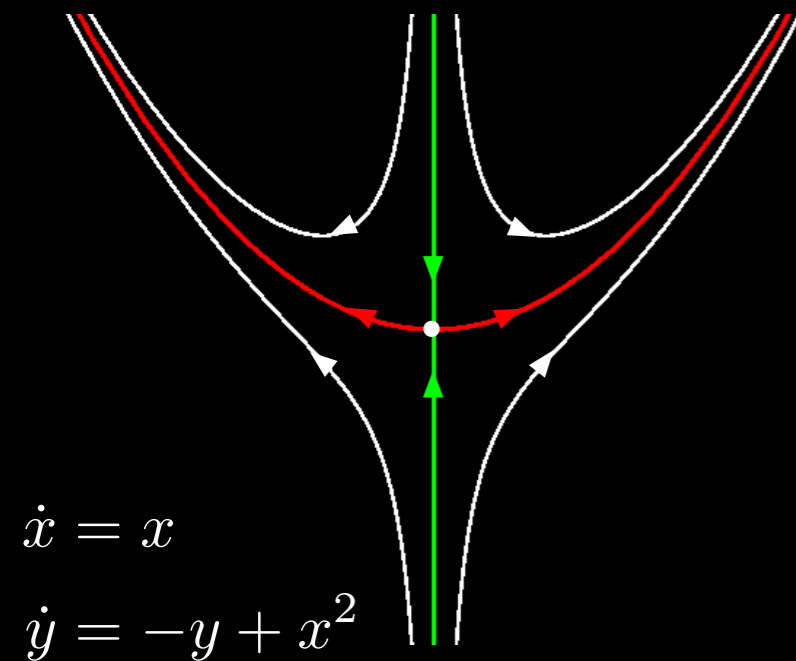
Φ_0^T - particle flow map

pLCS - positive-time LCS (repelling)

nLCS - negative-time LCS (attracting)

Haller, 2002;
Shadden et al., 2005

Attracting nLCS





Finite Time Lyapunov Exponents



Finite Time Lyapunov Exponents (FTLE)

Measure of stretching between neighboring particles

σ is time-dependent for unsteady flows

$$\sigma(\Phi_0^T; \mathbf{x}_0) = \frac{1}{|T|} \log \sqrt{\lambda_{\max}(\Delta(\mathbf{x}_0))}$$

where $\Delta = (\mathbf{D}\Phi_0^T)^* \mathbf{D}\Phi_0^T$

Lagrangian Coherent Structures (LCS)

LCS are hyperbolic ridges in the FTLE field

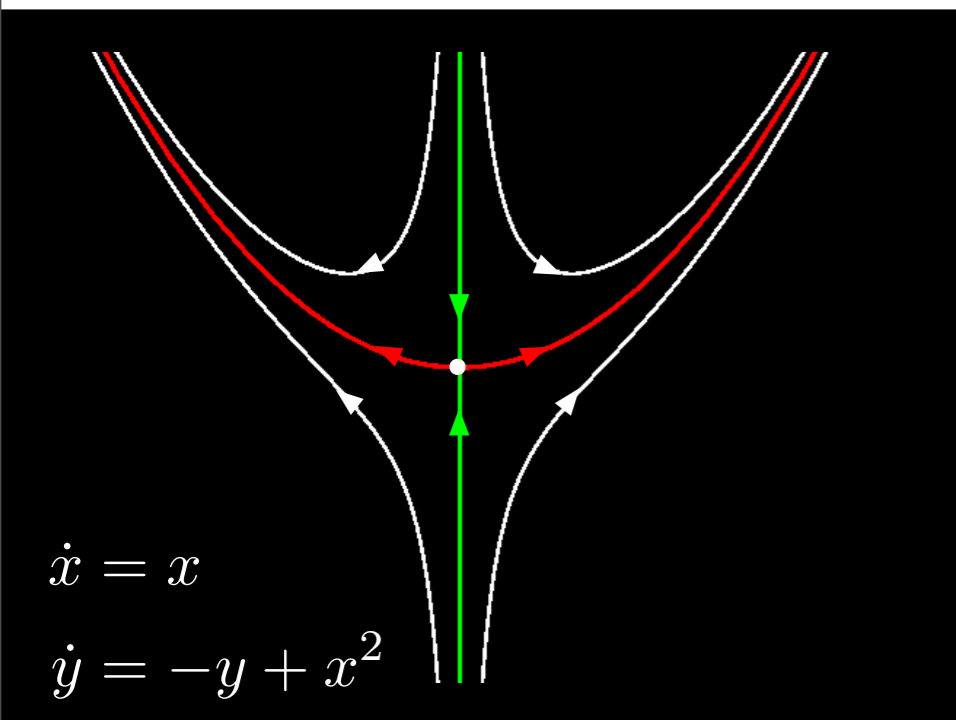
Generalize invariant manifolds for time varying flows

Φ_0^T - particle flow map

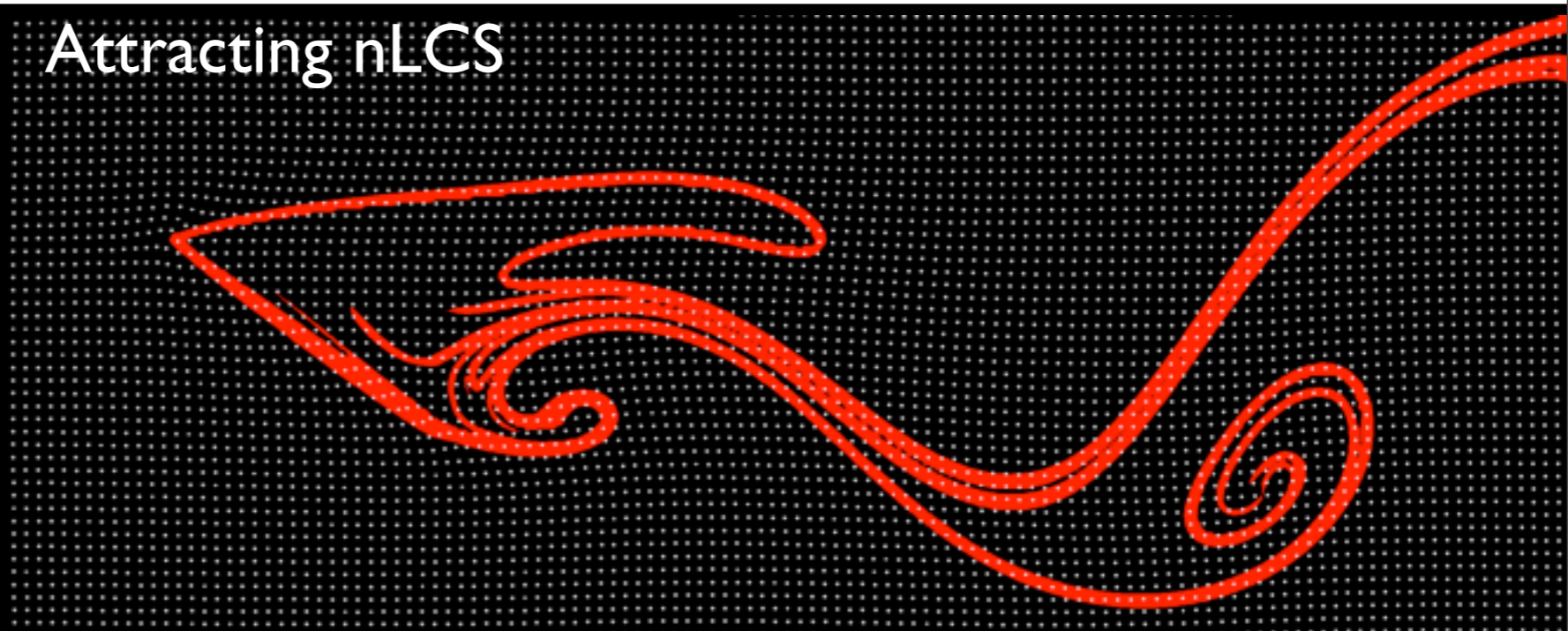
pLCS - positive-time LCS (repelling)

nLCS - negative-time LCS (attracting)

Haller, 2002;
Shadden et al., 2005



Attracting nLCS





Finite Time Lyapunov Exponents



Finite Time Lyapunov Exponents (FTLE)

Measure of stretching between neighboring particles

σ is time-dependent for unsteady flows

$$\sigma(\Phi_0^T; \mathbf{x}_0) = \frac{1}{|T|} \log \sqrt{\lambda_{\max}(\Delta(\mathbf{x}_0))}$$

where $\Delta = (\mathbf{D}\Phi_0^T)^* \mathbf{D}\Phi_0^T$

Lagrangian Coherent Structures (LCS)

LCS are hyperbolic ridges in the FTLE field

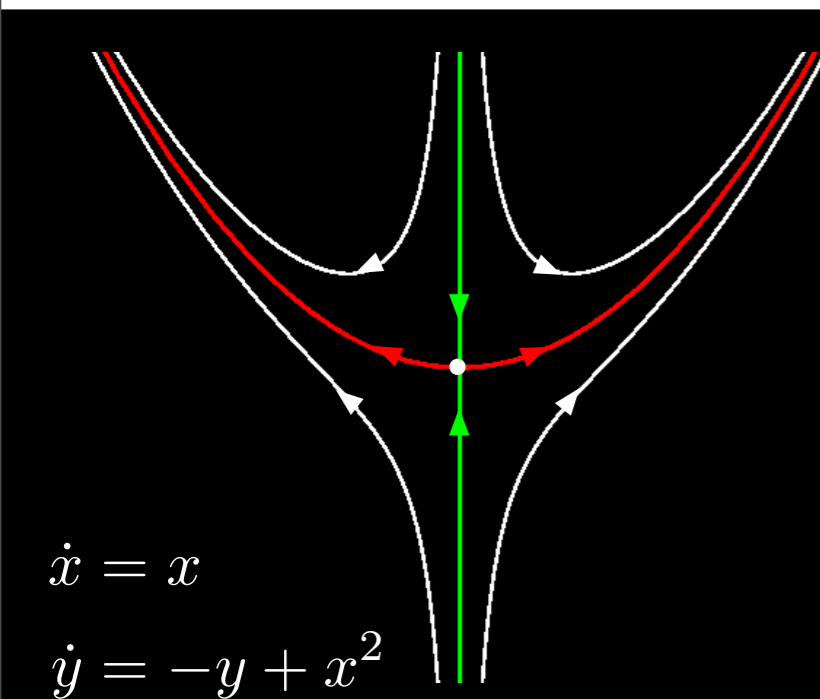
Generalize invariant manifolds for time varying flows

Φ_0^T - particle flow map

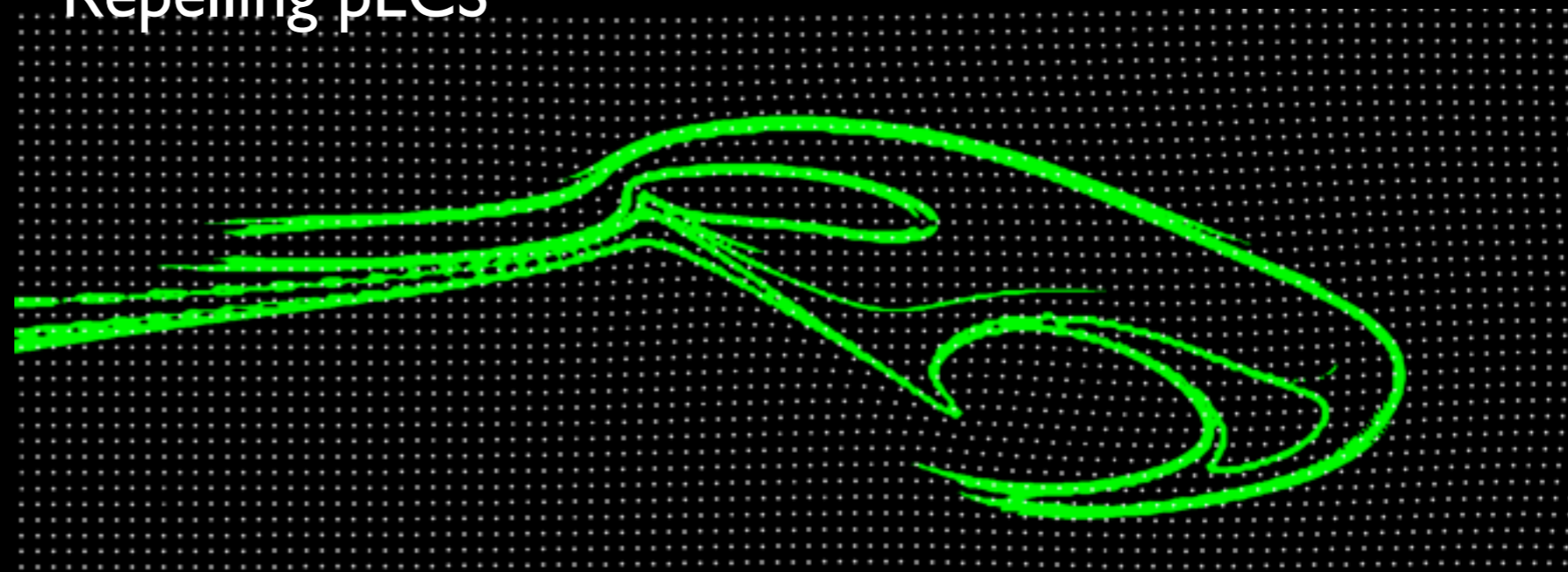
pLCS - positive-time LCS (repelling)

nLCS - negative-time LCS (attracting)

Haller, 2002;
Shadden et al., 2005



Repelling pLCS





Finite Time Lyapunov Exponents



Finite Time Lyapunov Exponents (FTLE)

Measure of stretching between neighboring particles

σ is time-dependent for unsteady flows

Lagrangian Coherent Structures (LCS)

LCS are hyperbolic ridges in the FTLE field

Generalize invariant manifolds for time varying flows

New Fast Method

Flow map composition removes redundant particle integrations for neighboring flow maps

10-100X speed-up

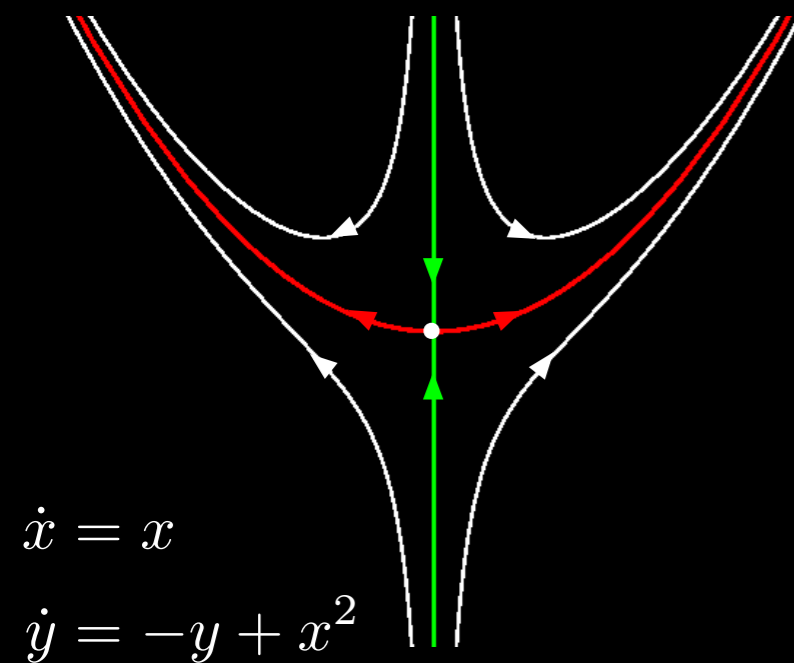
Accurate for 2D and 3D flows

For more information, see:

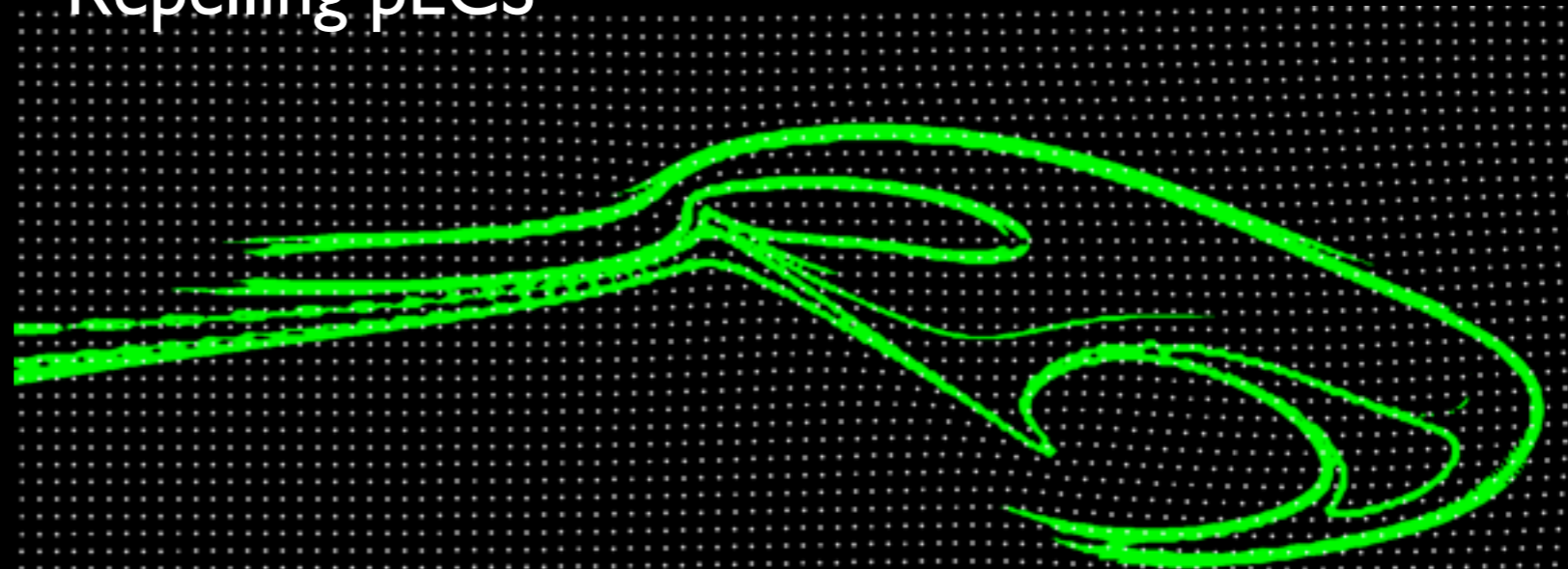
Fast computation of FTLE fields for unsteady flows: a comparison of methods

Brunton & Rowley, *Chaos* 20, 2010

Haller, 2002;
Shadden *et al.*, 2005

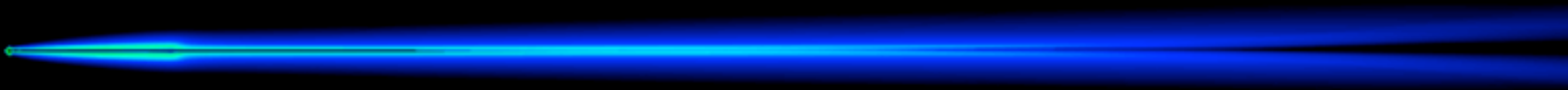
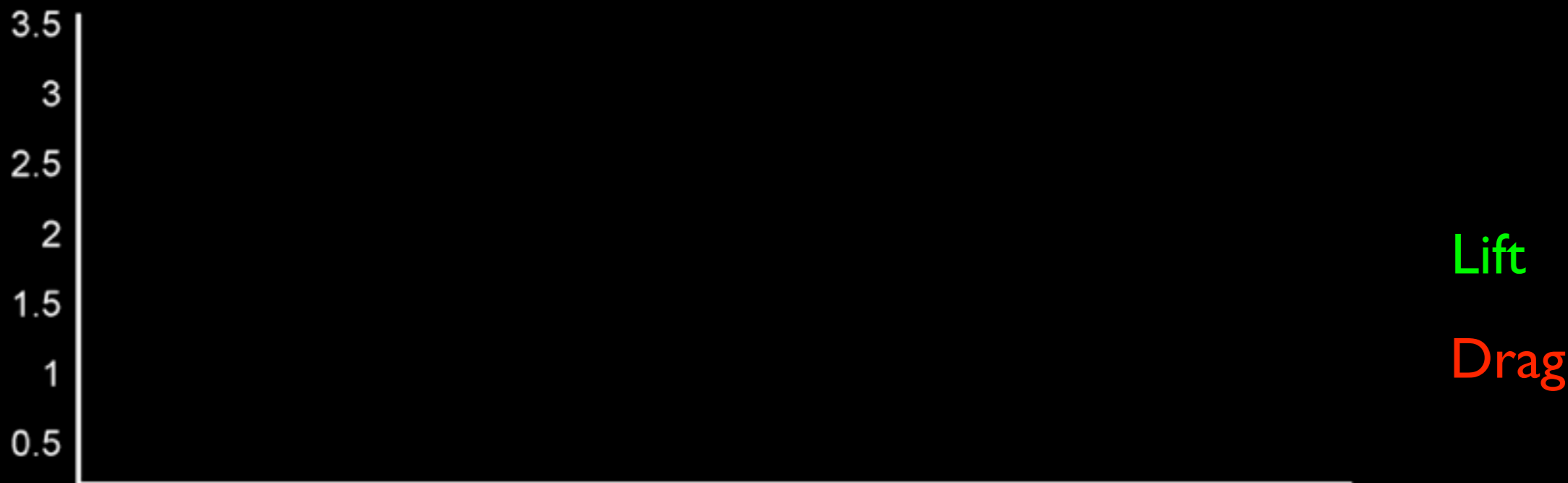


Repelling pLCS





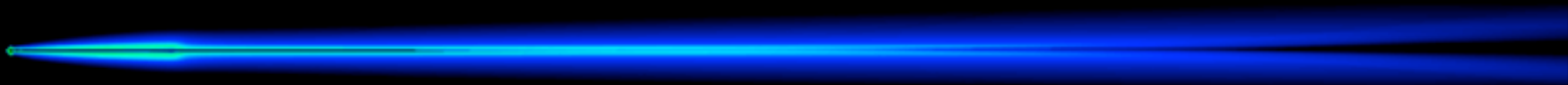
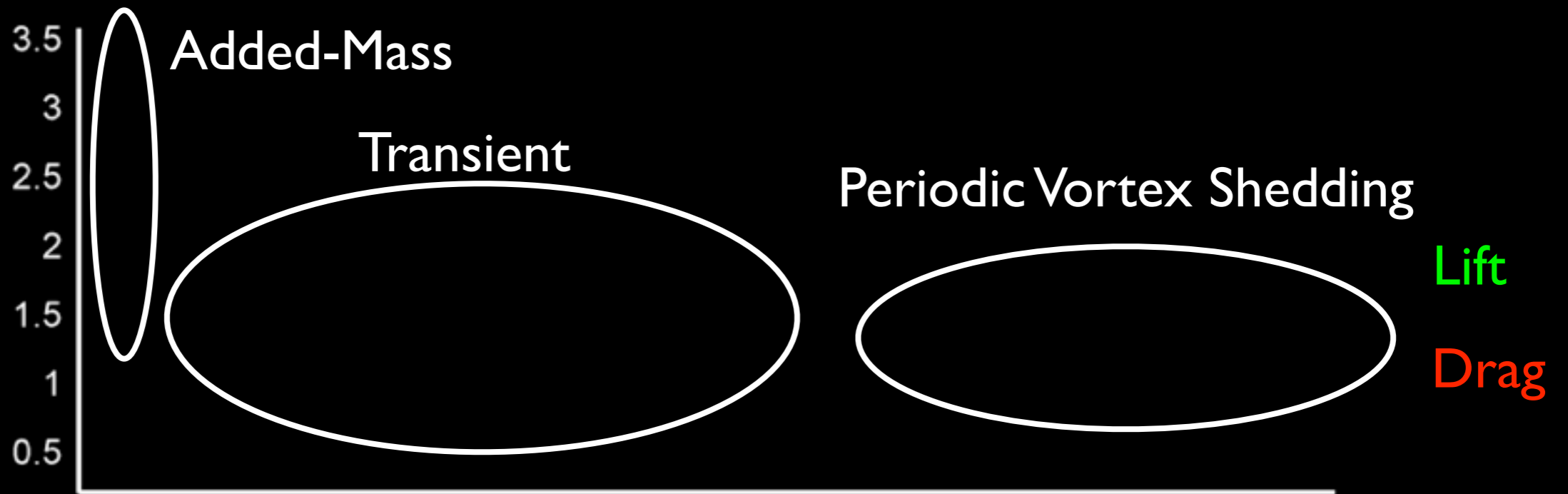
2D Model Problem



$Re = 300$
 $\alpha = 32^\circ$



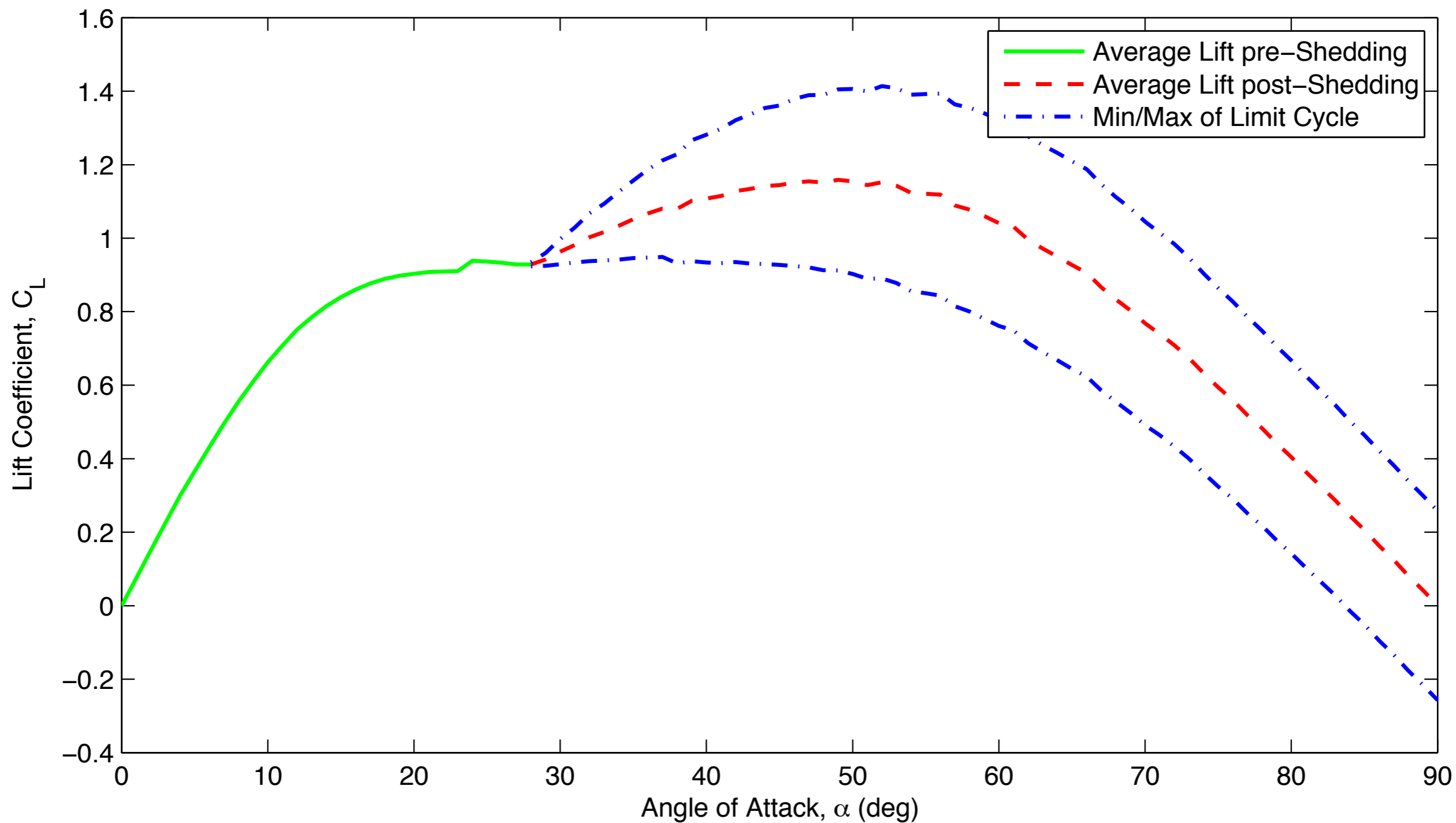
2D Model Problem



$Re = 300$
 $\alpha = 32^\circ$



Lift vs. Angle of Attack

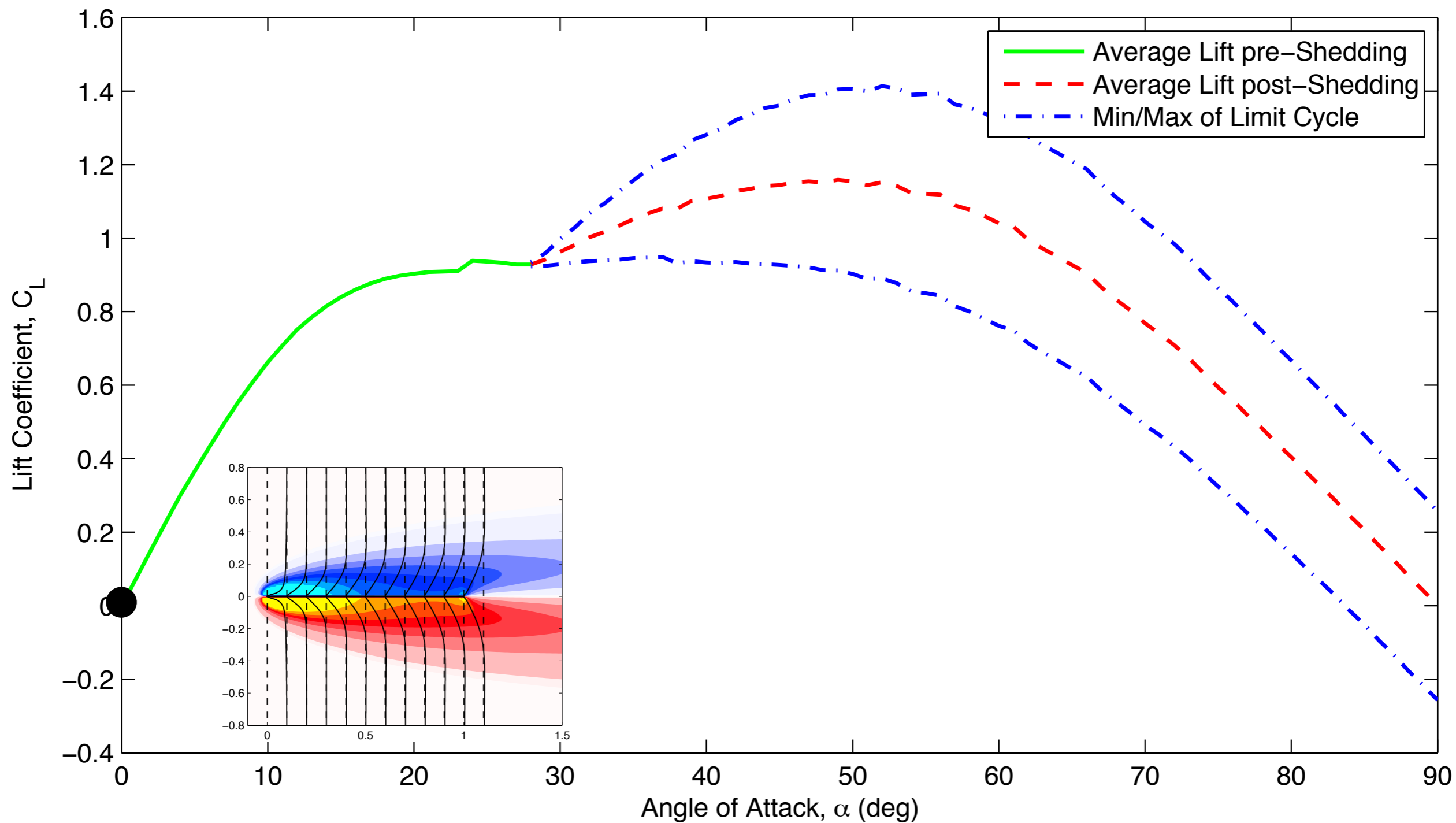


Low Reynolds number, (Re=100)

Hopf bifurcation at $\alpha_{\text{crit}} \approx 28^\circ$ (pair of imaginary eigenvalues pass into right half plane)



Lift vs. Angle of Attack

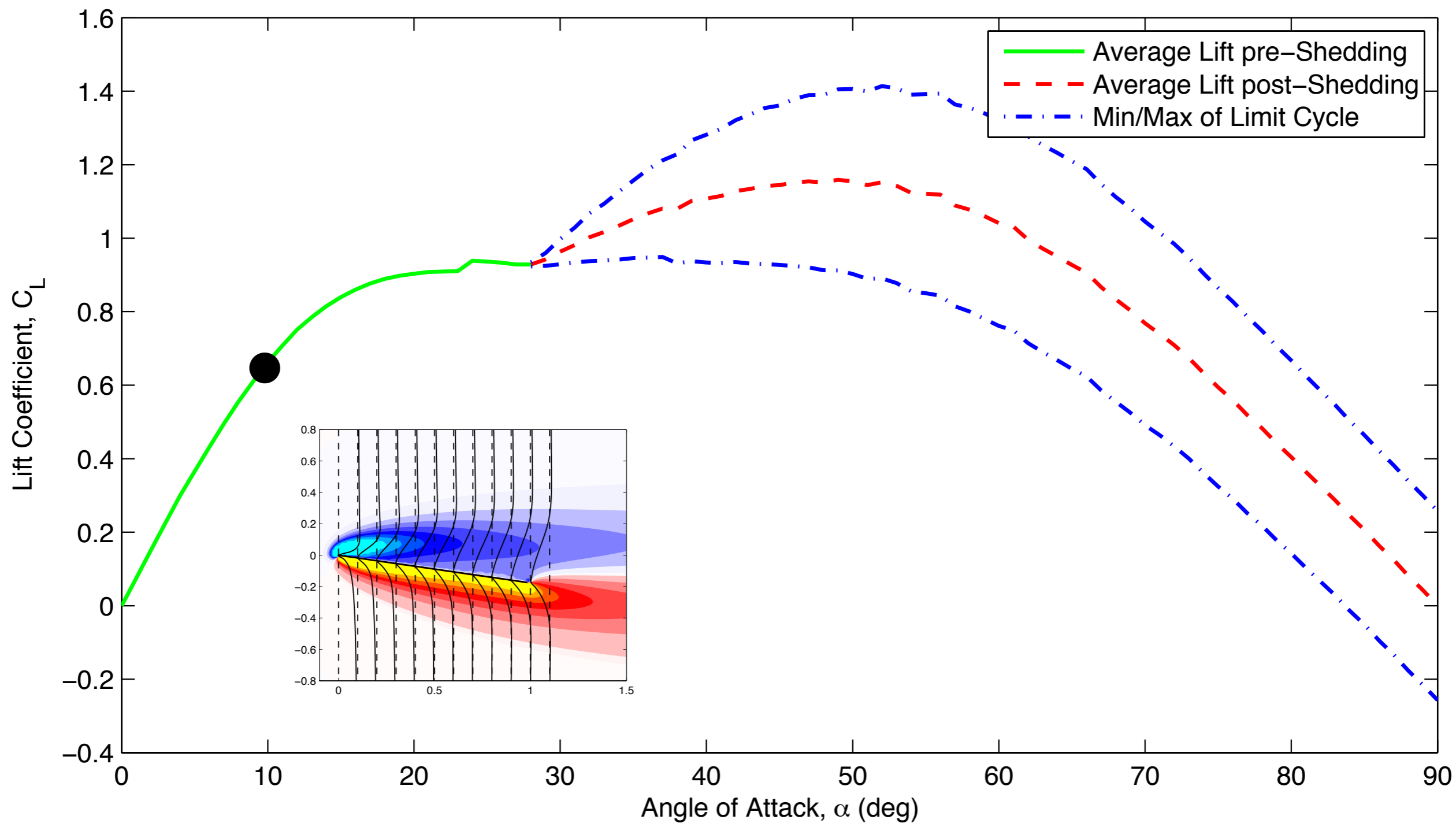


Low Reynolds number, (Re=100)

Hopf bifurcation at $\alpha_{crit} \approx 28^\circ$ (pair of imaginary eigenvalues pass into right half plane)



Lift vs. Angle of Attack

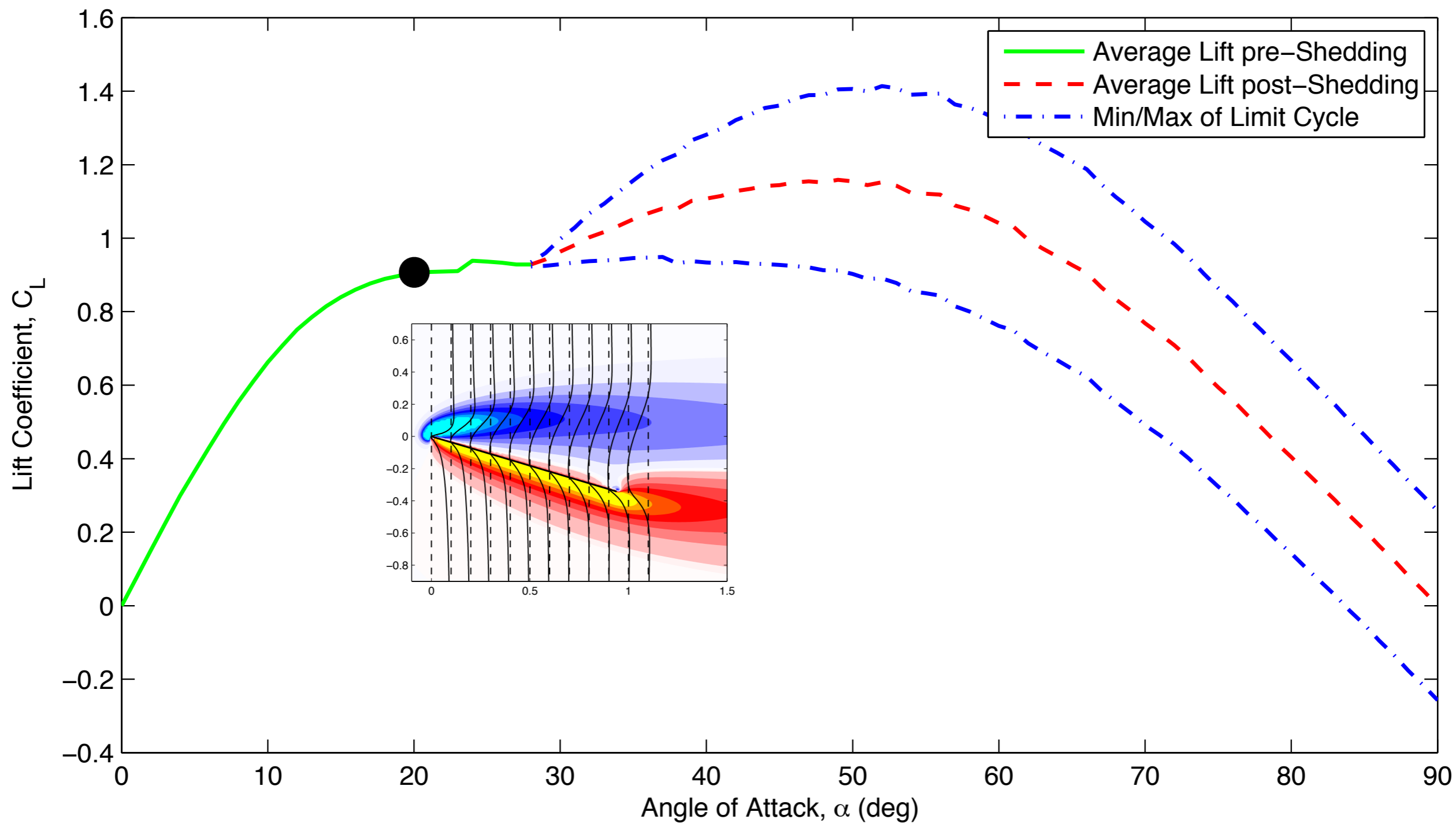


Low Reynolds number, (Re=100)

Hopf bifurcation at $\alpha_{crit} \approx 28^\circ$ (pair of imaginary eigenvalues pass into right half plane)



Lift vs. Angle of Attack

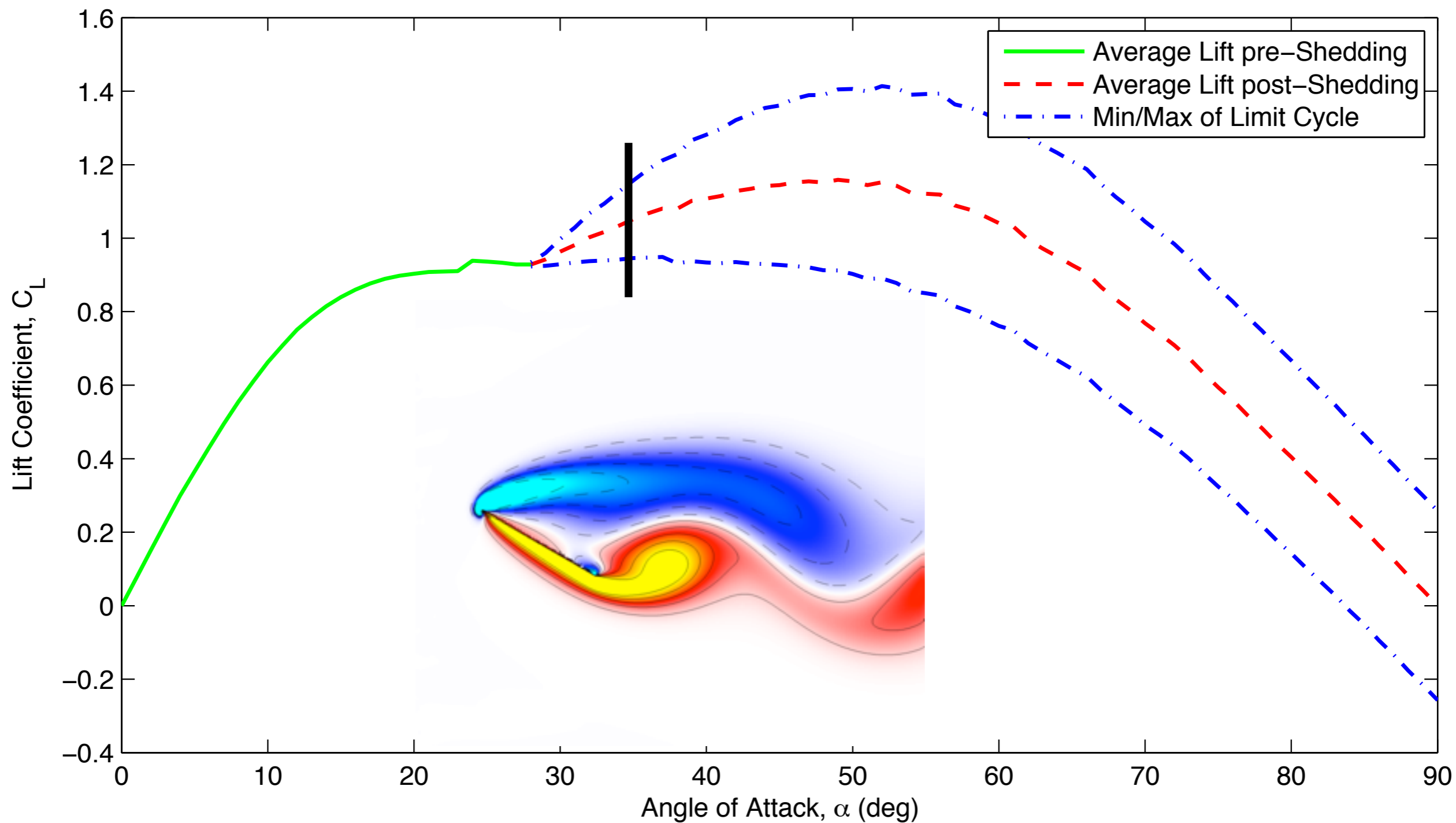


Low Reynolds number, (Re=100)

Hopf bifurcation at $\alpha_{crit} \approx 28^\circ$ (pair of imaginary eigenvalues pass into right half plane)



Lift vs. Angle of Attack



Low Reynolds number, (Re=100)

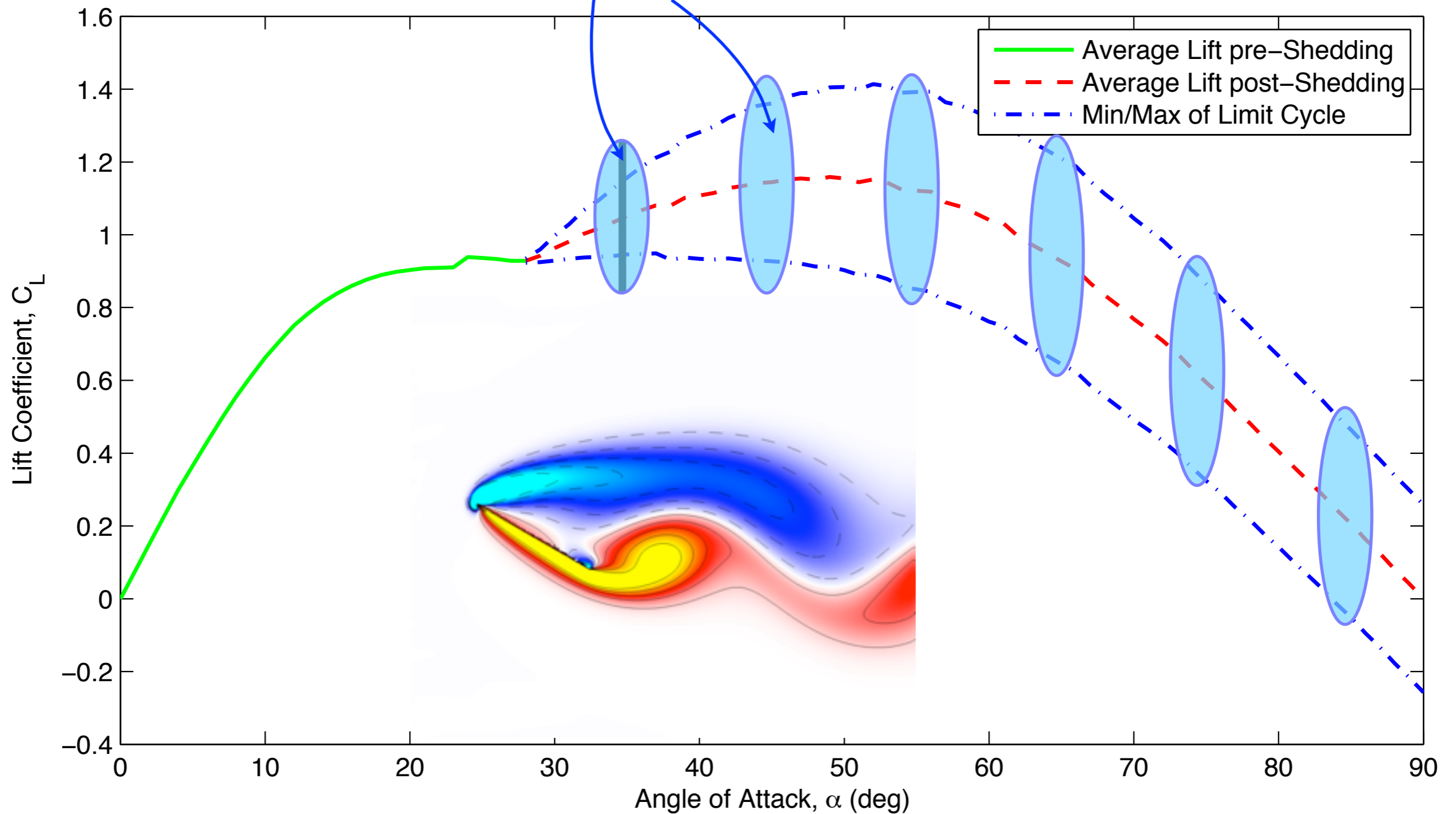
Hopf bifurcation at $\alpha_{crit} \approx 28^\circ$ (pair of imaginary eigenvalues pass into right half plane)



Lift vs. Angle of Attack



Models based on Hopf normal form capture vortex shedding



Low Reynolds number, (Re=100)

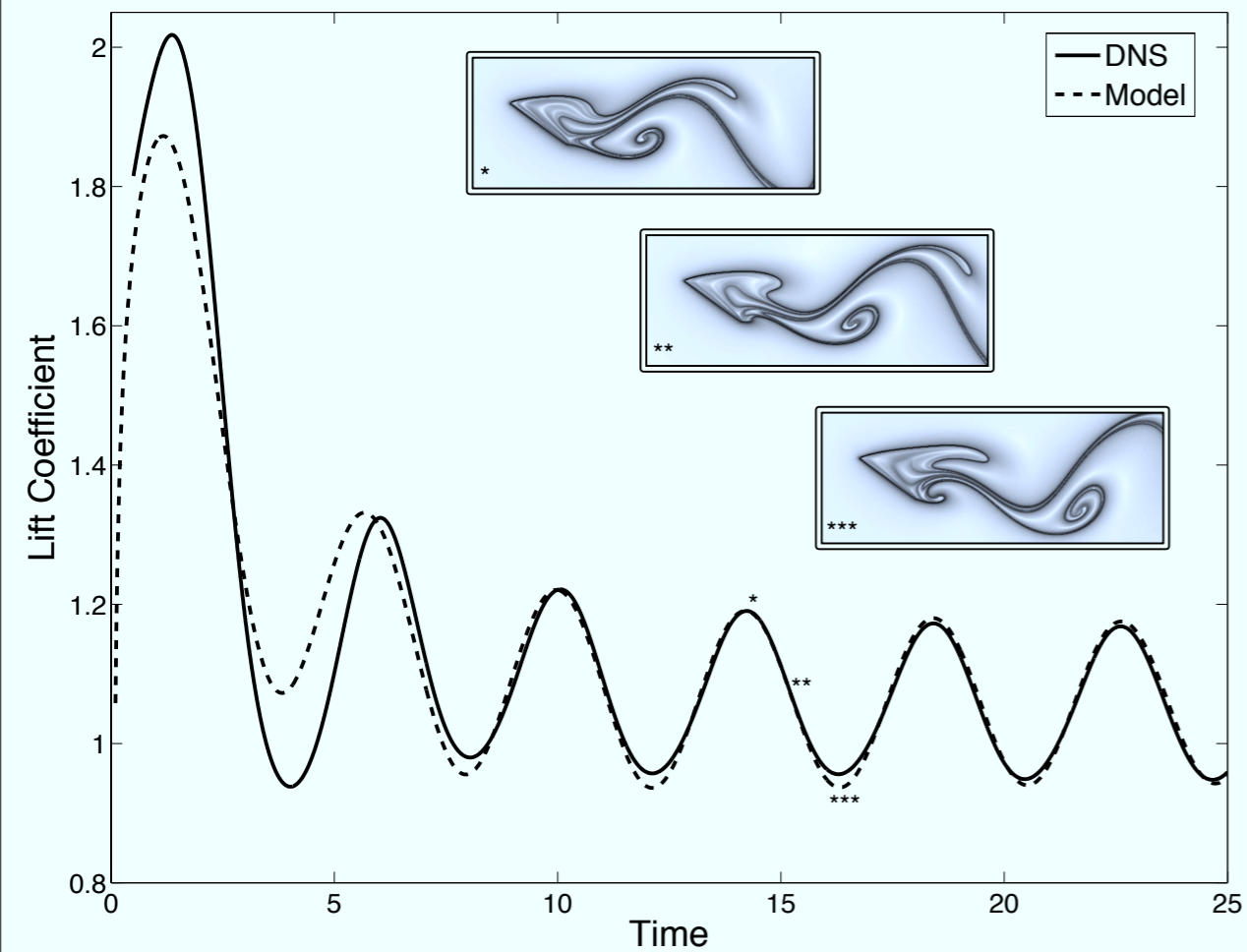
Hopf bifurcation at $\alpha_{crit} \approx 28^\circ$ (pair of imaginary eigenvalues pass into right half plane)



High angle of attack models



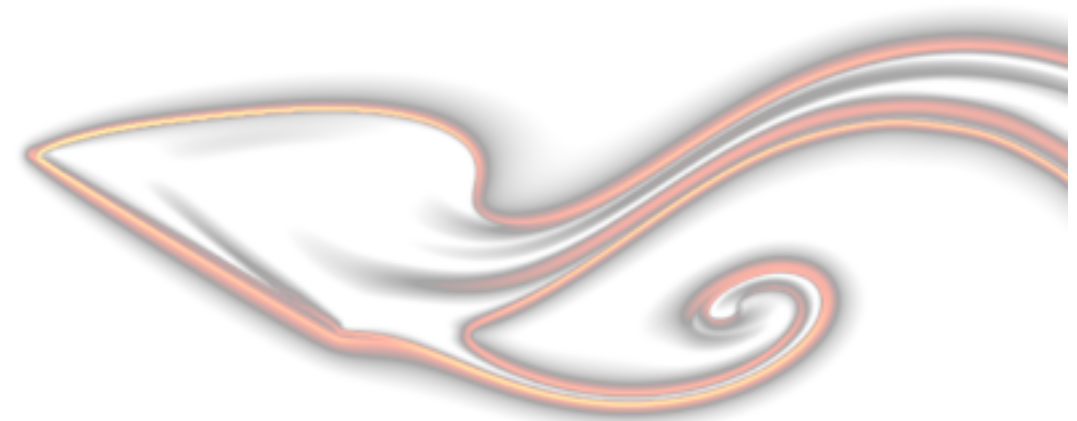
Heuristic Model



Galerkin Projection onto POD



Full DNS



Reconstruction

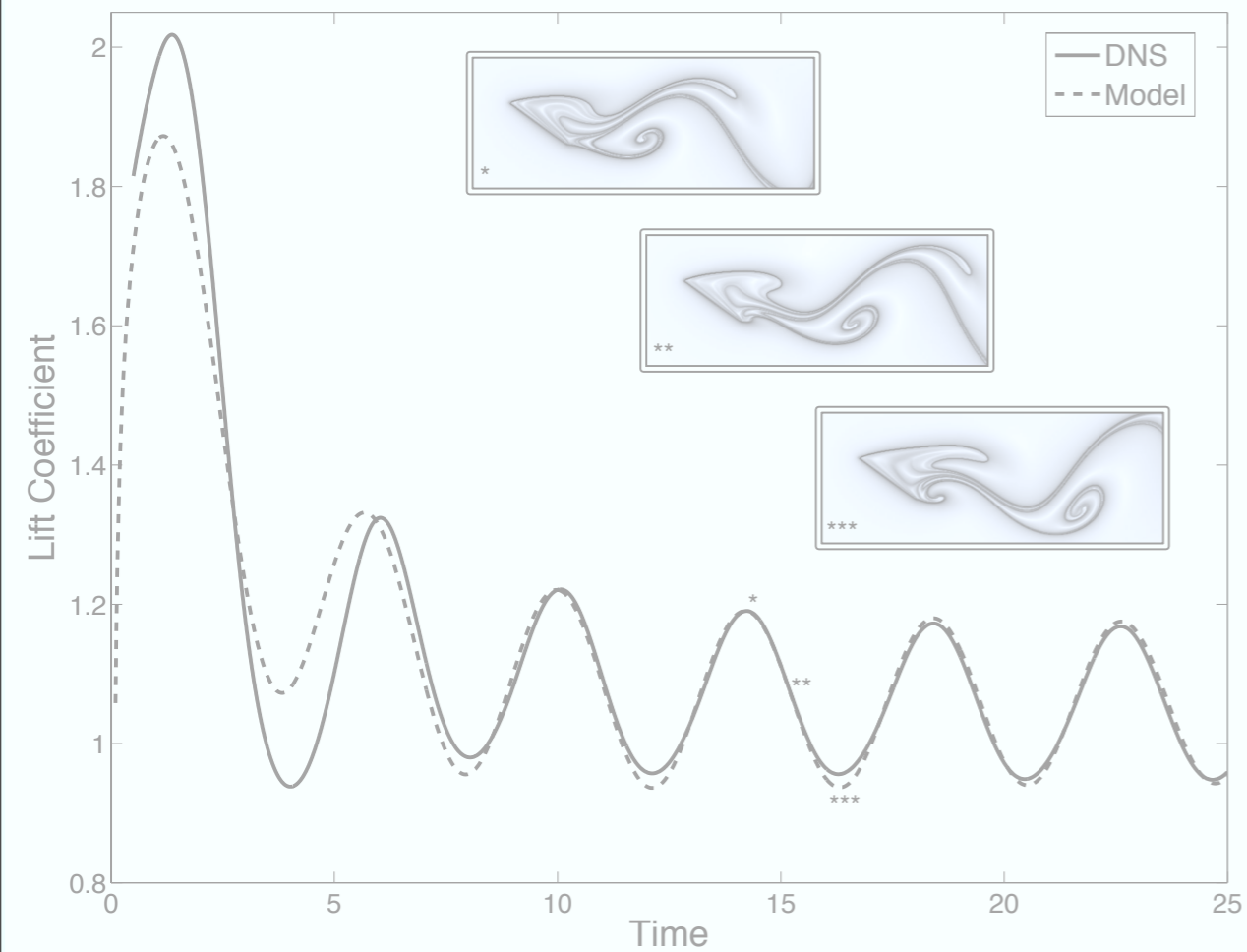
$$\left. \begin{aligned} \dot{x} &= (\alpha - \alpha_c)\mu x - \omega y - ax(x^2 + y^2) \\ \dot{y} &= (\alpha - \alpha_c)\mu y + \omega x - ay(x^2 + y^2) \\ \dot{z} &= -\lambda z \end{aligned} \right\} \implies \begin{aligned} \dot{r} &= r [(\alpha - \alpha_c)\mu - ar^2] \\ \dot{\theta} &= \omega \\ \dot{z} &= -\lambda z \end{aligned}$$



High angle of attack models



Heuristic Model



Galerkin Projection onto POD



Full DNS



Reconstruction

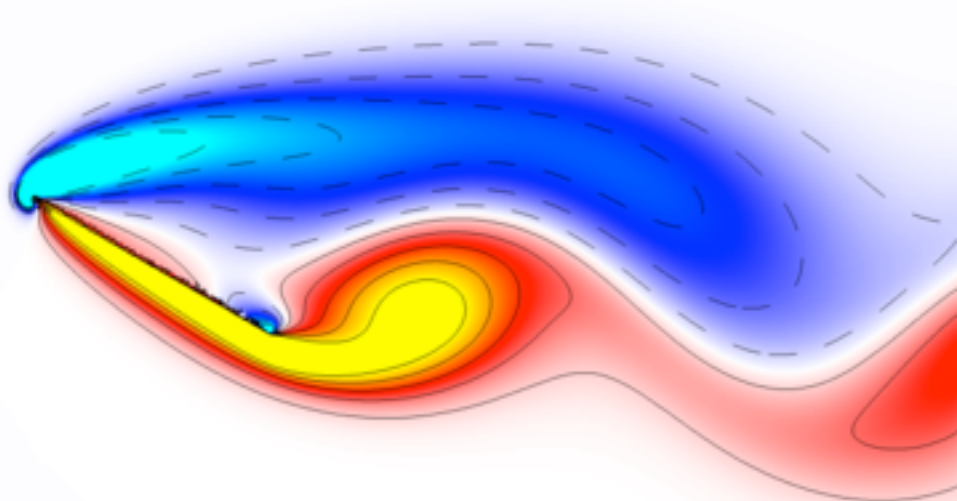
$$\left. \begin{aligned} \dot{x} &= (\alpha - \alpha_c)\mu x - \omega y - ax(x^2 + y^2) \\ \dot{y} &= (\alpha - \alpha_c)\mu y + \omega x - ay(x^2 + y^2) \\ \dot{z} &= -\lambda z \end{aligned} \right\} \implies \begin{aligned} \dot{r} &= r [(\alpha - \alpha_c)\mu - ar^2] \\ \dot{\theta} &= \omega \\ \dot{z} &= -\lambda z \end{aligned}$$



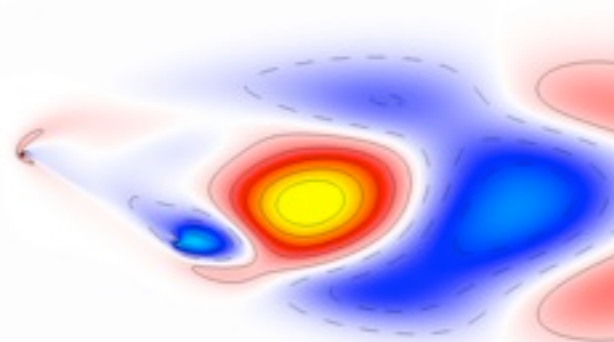
POD Modes for Stationary Plate



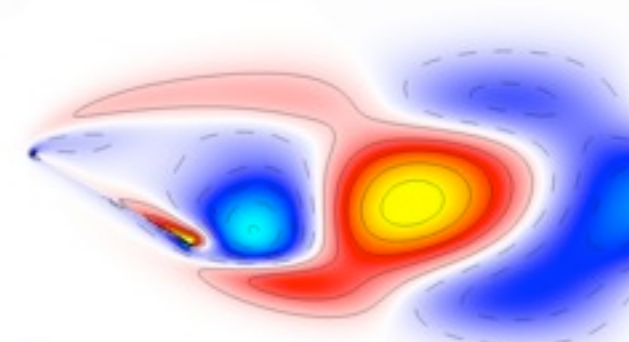
Full Flow



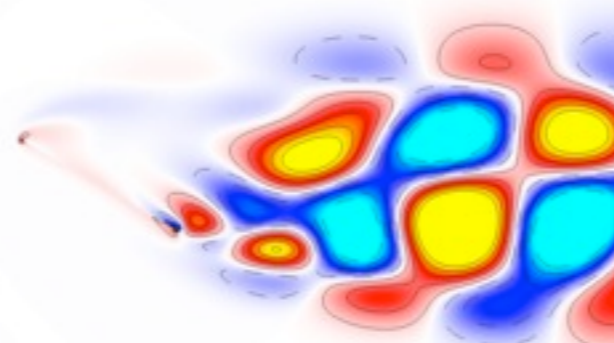
Mode 1



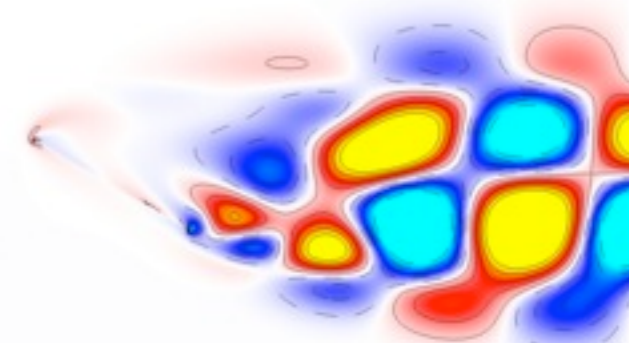
Mode 2



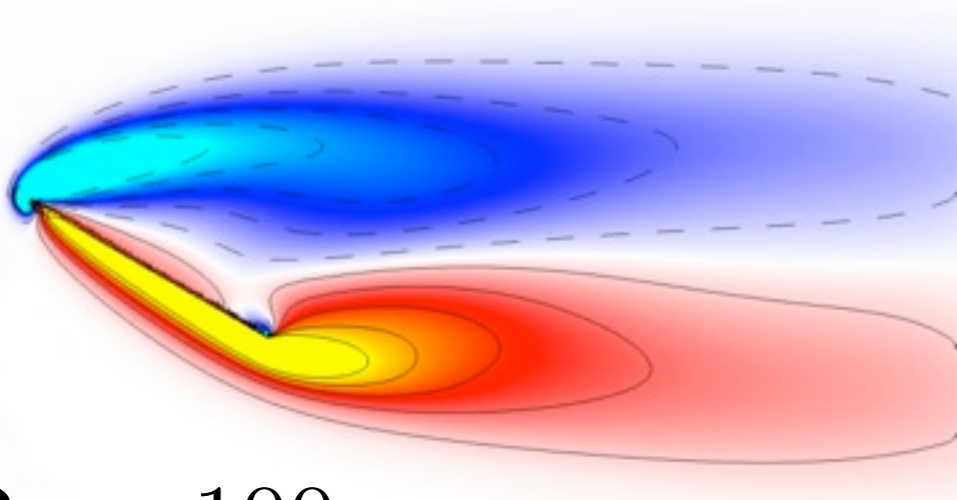
Mode 3



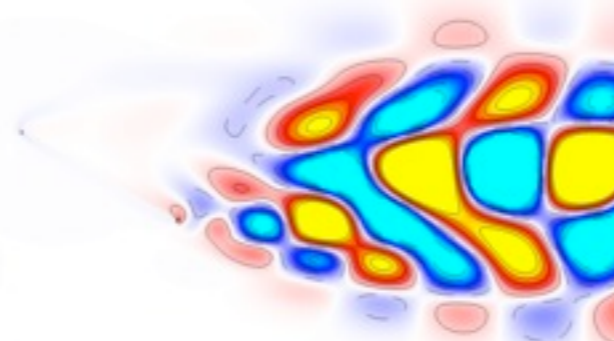
Mode 4



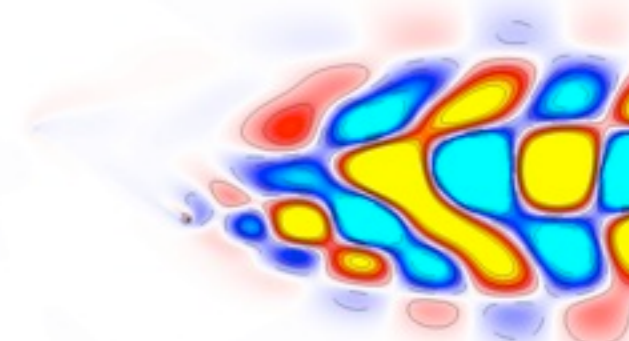
Mean Flow



Mode 5



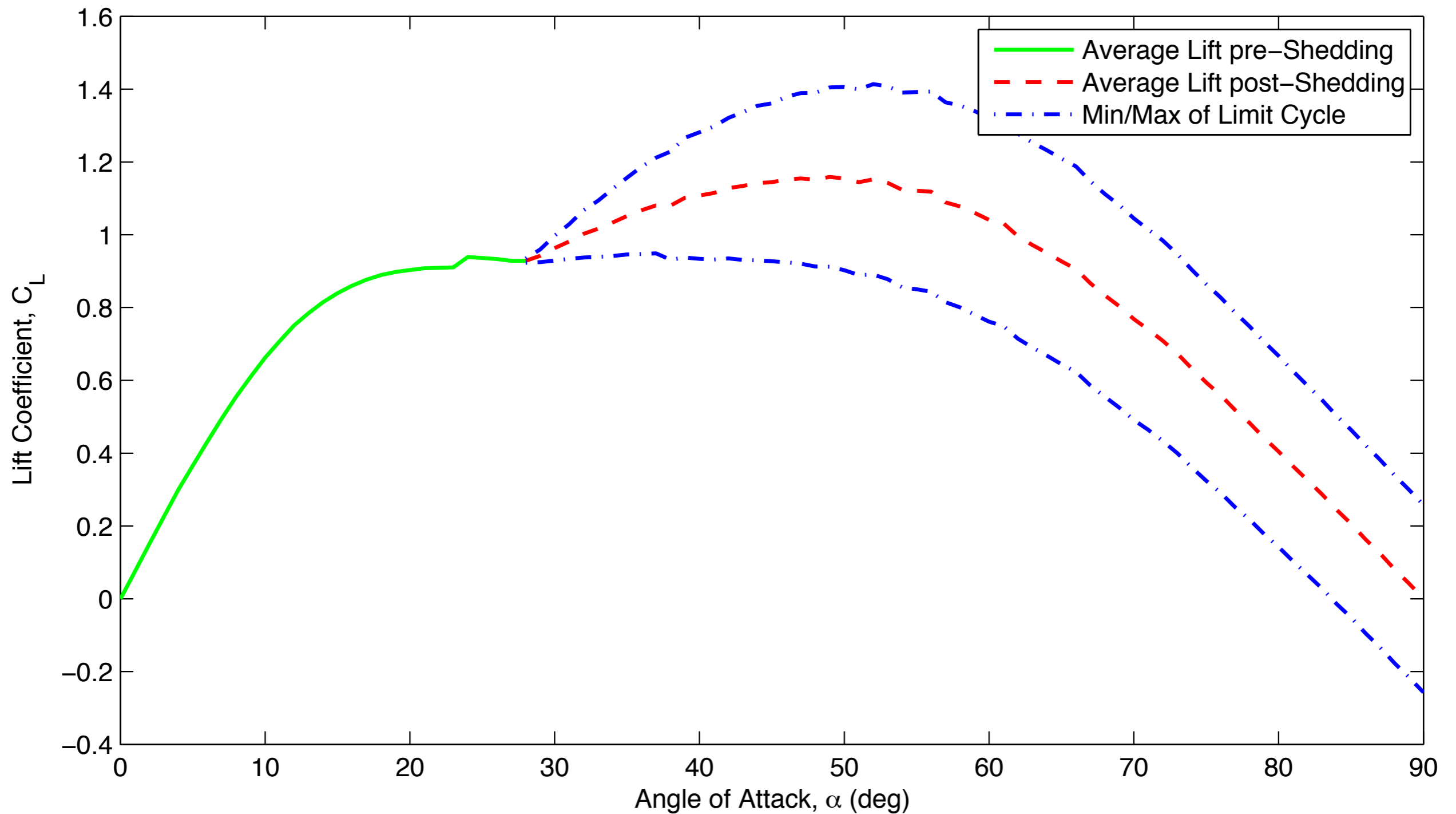
Mode 6



$Re = 100$
 $\alpha = 30^\circ$



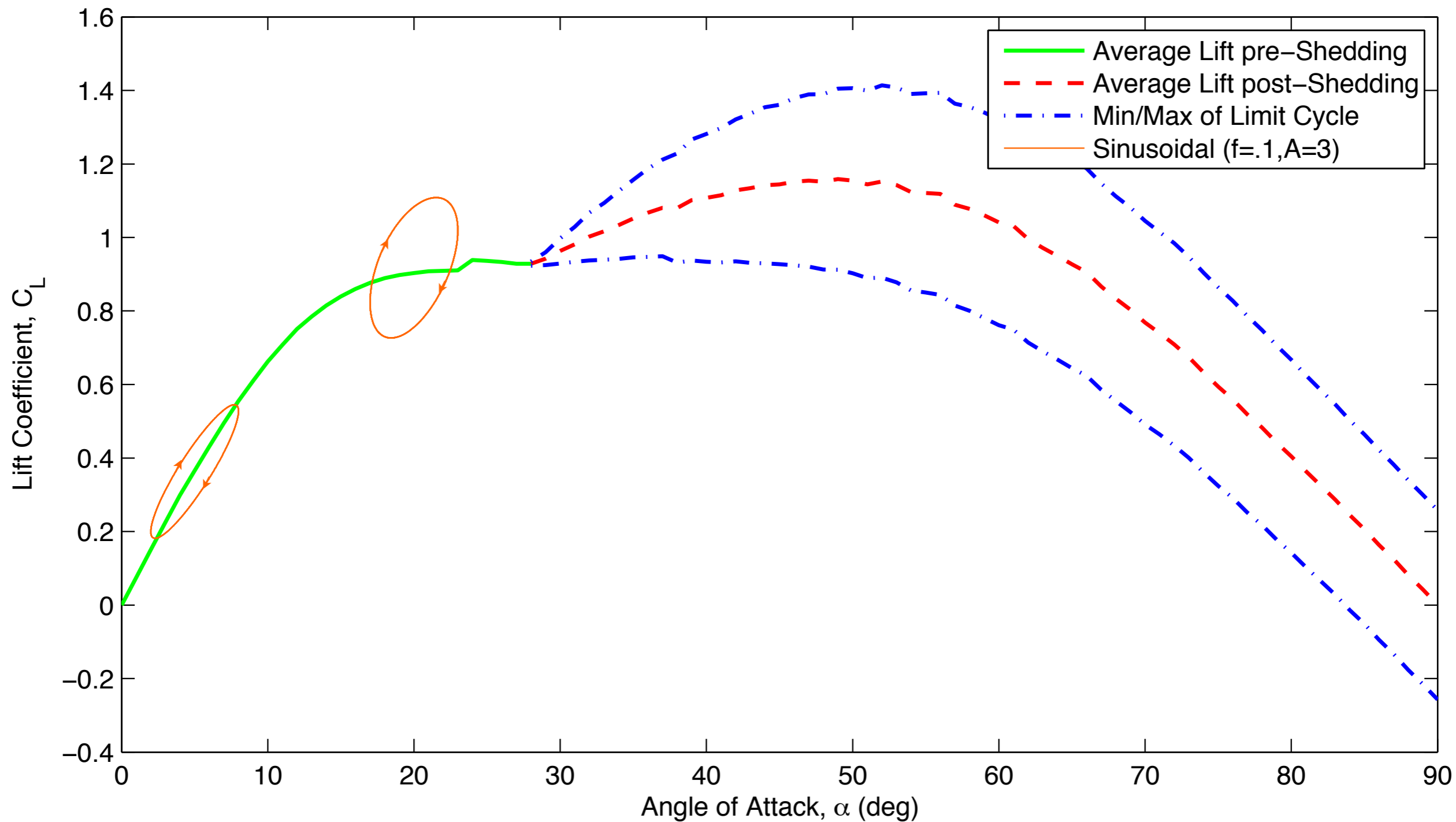
Lift vs. Angle of Attack



Need model that captures lift due to moving airfoil!



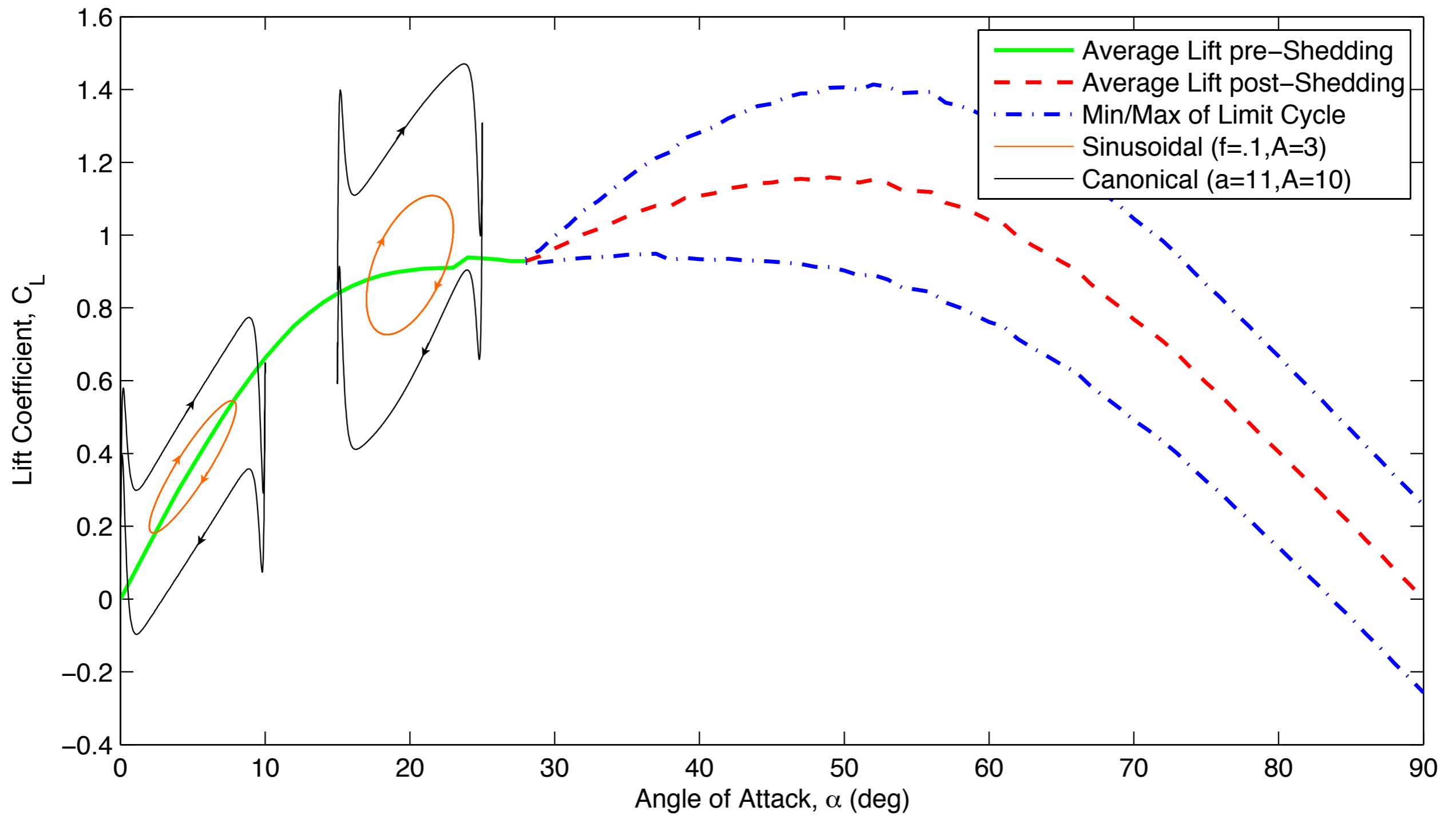
Lift vs. Angle of Attack



Need model that captures lift due to moving airfoil!



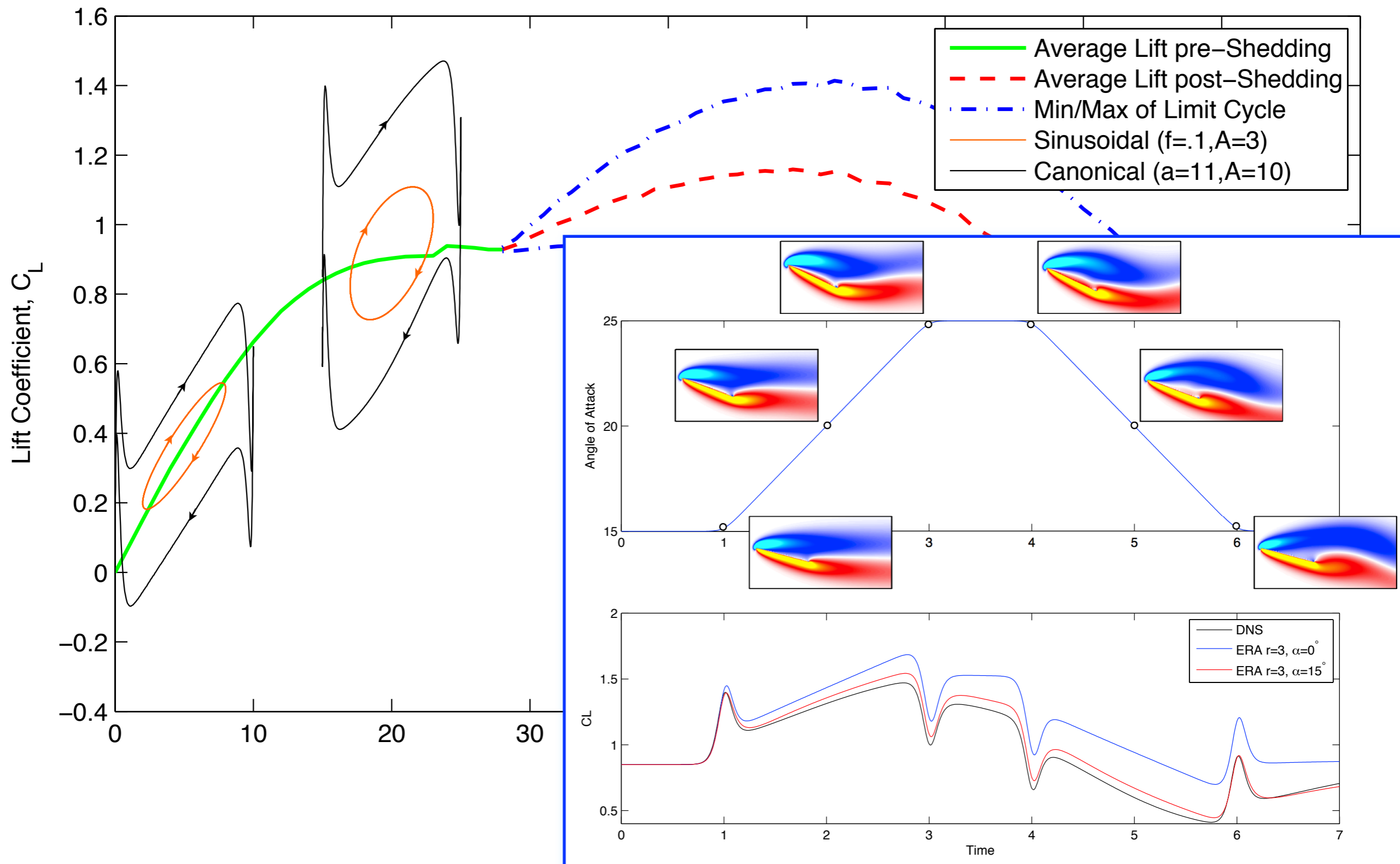
Lift vs. Angle of Attack



Need model that captures lift due to moving airfoil!



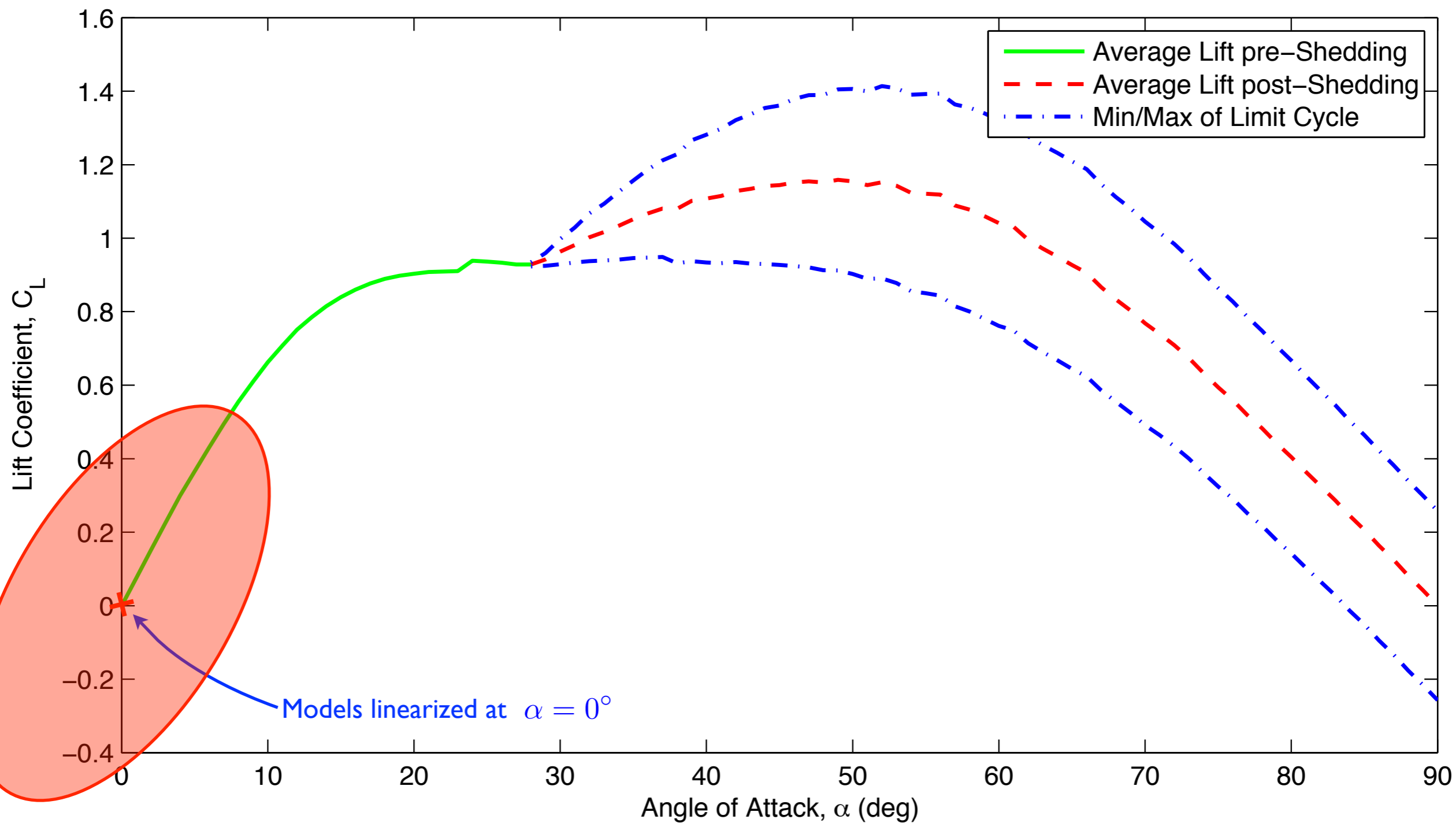
Lift vs. Angle of Attack



Need model that captures lift due to moving airfoil!



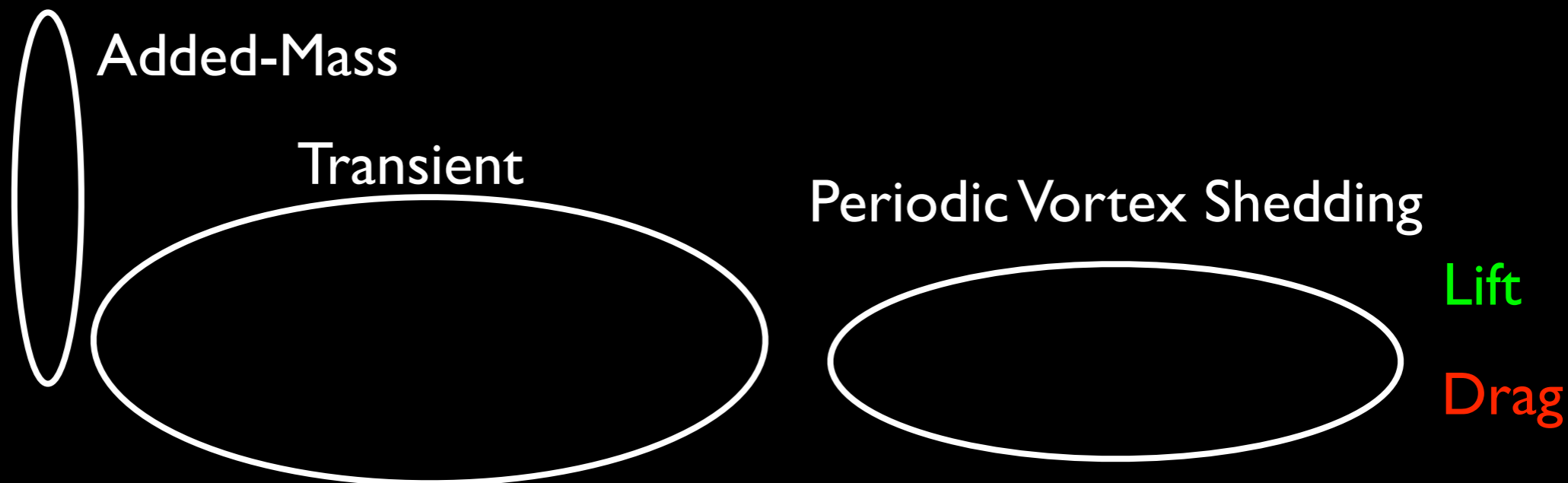
Lift vs. Angle of Attack



Need model that captures lift due to moving airfoil!



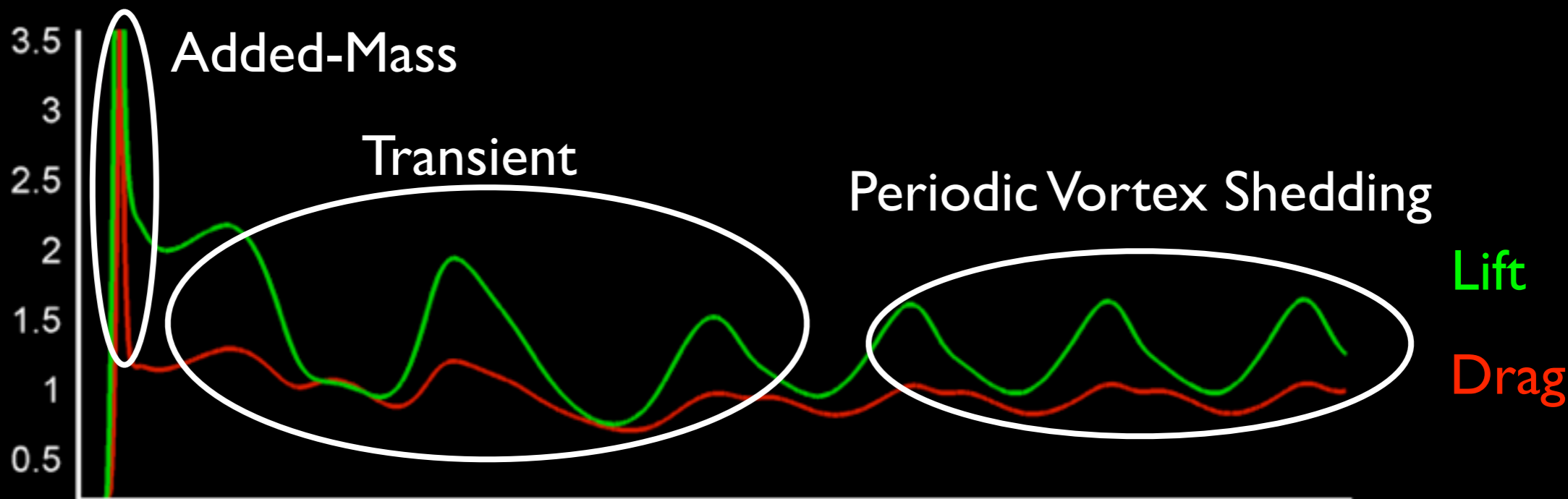
2D Model Problem



$$Re = 300$$
$$\alpha = 32^\circ$$



2D Model Problem



$Re = 300$
 $\alpha = 32^\circ$



Unsteady Aerodynamic Forces



Added Mass

Increasingly important for small/light aircraft

Unsteady potential flow forces ($F=ma$)

force needed to move air as plate accelerates

Circulatory/Viscous

Captures separation effects

Need improved models here

source of all lift in steady flight... and more



Unsteady Aerodynamic Forces



Added Mass

Increasingly important for small/light aircraft

Unsteady potential flow forces ($F=ma$)

force needed to move air as plate accelerates

Circulatory/Viscous

Captures separation effects

Need improved models here

source of all lift in steady flight... and more

The mass of the body and surrounding fluid are being accelerated, to different extents.

Kinetic energy T will be in some manner proportional to U (for potential and Stokes flows)

$$T = \rho \frac{I}{2} U^2 \quad \text{where} \quad I = \int_V \frac{u_i}{U} \cdot \frac{u_i}{U} dV$$

If body accelerates, T probably increases, and energy must be supplied:

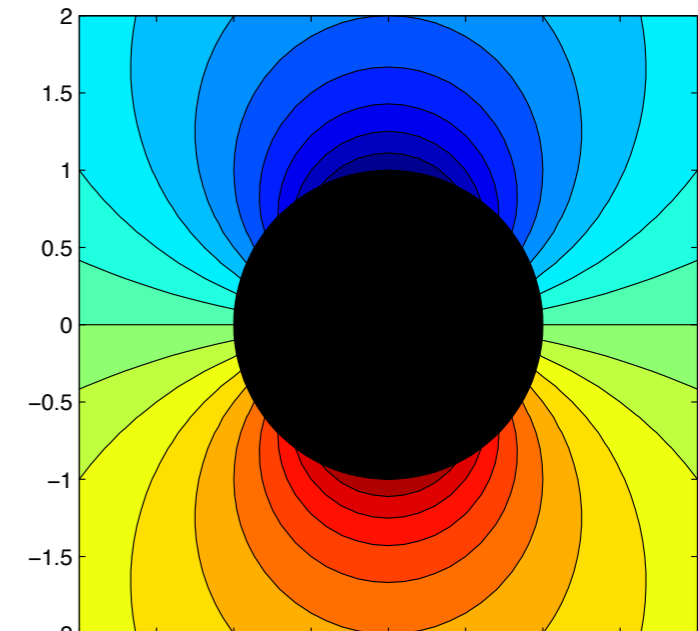
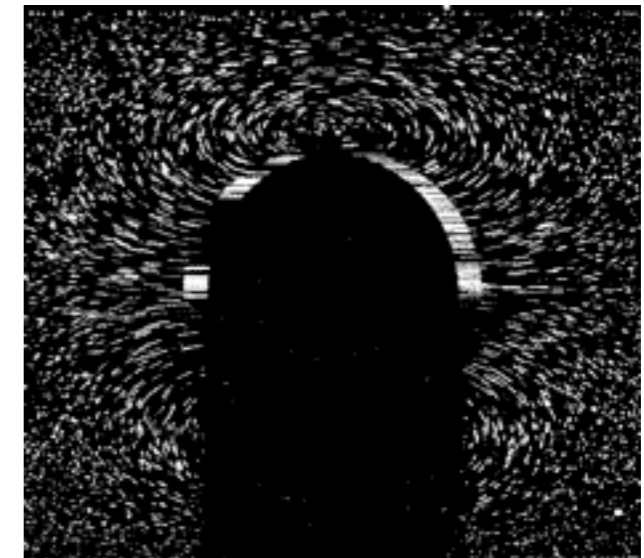
$$\frac{dT}{dt} = -FU \quad \implies \quad F_i = - \underbrace{\rho I_{ij}}_{\text{AM}} \dot{U}_j$$

Lamb, 1945.

Milne-Thompson, 1962

Newman, 1977.

cylinder moving in Lab frame





Unsteady Aerodynamic Forces



Added Mass

Increasingly important for small/light aircraft

Unsteady potential flow forces ($F=ma$)

force needed to move air as plate accelerates

Circulatory/Viscous

Captures separation effects

Need improved models here

source of all lift in steady flight... and more

The mass of the body and surrounding fluid are being accelerated, to different extents.

Kinetic energy T will be in some manner proportional to U (for potential and Stokes flows)

$$T = \rho \frac{I}{2} U^2 \quad \text{where} \quad I = \int_V \frac{u_i}{U} \cdot \frac{u_i}{U} dV$$

If body accelerates, T probably increases, and energy must be supplied:

$$\frac{dT}{dt} = -FU \quad \implies \quad F_i = - \underbrace{\rho I_{ij}}_{\text{AM}} \dot{U}_j$$

Lamb, 1945.

Milne-Thompson, 1962

Newman, 1977.

Beer bubble acceleration





Unsteady Aerodynamic Forces



Added Mass

Increasingly important for small/light aircraft

Unsteady potential flow forces ($F=ma$)

force needed to move air as plate accelerates

Circulatory/Viscous

Captures separation effects

Need improved models here

source of all lift in steady flight... and more



Boundary layer

Laminar separation bubble

Leading edge vortex

Periodic Vortex Shedding



Milne-Thompson, 1973.

Stengel, 2004.



Theodorsen's Model - 1935



Added Mass

Increasingly important for small/light aircraft

Unsteady potential flow forces ($F=ma$)

force needed to move air as plate accelerates

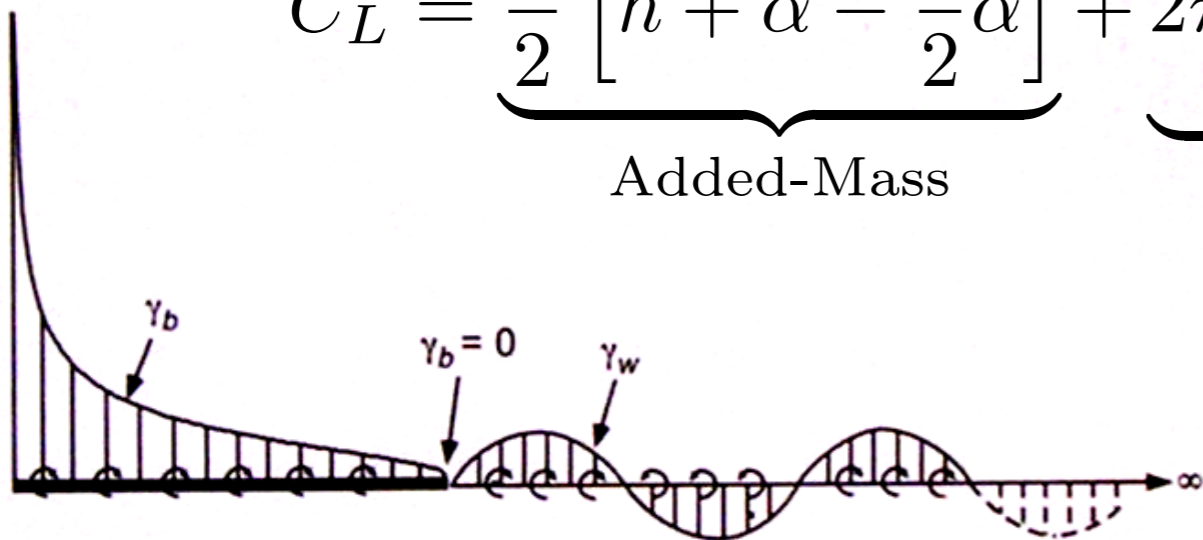
Circulatory/Viscous

Captures separation effects

Need improved models here

source of all lift in steady flight... and more

$$C_L = \underbrace{\frac{\pi}{2} \left[\ddot{h} + \dot{\alpha} - \frac{a}{2} \ddot{\alpha} \right]}_{\text{Added-Mass}} + \underbrace{2\pi \left[\alpha + \dot{h} + \frac{1}{2} \dot{\alpha} \left(\frac{1}{2} - a \right) \right]}_{\text{Circulatory}} C(k)$$

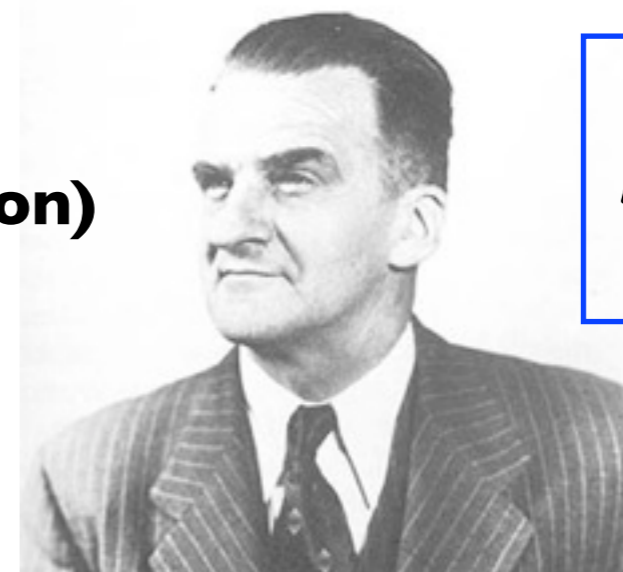


$$C(k) = \frac{H_1^{(2)}(k)}{H_1^{(2)}(k) + iH_0^{(2)}(k)}$$

2D Incompressible, inviscid model

Unsteady potential flow (w/ Kutta condition)

Linearized about zero angle of attack



$$k = \frac{\pi f c}{U_\infty}$$

Theodorsen, 1935.

Leishman, 2006.



Bode Plot of Theodorsen



$$C_L = \underbrace{\frac{\pi}{2} \left[\ddot{h} + \dot{\alpha} - \frac{a}{2} \ddot{\alpha} \right]}_{\text{Added-Mass}} + \underbrace{2\pi \left[\alpha + \dot{h} + \frac{1}{2} \dot{\alpha} \left(\frac{1}{2} - a \right) \right]}_{\text{Circulatory}} C(k)$$

$$k = \frac{\pi f c}{U_\infty}$$

Frequency response

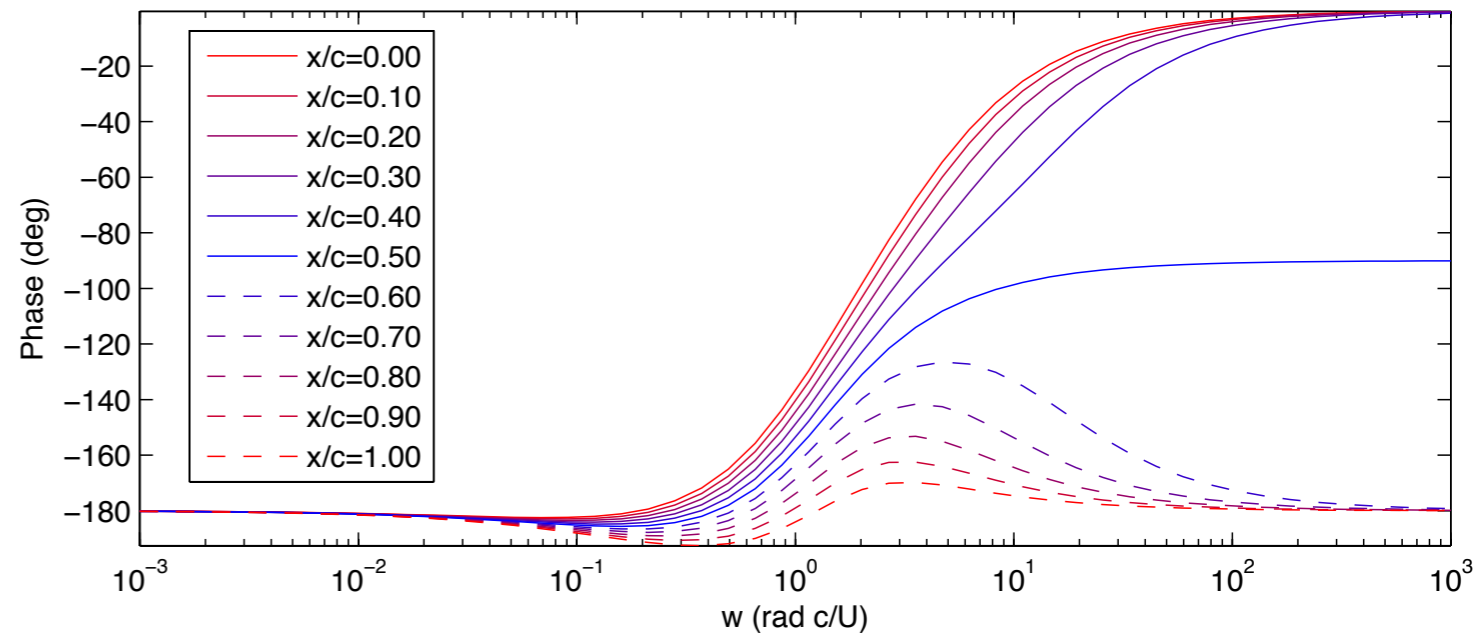
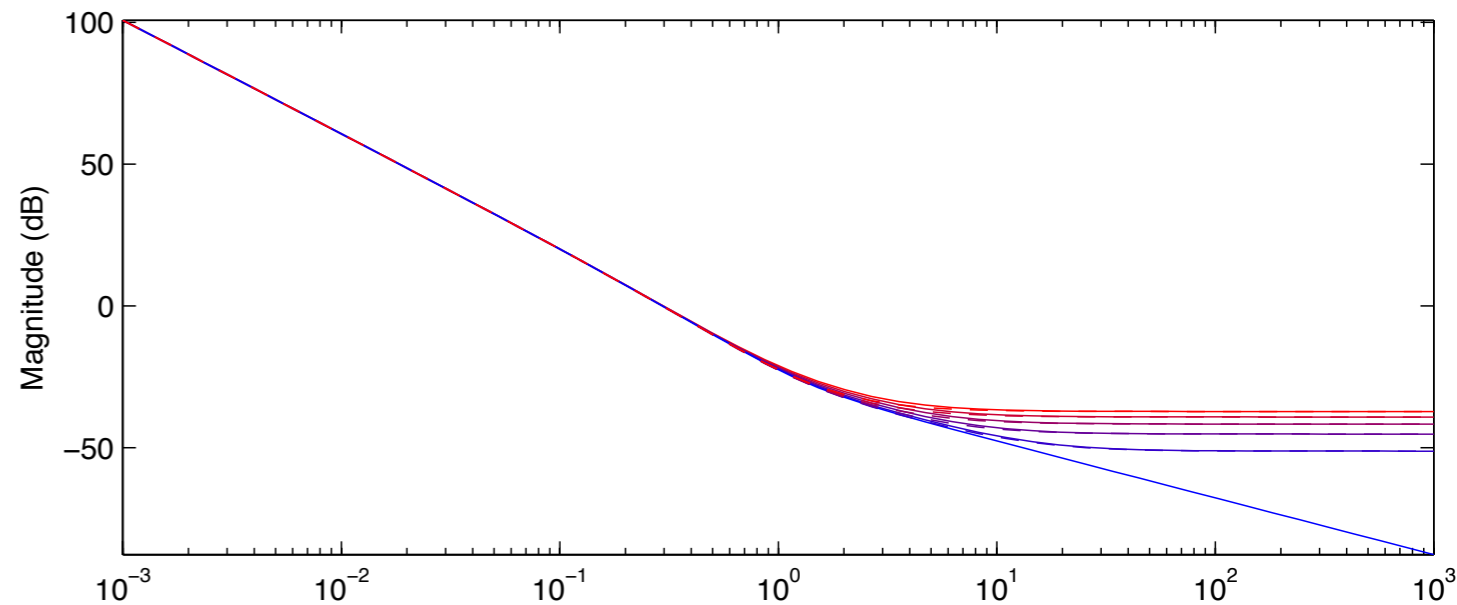
input is $\ddot{\alpha}$ (α is angle of attack)

output is lift coefficient C_L

Low frequencies dominated by quasi-steady forces

High frequencies dominated by added-mass forces

Intermediate frequencies determined by Theodorsen's function $C(k)$

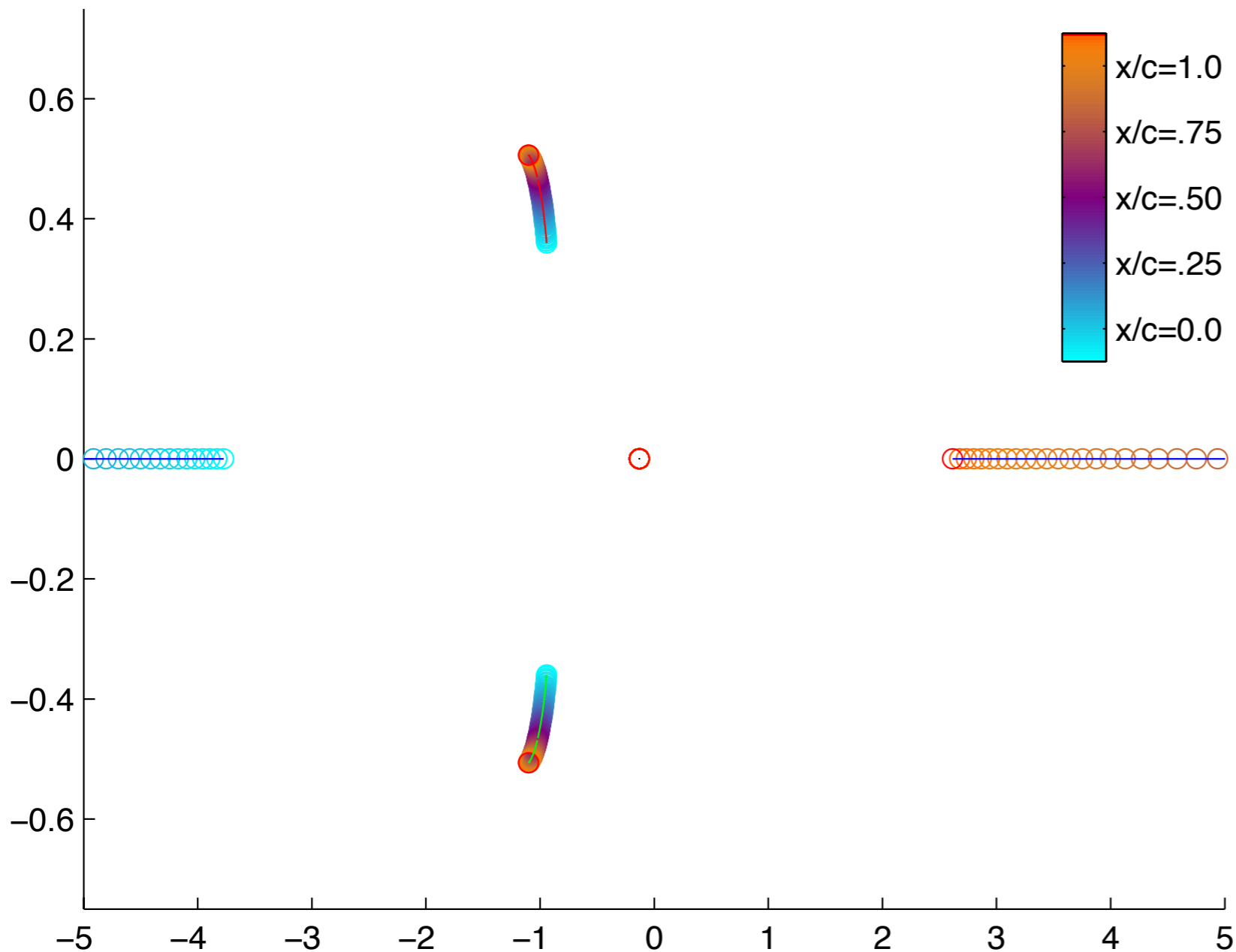




Zeros of Theodorsen's Model



Zeros of Theodorsen Model, Varying Pitch Point



All Theodorsen pitch models have same poles, different zeros

As pitch point moves aft of center, zero enters RHP at +infinity.

non-minimum phase response:

Given a step in angle of attack, lift initially moves in opposite direction (because of negative added-mass forces), before the circulatory lift forces have a change to catch up and system relaxes to a positive lift steady state.



Indicial Response Models



Given an impulse in angle of attack, $\alpha = \delta(t)$, the time history of Lift is $C_L^\delta(t)$

The response to an arbitrary input $\alpha(t)$ is given by linear superposition:

$$C_L(t) = \int_0^t C_L^\delta(t - \tau)\alpha(\tau)d\tau = (C_L^\delta * \alpha)(t)$$

Given a step in angle of attack, $\dot{\alpha} = \delta(t)$, the time history of Lift is $C_L^S(t)$

The response to an arbitrary input $\alpha(t)$ is given by:

$$C_L(t) = C_L^S(t)\alpha(0) + \int_0^t C_L^S(t - \tau)\dot{\alpha}(\tau)d\tau$$

Model Summary

Reconstructs Lift for arbitrary input

Linear time-invariant (LTI) models

Based on experiment, simulation or theory

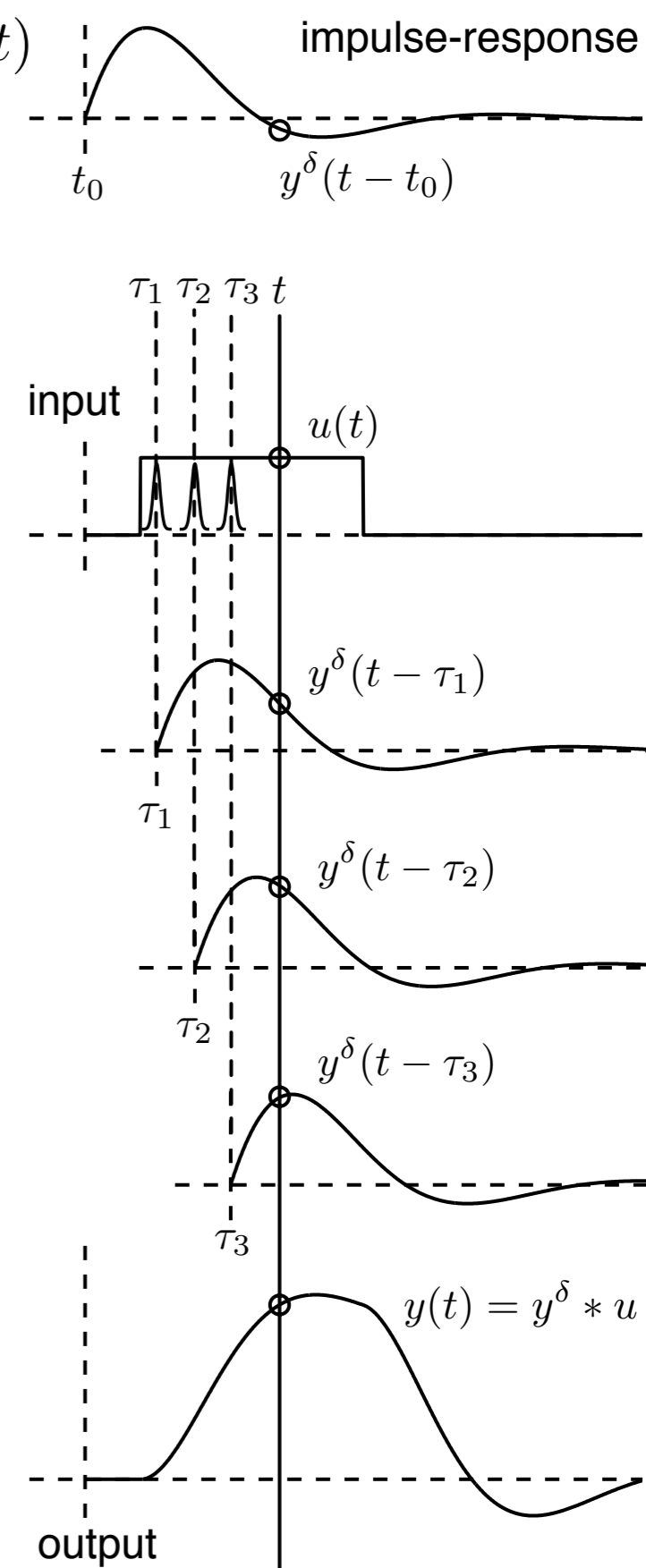
Wagner developed indicial response analytically using same approximations as Theodorsen

convolution integral inconvenient for feedback control design

Wagner, 1925.

Reisenthel, 1996.

Leishman, 2006.





Indicial Response Models



Given an impulse in angle of attack, $\alpha = \delta(t)$, the time history of Lift is $C_L^\delta(t)$

The response to an arbitrary input $\alpha(t)$ is given by linear superposition:

$$C_L(t) = \int_0^t C_L^\delta(t - \tau)\alpha(\tau)d\tau = (C_L^\delta * \alpha)(t)$$

Given a step in angle of attack, $\dot{\alpha} = \delta(t)$, the time history of Lift is $C_L^S(t)$

The response to an arbitrary input $\alpha(t)$ is given by:

$$C_L(t) = C_L^S(t)\alpha(0) + \int_0^t C_L^S(t - \tau)\dot{\alpha}(\tau)d\tau$$

Model Summary

Reconstructs Lift for arbitrary input

Linear time-invariant (LTI) models

Based on experiment, simulation or theory

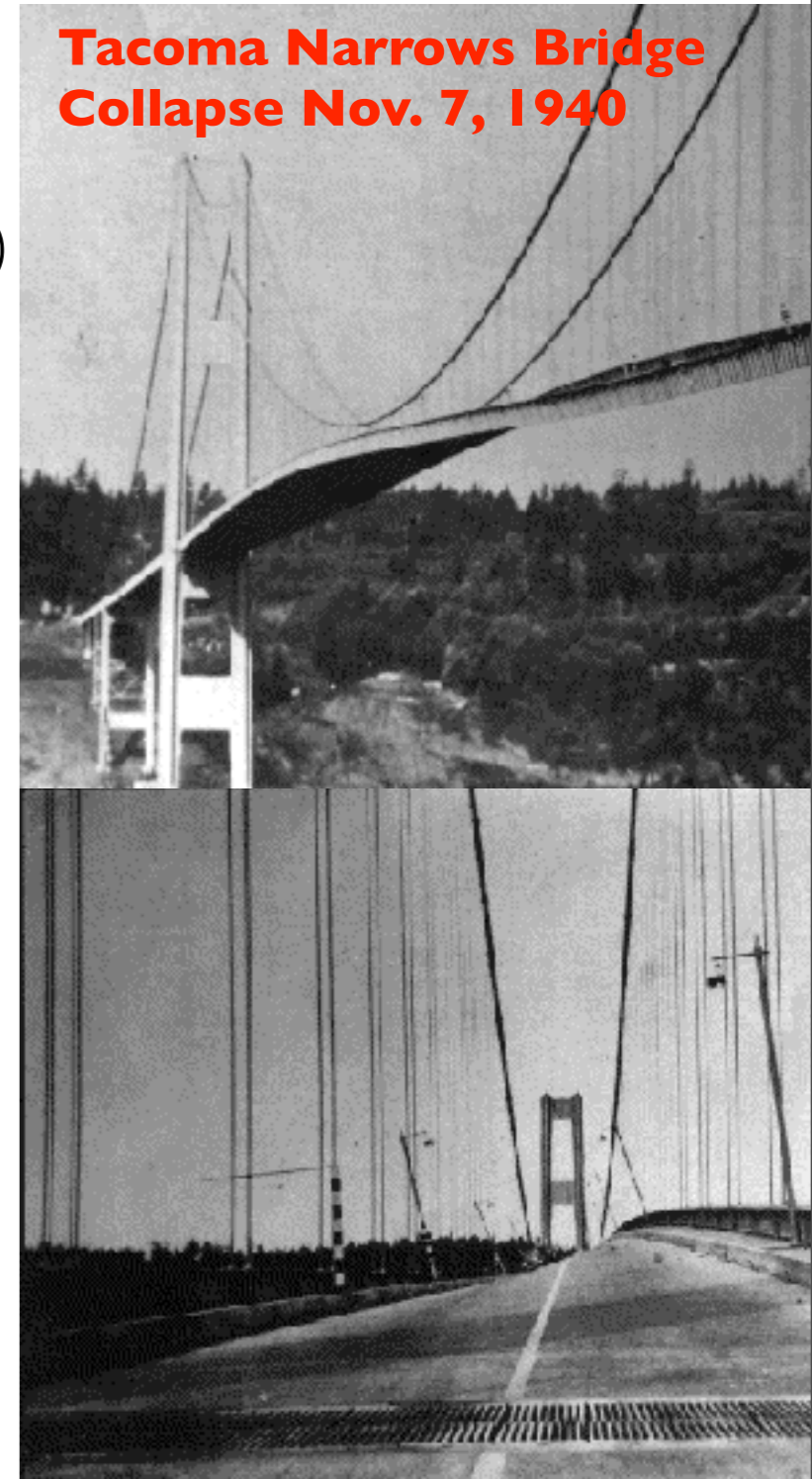
Wagner developed indicial response analytically using same approximations as Theodorsen

convolution integral inconvenient for feedback control design

Wagner, 1925.

Reisenthel, 1996.

Leishman, 2006.





State-Space Indicial Response



Indicial Response

Tuned to specific geometry, Re #

$$C_L(t) = C_L^\delta(t)\alpha(0) + \int_0^t C_L^\delta(t - \tau)\dot{\alpha}(\tau)d\tau$$

Theodorsen's Model

Physically motivated components

Parametrized by pitch point

Frequency domain, idealized assumptions

$$C_L = \underbrace{\frac{\pi}{2} \left[\ddot{h} + \dot{\alpha} - \frac{a}{2}\ddot{\alpha} \right]}_{\text{Added-Mass}} + 2\pi \underbrace{\left[\alpha + \dot{h} + \frac{1}{2}\dot{\alpha} \left(\frac{1}{2} - a \right) \right]}_{\text{Circulatory}} C(k)$$

State-Space Model

Captures input output dynamics accurately

Computationally tractable

fits into control framework

transient dynamics

$$\frac{d}{dt} \begin{bmatrix} \mathbf{x} \\ \alpha \\ \dot{\alpha} \end{bmatrix} = \begin{bmatrix} A_r & 0 & 0 \\ 0 & 0 & 1 \\ 0 & 0 & 0 \end{bmatrix} \begin{bmatrix} \mathbf{x} \\ \alpha \\ \dot{\alpha} \end{bmatrix} + \begin{bmatrix} B_r \\ 0 \\ 1 \end{bmatrix} \ddot{\alpha}$$

$$C_L = \begin{bmatrix} C_r & C_{L\alpha} & C_{L\dot{\alpha}} \end{bmatrix} \begin{bmatrix} \mathbf{x} \\ \alpha \\ \dot{\alpha} \end{bmatrix} + C_{L\ddot{\alpha}} \ddot{\alpha}$$

quasi-steady and added-mass

Brunton and Rowley, in preparation.



State-Space Indicial Response



Stability derivatives plus fast dynamics

$$C_L(\alpha, \dot{\alpha}, \ddot{\alpha}, \mathbf{x}) = C_{L_\alpha} \alpha + C_{L_{\dot{\alpha}}} \dot{\alpha} + C_{L_{\ddot{\alpha}}} \ddot{\alpha} + C\mathbf{x}$$

Quasi-steady and added-mass

Transient dynamics

Transfer Function

$$Y(s) = \left[\frac{C_{L_\alpha}}{s^2} + \frac{C_{L_{\dot{\alpha}}}}{s} + C_{L_{\ddot{\alpha}}} + G(s) \right] s^2 U(s)$$

State-Space Model

Captures input output dynamics accurately

Computationally tractable

fits into control framework

transient dynamics

$$\frac{d}{dt} \begin{bmatrix} \mathbf{x} \\ \alpha \\ \dot{\alpha} \end{bmatrix} = \begin{bmatrix} A_r & 0 & 0 \\ 0 & 0 & 1 \\ 0 & 0 & 0 \end{bmatrix} \begin{bmatrix} \mathbf{x} \\ \alpha \\ \dot{\alpha} \end{bmatrix} + \begin{bmatrix} B_r \\ 0 \\ 1 \end{bmatrix} \ddot{\alpha}$$

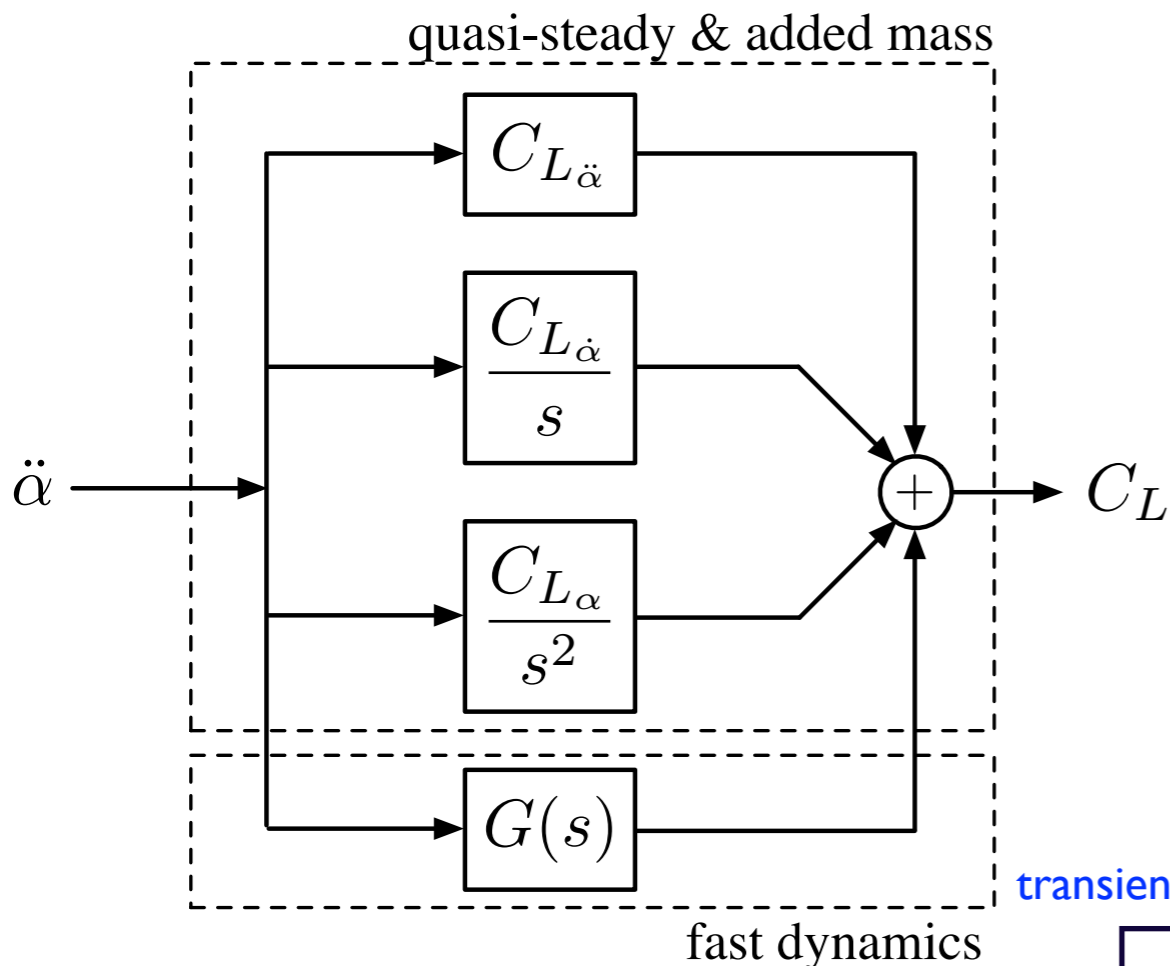
$$C_L = \begin{bmatrix} C_r & C_{L_\alpha} & C_{L_{\dot{\alpha}}} \end{bmatrix} \begin{bmatrix} \mathbf{x} \\ \alpha \\ \dot{\alpha} \end{bmatrix} + C_{L_{\ddot{\alpha}}} \ddot{\alpha}$$

quasi-steady and added-mass

Brunton and Rowley, in preparation.



State-Space Indicial Response



Model Summary

Linearized about $\alpha = 0$

Based on experiment, simulation or theory

Recovers stability derivatives $C_{L\alpha}$, $C_{L\dot{\alpha}}$, $C_{L\ddot{\alpha}}$ associated with quasi-steady and added-mass

ODE model ideal for control design

transient dynamics

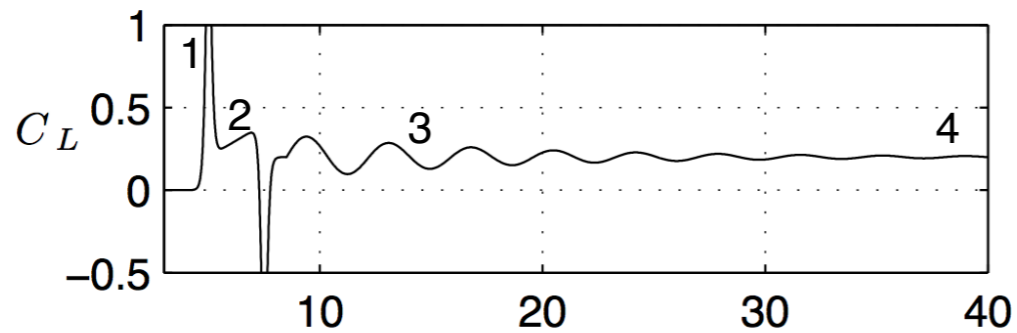
$$\frac{d}{dt} \begin{bmatrix} \mathbf{x} \\ \alpha \\ \dot{\alpha} \end{bmatrix} = \begin{bmatrix} A_r & 0 & 0 \\ 0 & 0 & 1 \\ 0 & 0 & 0 \end{bmatrix} \begin{bmatrix} \mathbf{x} \\ \alpha \\ \dot{\alpha} \end{bmatrix} + \begin{bmatrix} B_r \\ 0 \\ 1 \end{bmatrix} \ddot{\alpha}$$

$$C_L = \begin{bmatrix} C_r & C_{L\alpha} & C_{L\dot{\alpha}} \end{bmatrix} \begin{bmatrix} \mathbf{x} \\ \alpha \\ \dot{\alpha} \end{bmatrix} + C_{L\ddot{\alpha}} \ddot{\alpha}$$

quasi-steady and added-mass

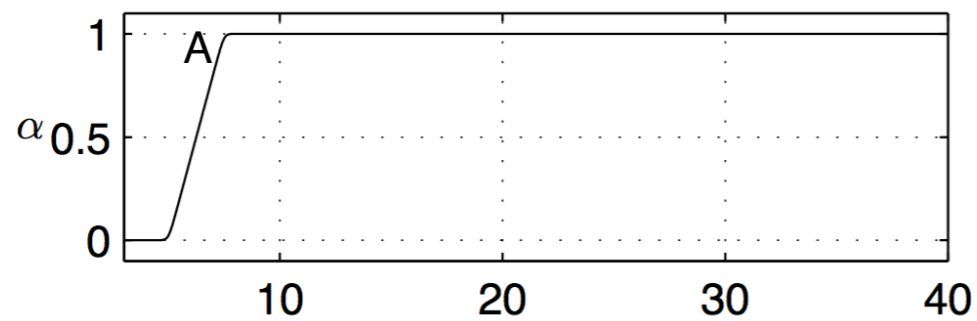


Identifying Model from Simulations

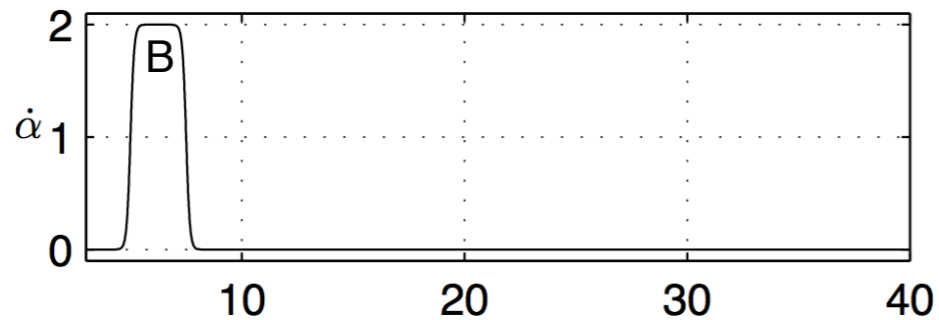


1 - added-mass from $\ddot{\alpha}$ (C)

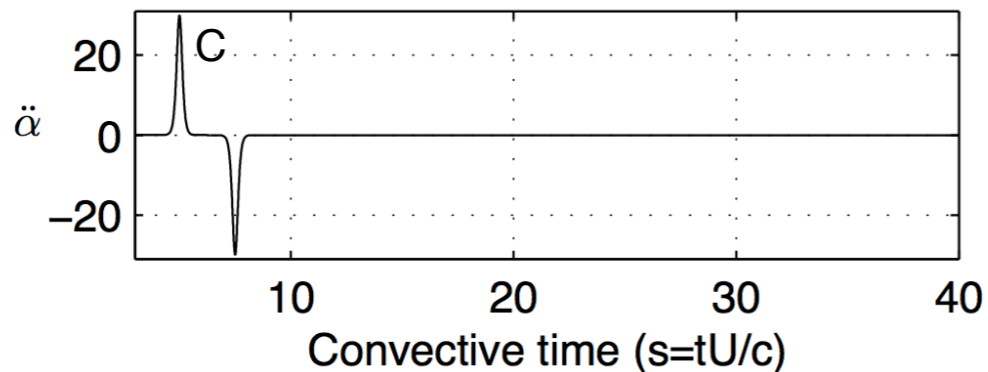
2 - added-mass from $\dot{\alpha}$ (B) and quasi-steady α (A)



3 - fast dynamics (G) and quasi-steady from α (A)



4 - quasi-steady from α (A)



Cartoon illustration of aerodynamic step response

4-6 orders of magnitude frequency and scale separation in response

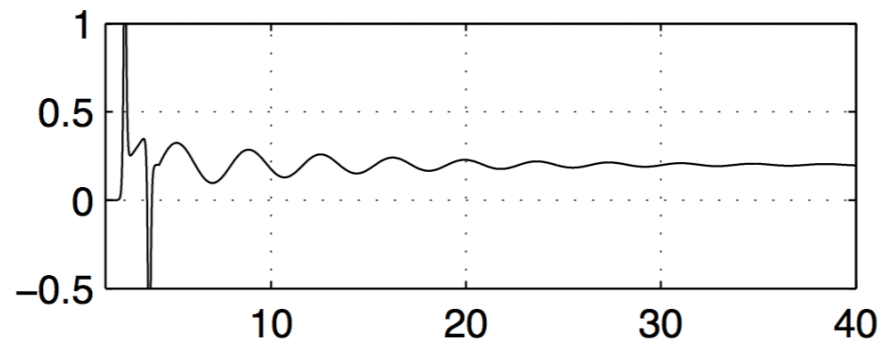
Brunton and Rowley, in preparation.



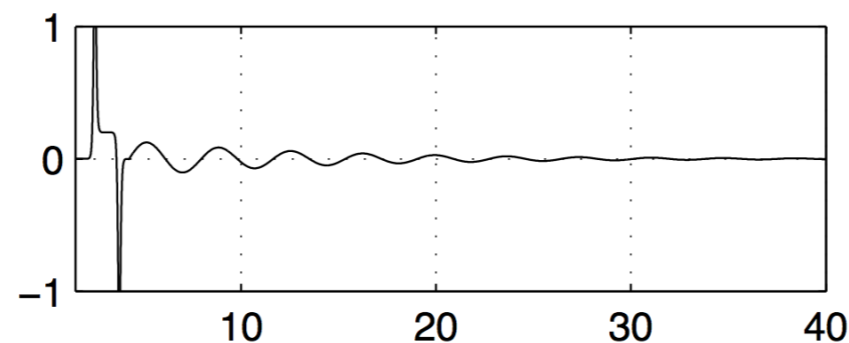
Method I



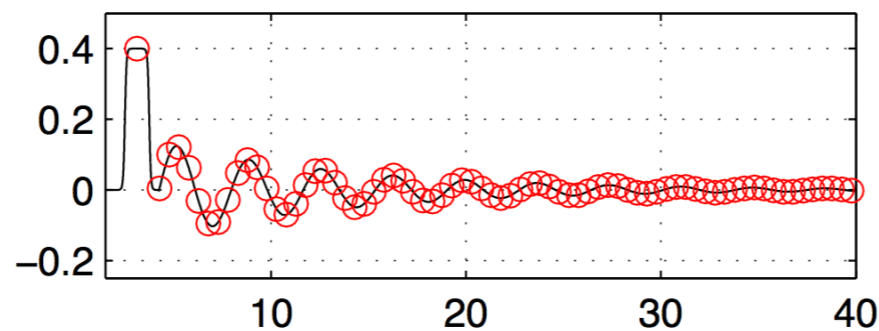
step maneuver in α
 $\dot{\alpha} = \delta$ (resolved in time)



subtract off $\alpha \cdot C_{L\alpha}$
(low frequency asymptote)



subtract off $\ddot{\alpha} \cdot C_{\ddot{\alpha}}$
(high frequency asymptote)



$$\frac{d}{dt} \begin{bmatrix} x \\ \alpha \\ \dot{\alpha} \end{bmatrix} = \begin{bmatrix} A & 0 & B \\ 0 & 0 & 1 \\ 0 & 0 & 0 \end{bmatrix} \begin{bmatrix} x \\ \alpha \\ \dot{\alpha} \end{bmatrix} + \begin{bmatrix} 0 \\ 0 \\ 1 \end{bmatrix} \ddot{\alpha}$$

$$y = [C \quad C_\alpha \quad C_{\dot{\alpha}}] \begin{bmatrix} x \\ \alpha \\ \dot{\alpha} \end{bmatrix} + D\ddot{\alpha}$$

Isolate high and low frequency asymptotes and identify transient fluid dynamics with ERA

Transient dynamics modeled using ERA model

$$\dot{\alpha} \rightarrow (A, B, C, C_{\dot{\alpha}}) \rightarrow C_L$$

ERA - Eigensystem realization algorithm

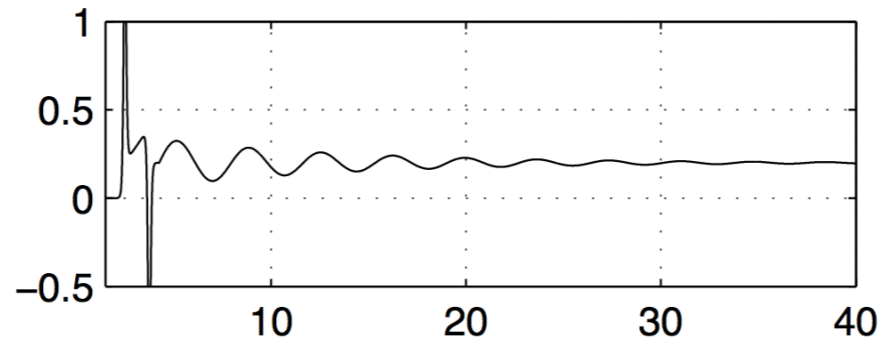
Brunton and Rowley, in preparation.



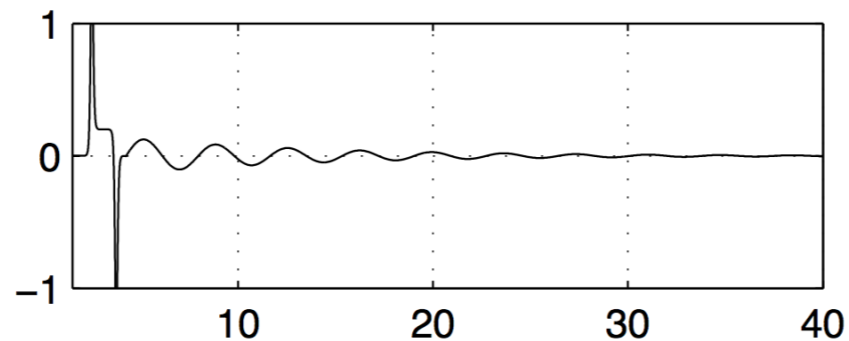
Method II



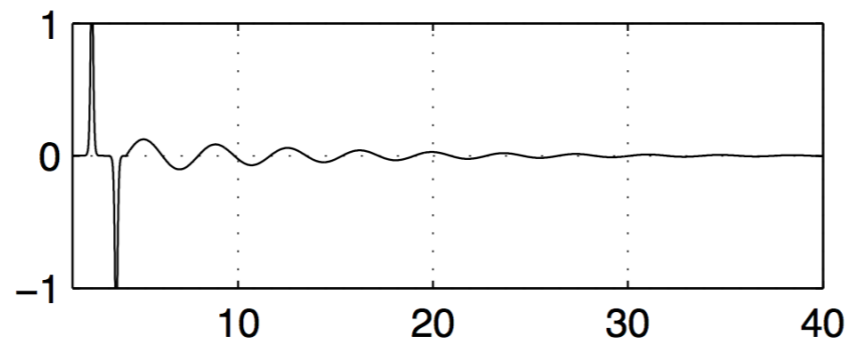
step maneuver in α
 $\dot{\alpha} = \delta$ (resolved in time)



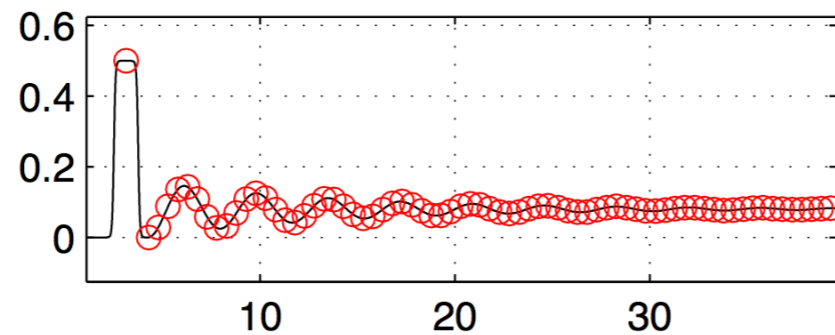
subtract off $\alpha \cdot C_{L\alpha}$
(low frequency asymptote)



subtract off $\dot{\alpha} \cdot C_{\dot{\alpha}}$



integrate to obtain $\ddot{\alpha} = \delta$
(less $C_{L\alpha}$ and $C_{\dot{\alpha}}$ terms)



$$\frac{d}{dt} \begin{bmatrix} x \\ \alpha \\ \dot{\alpha} \end{bmatrix} = \begin{bmatrix} A & 0 & 0 \\ 0 & 0 & 1 \\ 0 & 0 & 0 \end{bmatrix} \begin{bmatrix} x \\ \alpha \\ \dot{\alpha} \end{bmatrix} + \begin{bmatrix} B \\ 0 \\ 1 \end{bmatrix} \ddot{\alpha}$$

$$y = \begin{bmatrix} C & C_{\alpha} & C_{\dot{\alpha}} \end{bmatrix} \begin{bmatrix} x \\ \alpha \\ \dot{\alpha} \end{bmatrix} + D\ddot{\alpha}$$

Transient dynamics modeled using ERA model

$$\dot{\alpha} \rightarrow (A, B, C, D) \rightarrow C_L$$



Summary of Methods



Method I

$$\frac{d}{dt} \begin{bmatrix} x \\ \alpha \\ \dot{\alpha} \end{bmatrix} = \begin{bmatrix} A & 0 & B \\ 0 & 0 & 1 \\ 0 & 0 & 0 \end{bmatrix} \begin{bmatrix} x \\ \alpha \\ \dot{\alpha} \end{bmatrix} + \begin{bmatrix} 0 \\ 0 \\ 1 \end{bmatrix} \ddot{\alpha}$$

$$y = \begin{bmatrix} C & C_\alpha & C_{\dot{\alpha}} \end{bmatrix} \begin{bmatrix} x \\ \alpha \\ \dot{\alpha} \end{bmatrix} + D\ddot{\alpha}$$

Method II

$$\frac{d}{dt} \begin{bmatrix} x \\ \alpha \\ \dot{\alpha} \end{bmatrix} = \begin{bmatrix} A & 0 & 0 \\ 0 & 0 & 1 \\ 0 & 0 & 0 \end{bmatrix} \begin{bmatrix} x \\ \alpha \\ \dot{\alpha} \end{bmatrix} + \begin{bmatrix} B \\ 0 \\ 1 \end{bmatrix} \ddot{\alpha}$$

$$y = \begin{bmatrix} C & C_\alpha & C_{\dot{\alpha}} \end{bmatrix} \begin{bmatrix} x \\ \alpha \\ \dot{\alpha} \end{bmatrix} + D\ddot{\alpha}$$

General procedure

1. Obtain time-resolved step response in pitch angle
2. Identify some or all of the quasi-steady and added mass parameters $C_{L_\alpha}, C_{\dot{\alpha}}, C_{\ddot{\alpha}}$
3. Model remaining transient dynamic with Eigensystem realization algorithm (**ERA**)

ERA was recently shown to be equivalent to balanced proper orthogonal decomposition (BPOD)

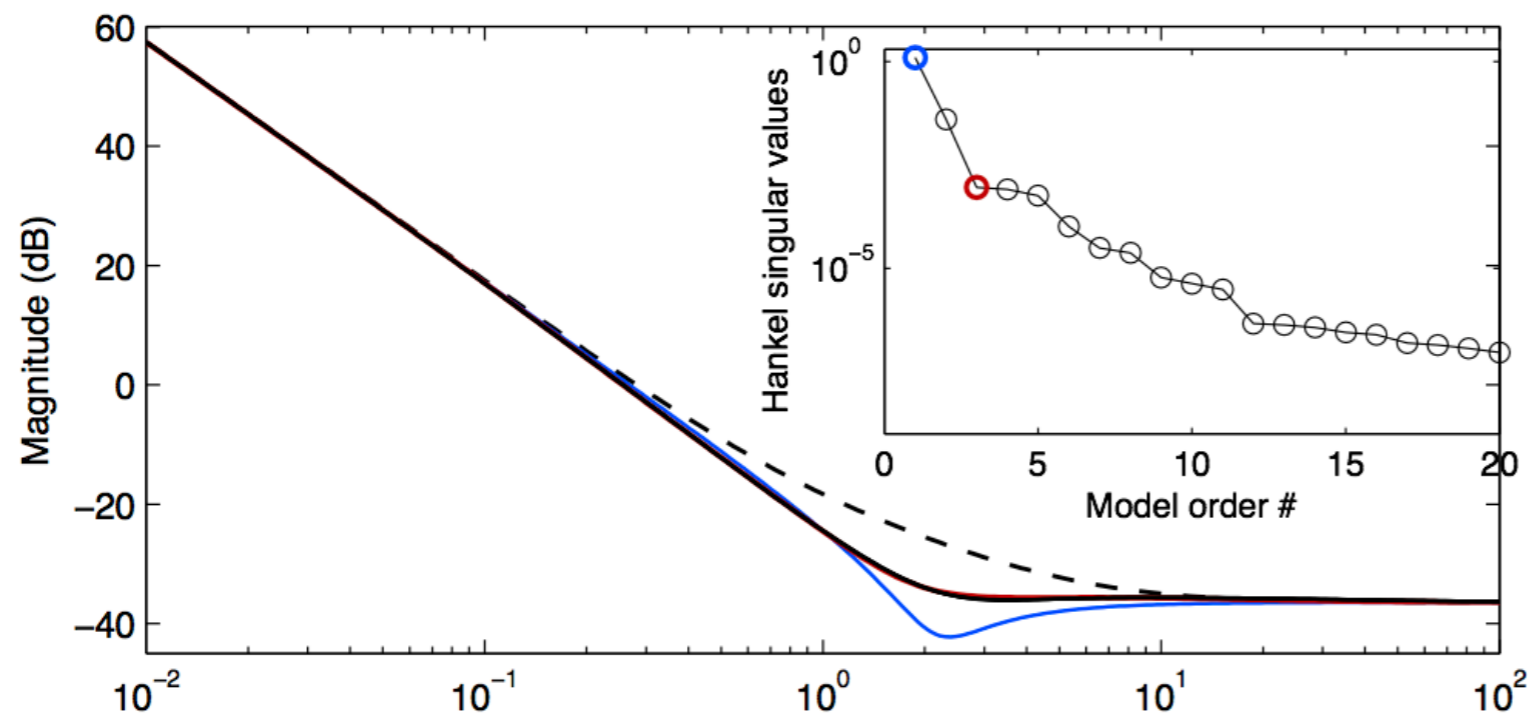
Ma, Ahuja, & Rowley (2011)

Highly flexible

1. Extensions for pitch, plunge, and surge motions
2. Multiple input, multiple output models possible with ERA



Bode Plot - Pitch (LE)

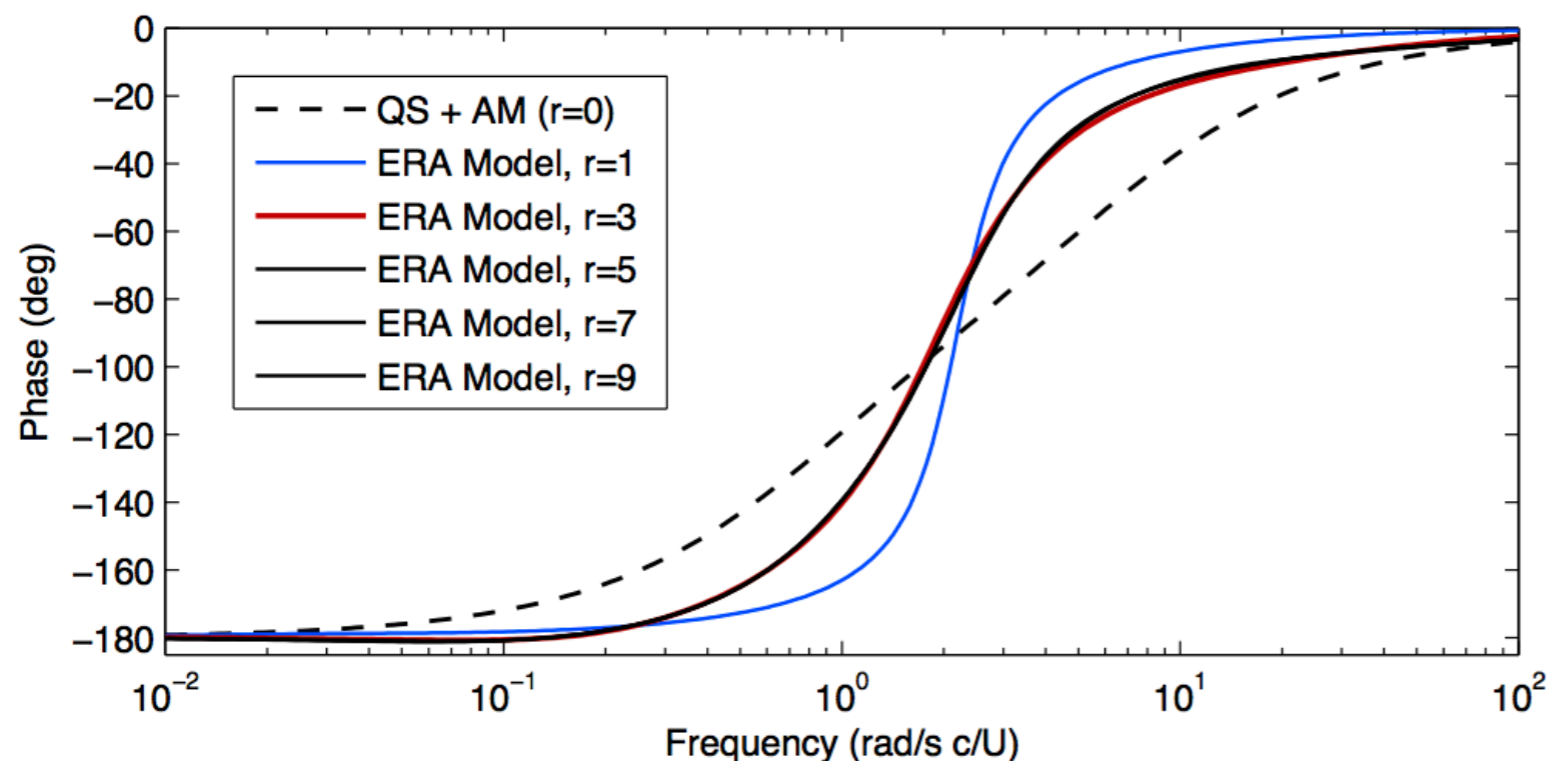


Frequency response

input is $\ddot{\alpha}$ (α is angle of attack)

output is lift coefficient C_L

Pitching at leading edge



Model without additional dynamics [QS+AM (r=0)] is inaccurate in crossover region

Models with fast dynamics of ERA model order >3 are converged

Punchline: additional fast dynamics (ERA model) are essential

Brunton and Rowley, in preparation.



Bode Plot - Pitch (QC)



Frequency response

input is $\ddot{\alpha}$ (α is angle of attack)

output is lift coefficient C_L

Pitching at quarter chord

Reduced order model with ERA $r=7$
accurately reproduces Indicial Response

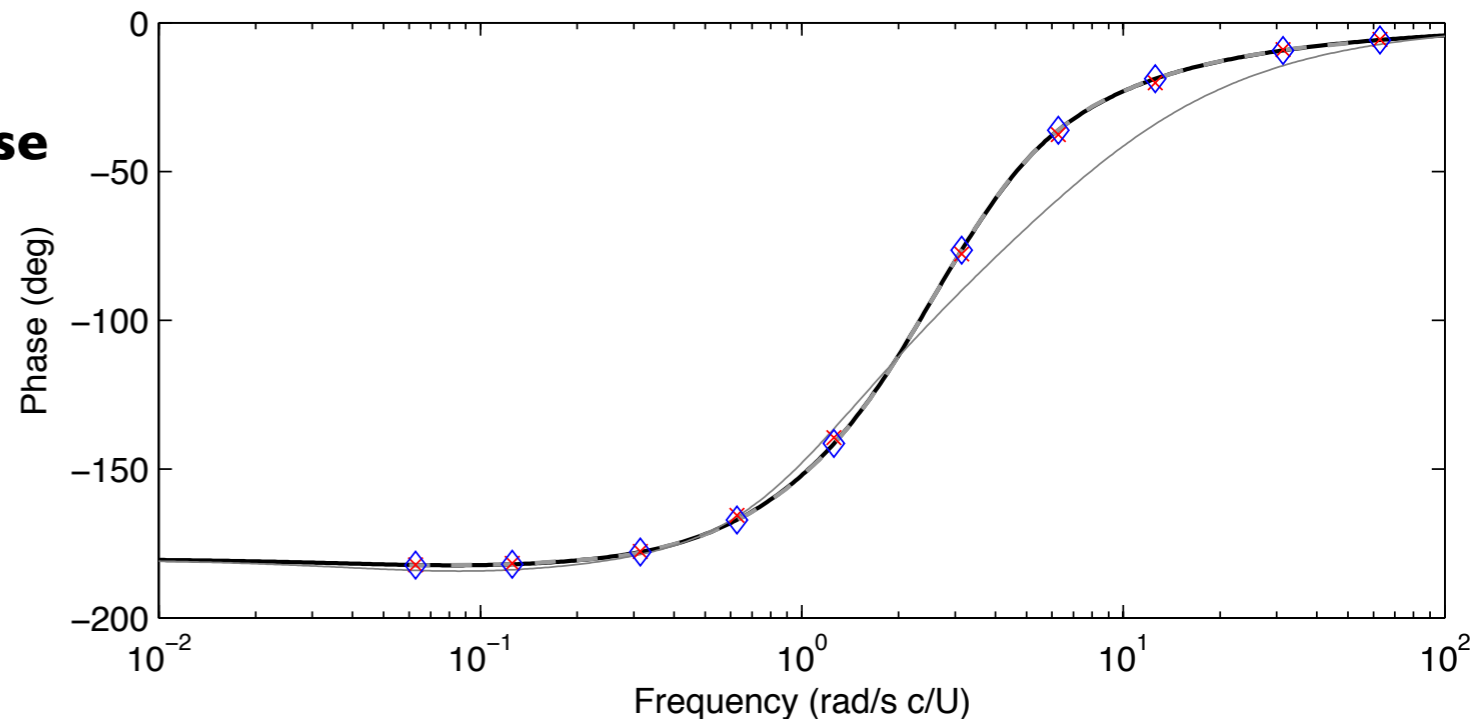
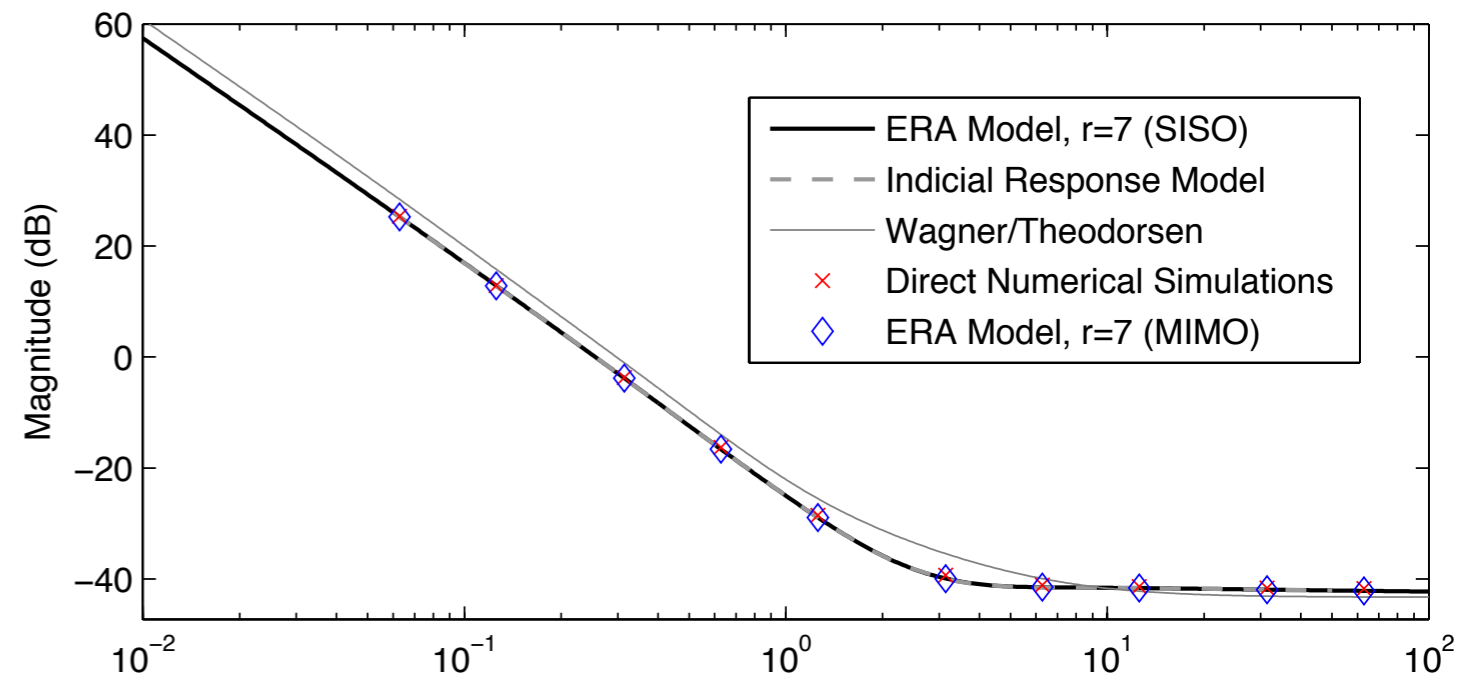
Indicial Response and model agree better with
DNS than Theodorsen's model.

Asymptotes are correct for Indicial Response
because it is based on simulations

Model for pitch/plunge dynamics
[ERA, $r=7$ (MIMO)] works as well,
for the same order model

Brunton and Rowley, *in preparation*.

Quarter-Chord Pitching

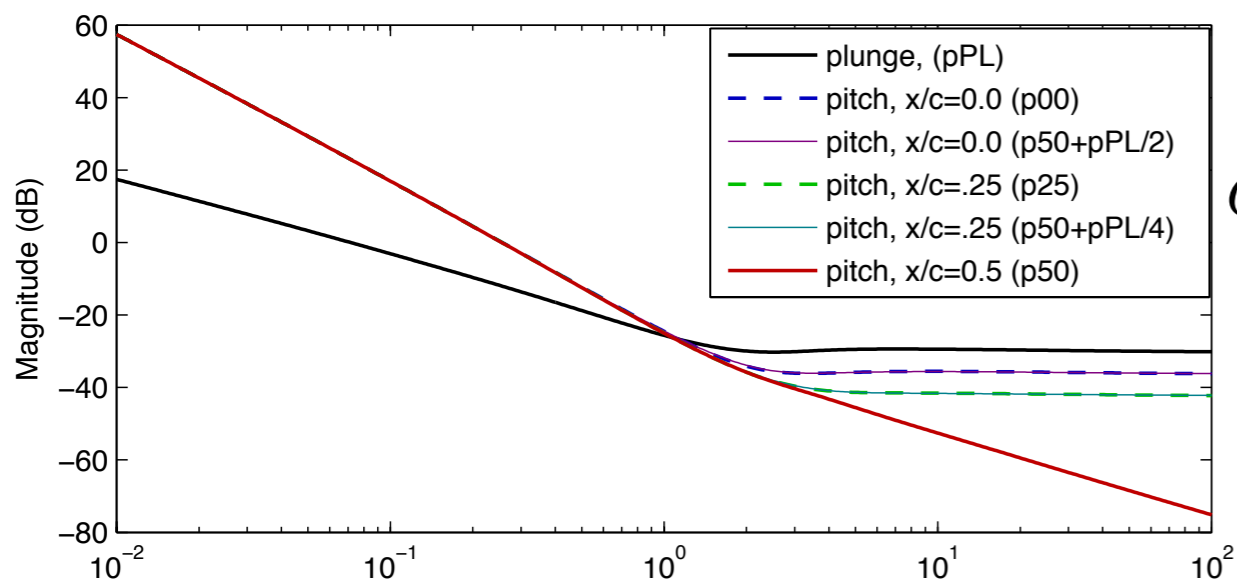




Parametrized by Pitch Point



$$\frac{d}{dt} \begin{bmatrix} \mathbf{x} \\ \alpha \\ \dot{\alpha} \\ \dot{h} \end{bmatrix} = \begin{bmatrix} A & 0 & 0 & 0 \\ 0 & 0 & 1 & 0 \\ 0 & 0 & 0 & 0 \\ 0 & 0 & 0 & 0 \end{bmatrix} \begin{bmatrix} \mathbf{x} \\ \alpha \\ \dot{\alpha} \\ \dot{h} \end{bmatrix} + \begin{bmatrix} B_1 & -\frac{a}{2}B_2 & B_2 \\ 0 & 0 & 0 \\ 1 & 0 & 0 \\ -\frac{a}{2} & 0 & 1 \end{bmatrix} \begin{bmatrix} \ddot{\alpha} \\ \ddot{h} \end{bmatrix}$$



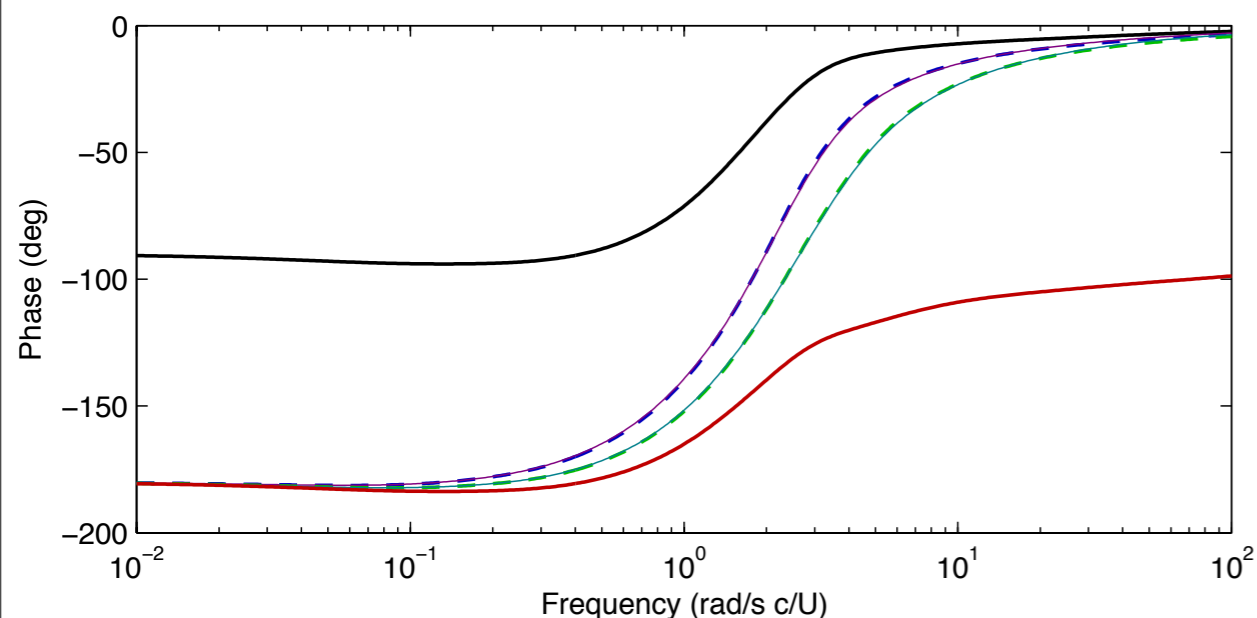
$$C_L = \begin{bmatrix} C & C_\alpha & C_{\dot{\alpha}} & C_{\dot{h}} \end{bmatrix} \begin{bmatrix} \mathbf{x} \\ \alpha \\ \dot{\alpha} \\ \dot{h} \end{bmatrix} + \begin{bmatrix} C_{\ddot{\alpha}} & -\frac{a}{2}C_{\ddot{h}} & C_{\ddot{h}} \end{bmatrix} \begin{bmatrix} \ddot{\alpha} \\ \ddot{h} \end{bmatrix}$$

(A, B_1, C) **model for pitch at mid-chord**

(A, B_2, C) **model for plunge**

Pitch about any point is linear combination of pitch at mid-chord and plunge motion

Models all have same poles, different zeros (similar to Theodorsen's model)

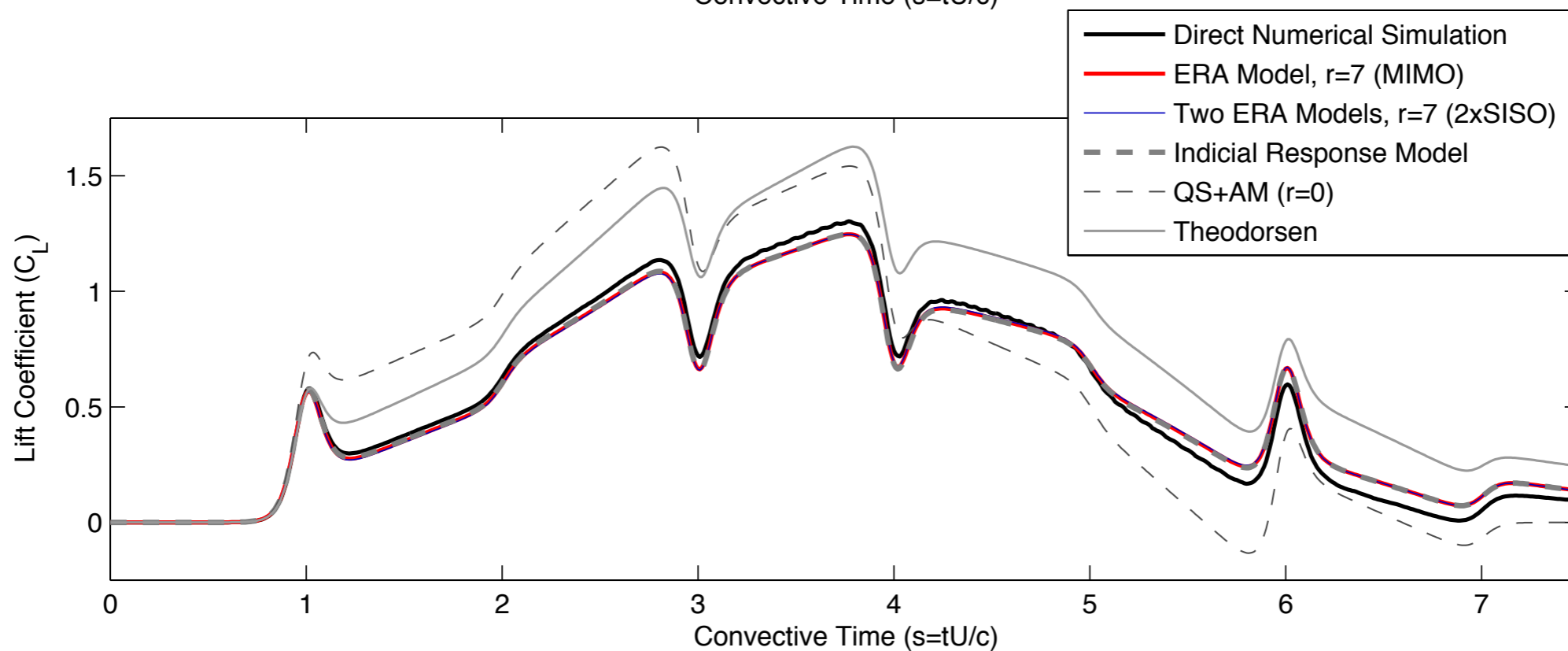
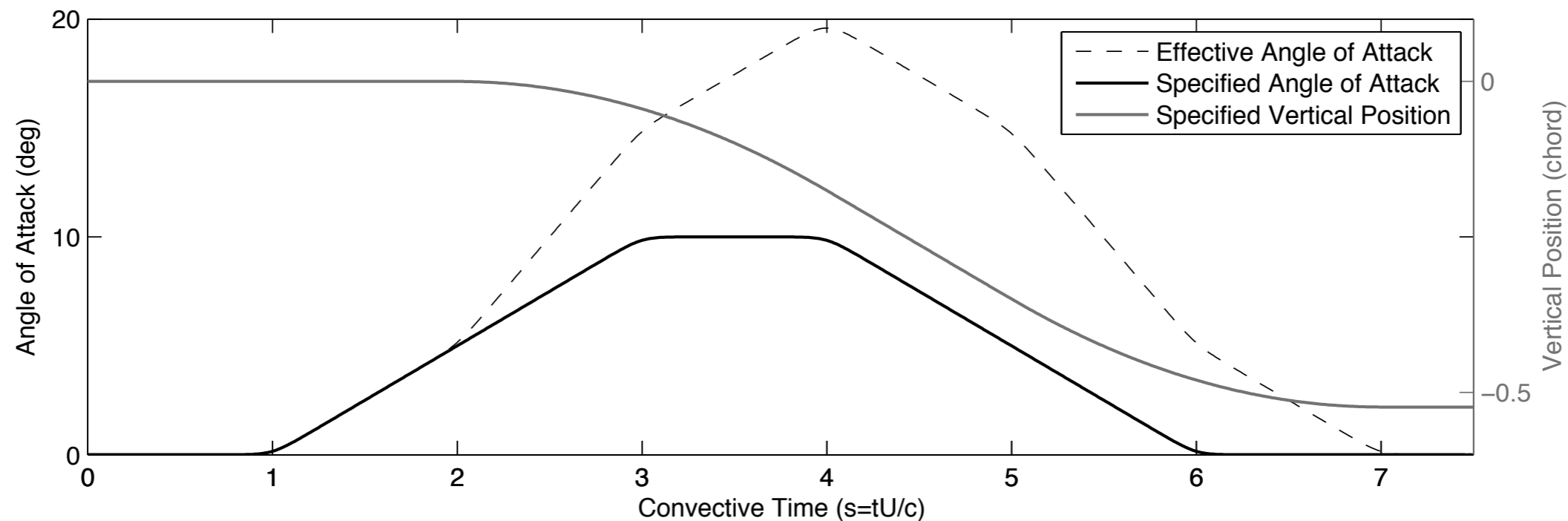




Pitch/Plunge Maneuver



Canonical pitch-up, hold, pitch-down maneuver, followed by step-down in vertical position

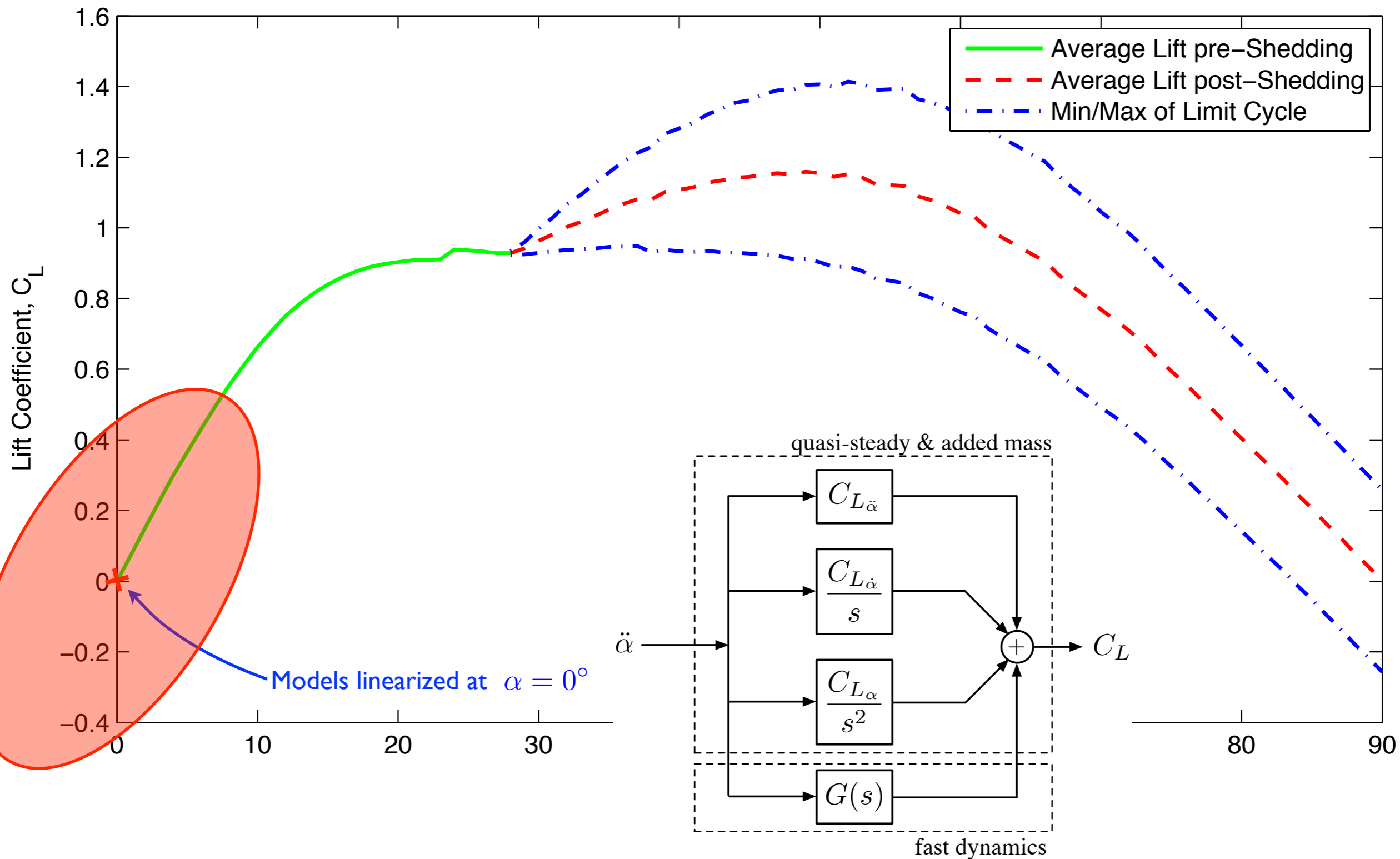


OL, Altman, Eldredge, Garmann, and Lian, 2010
Brunton and Rowley, *in preparation*.

**Reduced order model accurately captures
lift coefficient history from DNS**

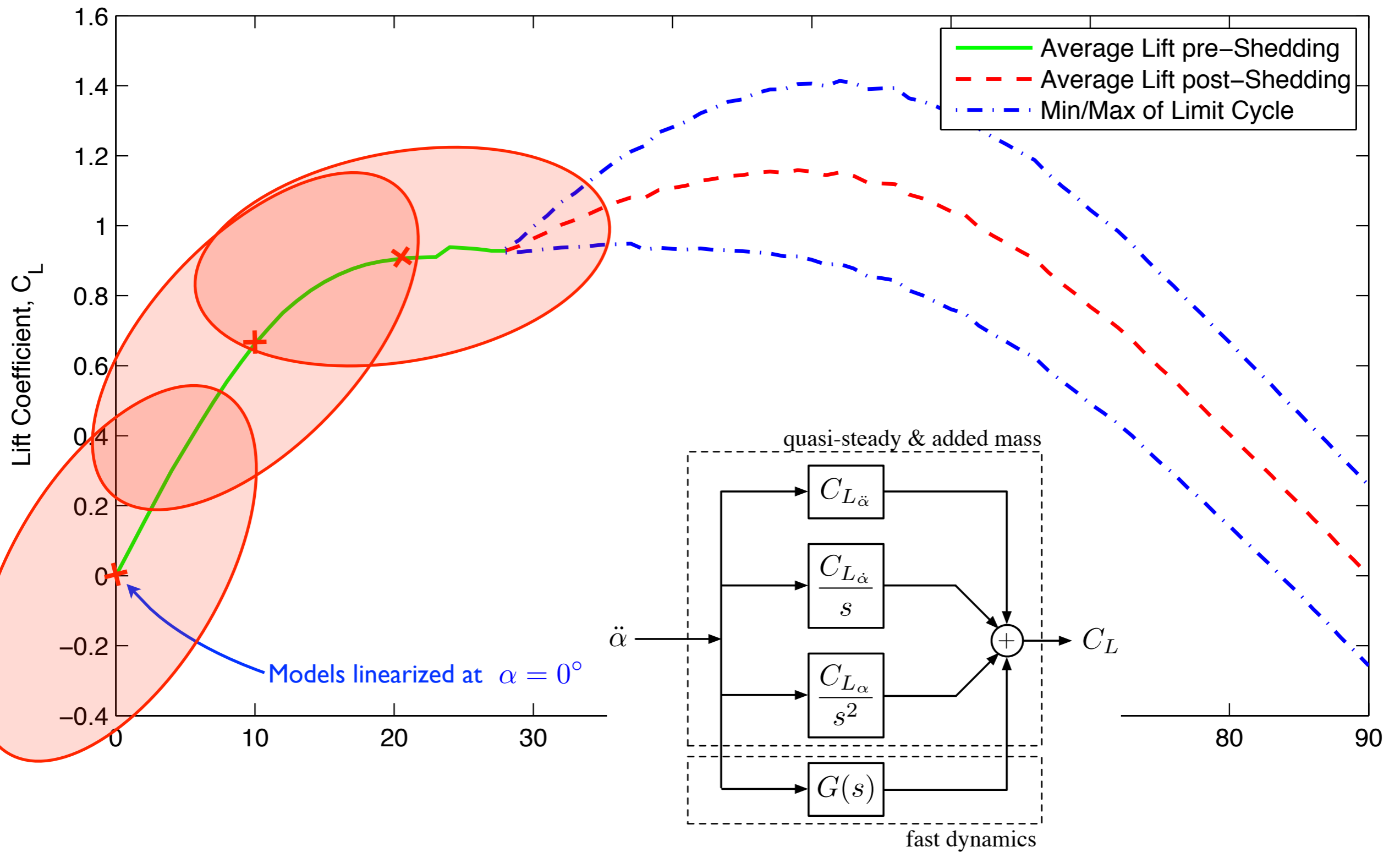


Lift vs. Angle of Attack





Lift vs. Angle of Attack





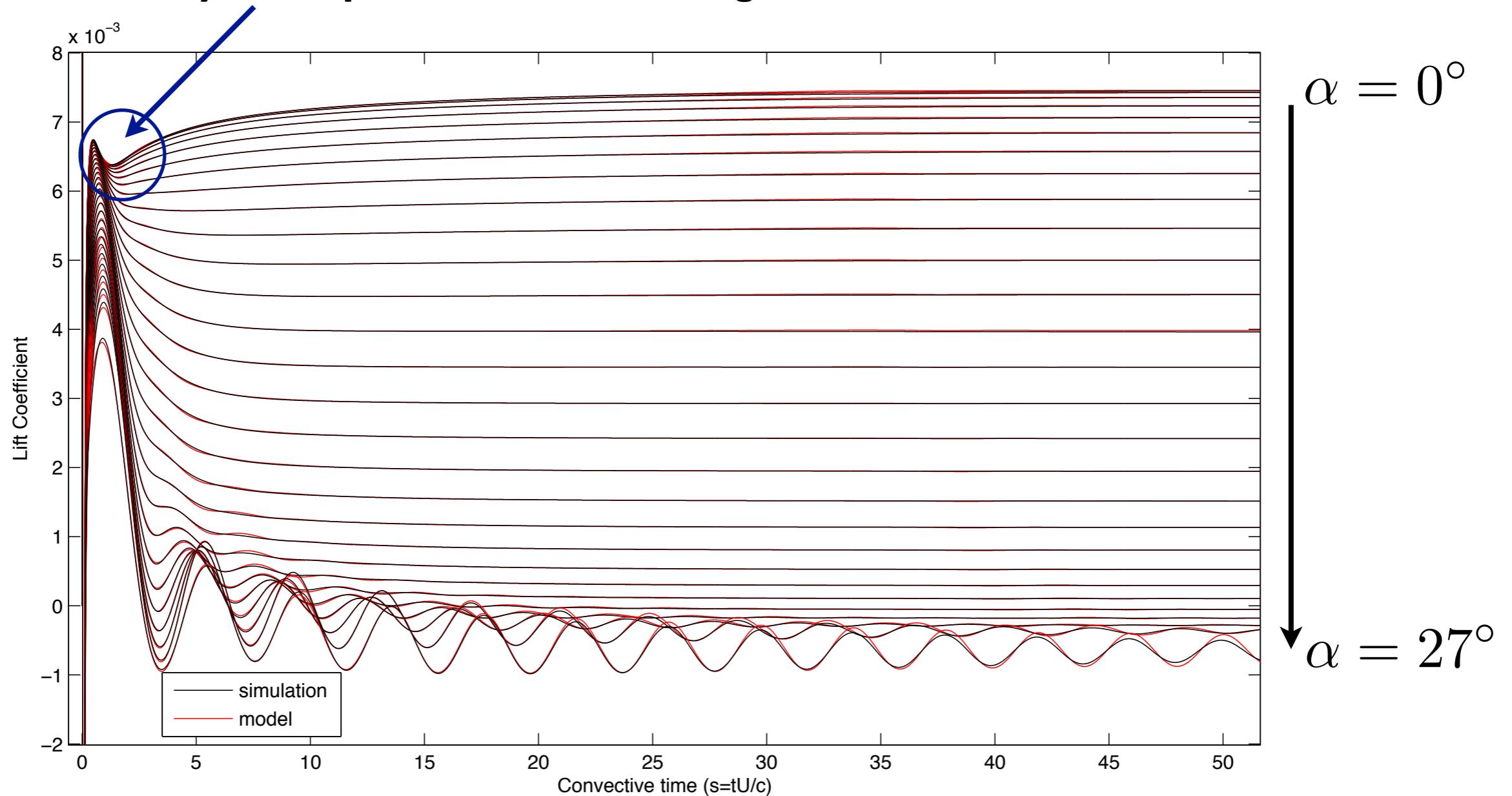
Models at various angle of attack



Impulse response simulations after rapid step-up $\alpha \in [0^\circ, 27^\circ]$

Initial lift $C_L(\alpha_0)$ **subtracted off**

Model with order $r=7$ required to capture this flow feature, eventually develops into vortex shedding mode





Bode Plot of ERA Models

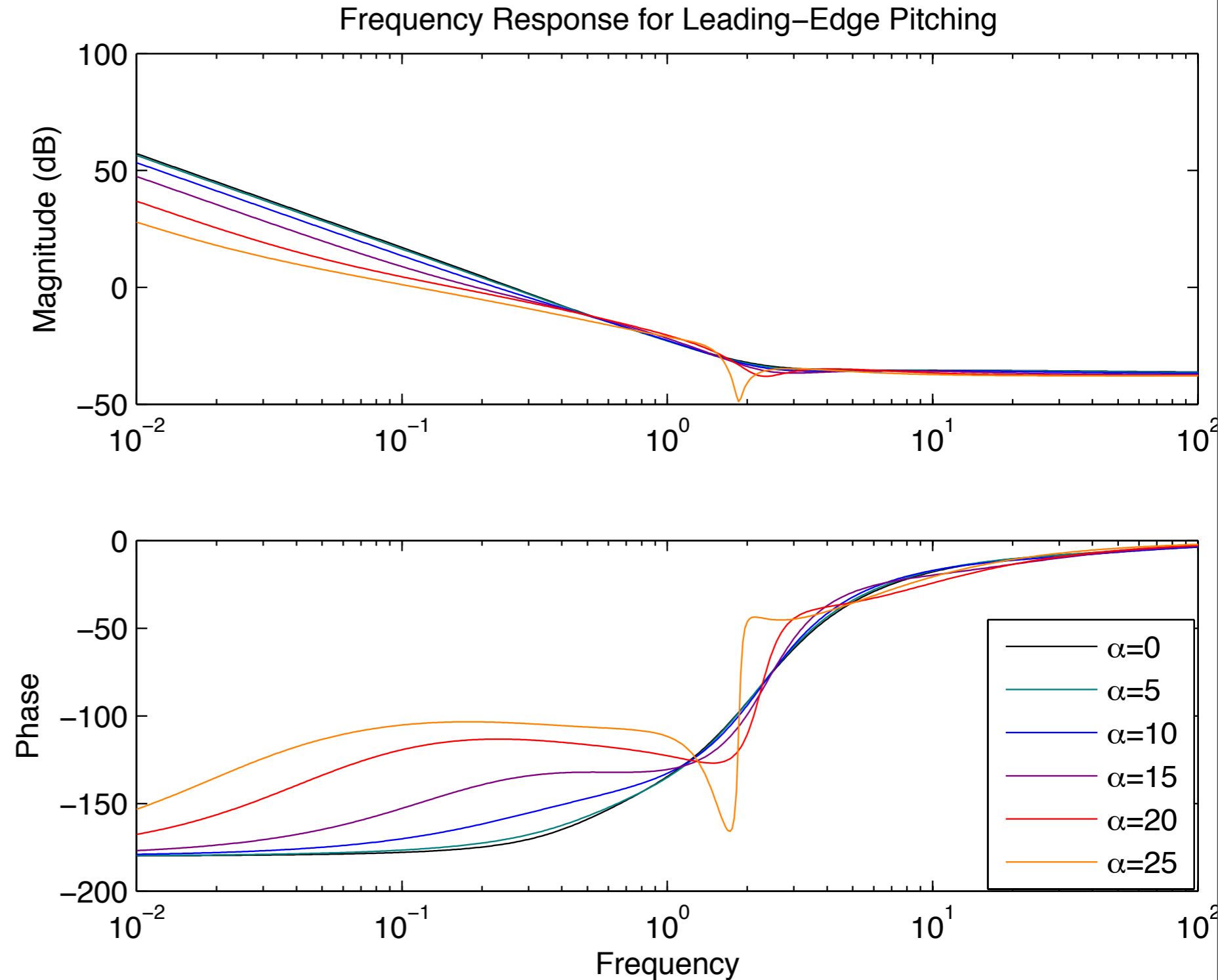


Results

Lift slope decreases for increasing angle of attack, so magnitude of low frequency motions decreases for increasing angle of attack.

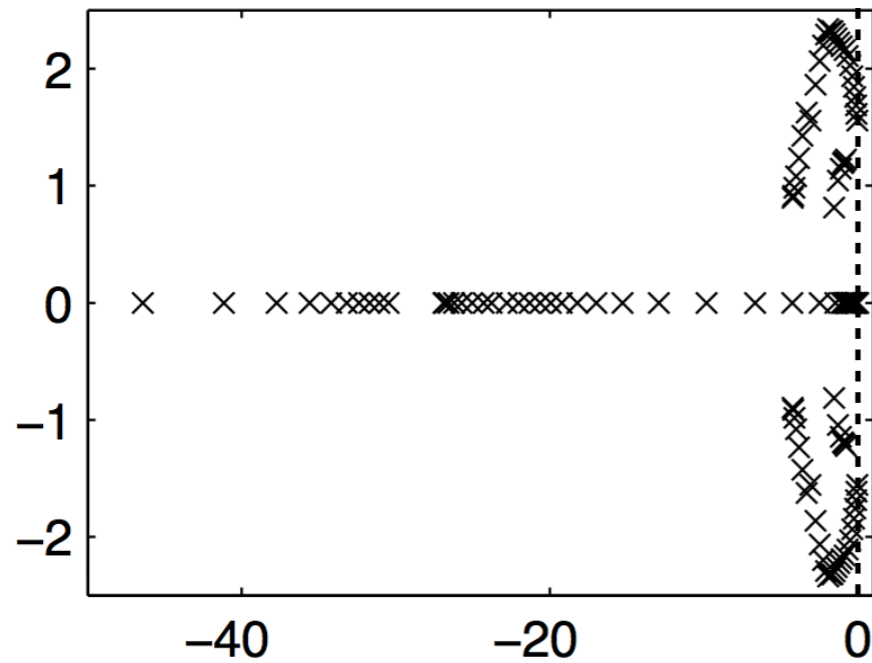
At larger angle of attack, phase converges to -180 at much lower frequencies. I.e., solutions take longer to reach equilibrium in time domain.

Consistent with fact that for large angle of attack, system is closer to Hopf instability, and a pair of eigenvalues are moving closer to imaginary axis.

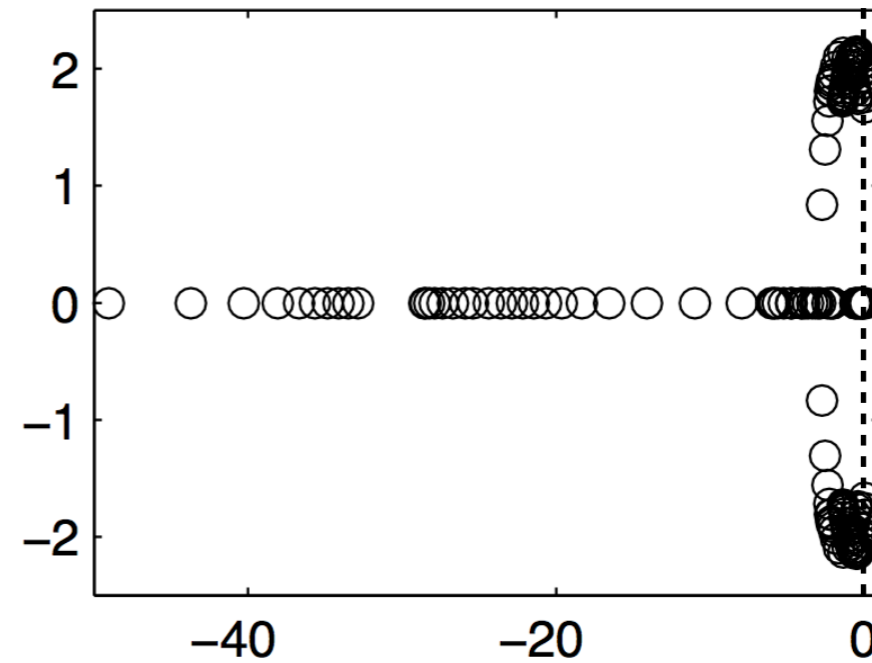




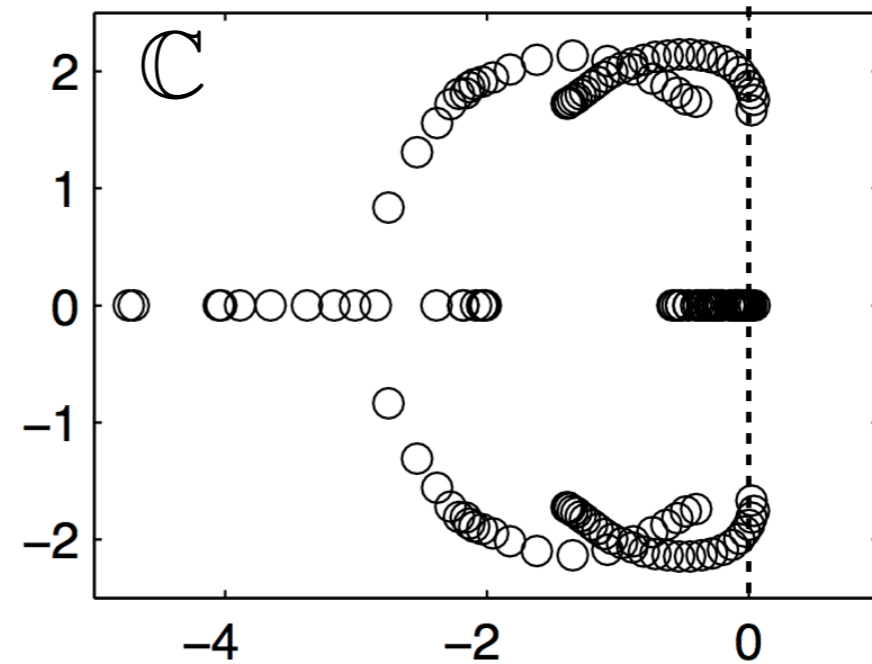
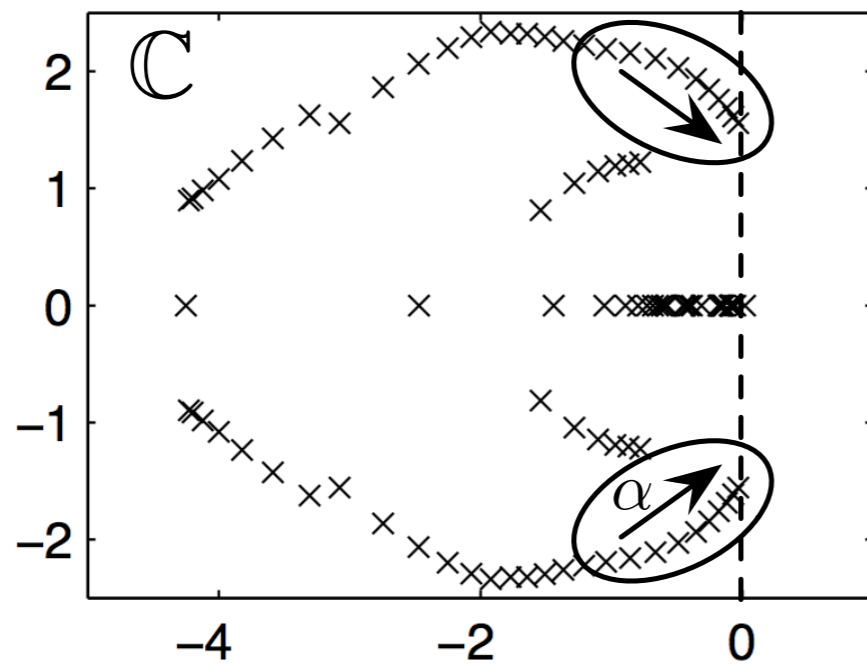
Poles and Zeros of ERA Models



Poles



Zeros

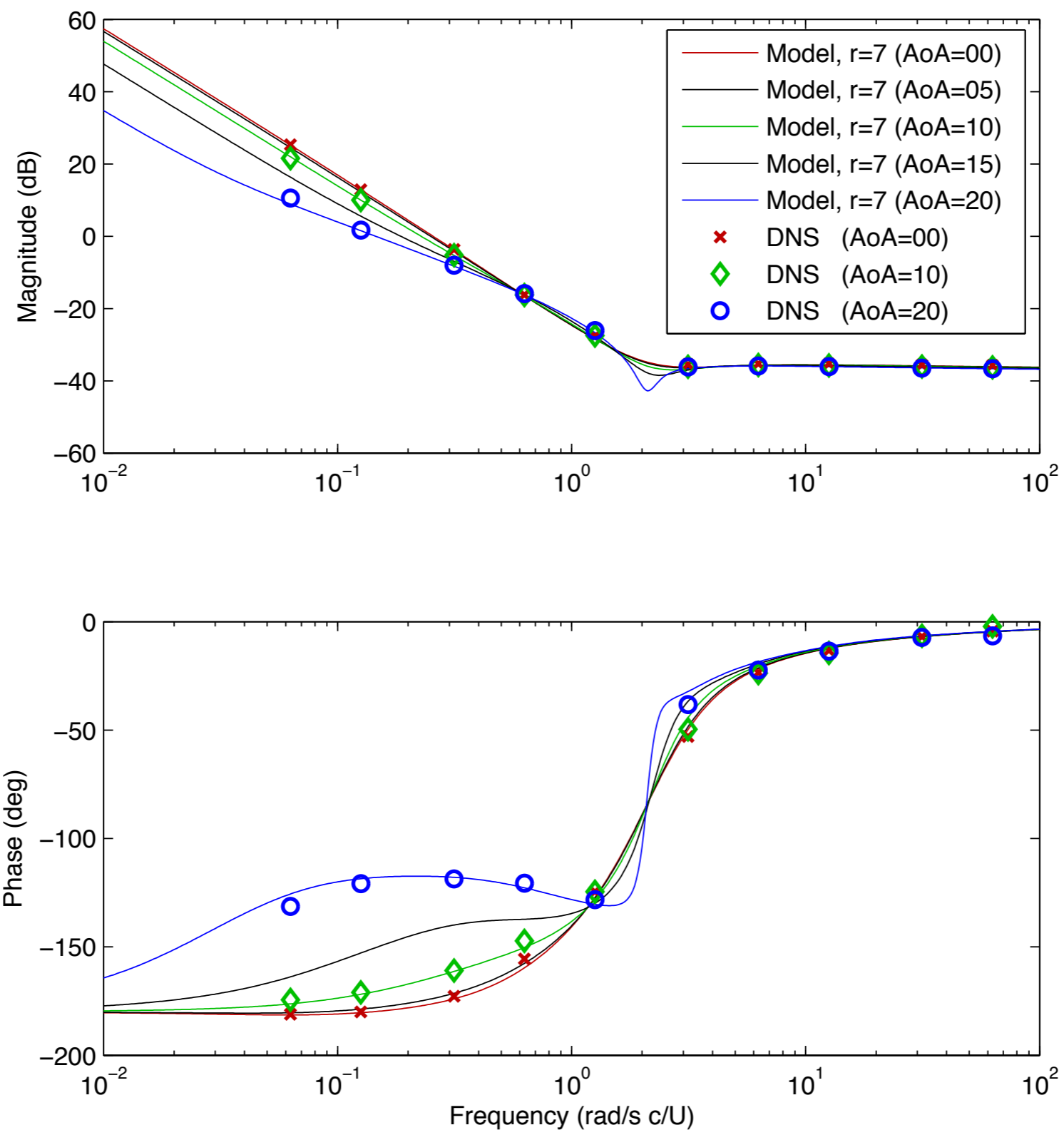


As angle of attack increases, pair of poles (and pair of zeros) march towards imaginary axis.

This is a good thing, because a Hopf bifurcation occurs at $\alpha_{crit} \approx 28^\circ$



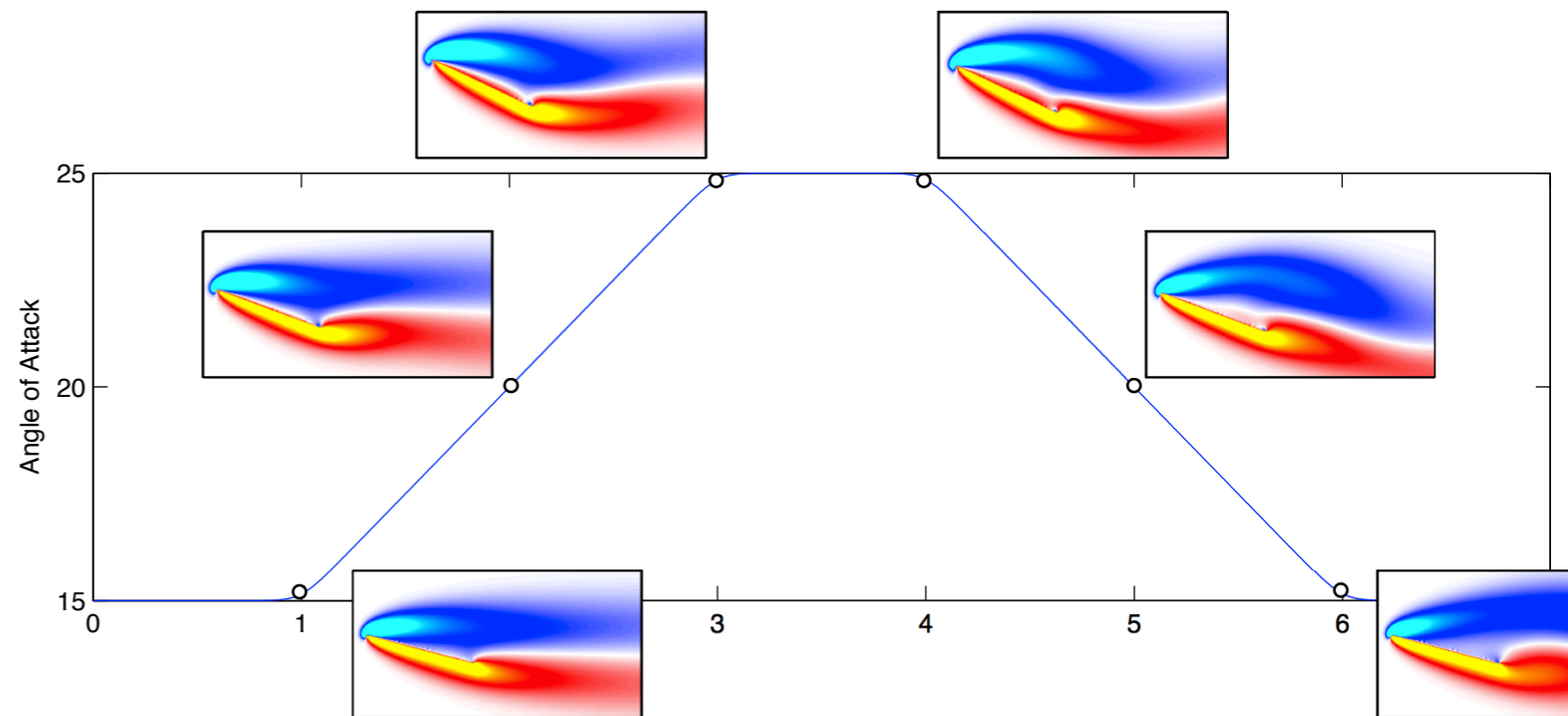
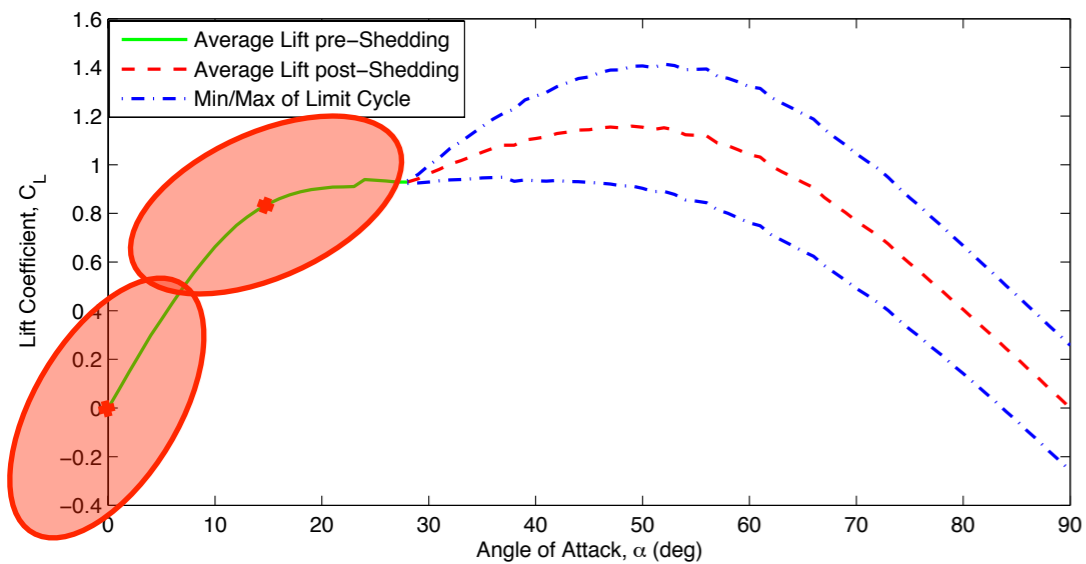
Bode Plot of Model (-) vs Data (x)



Direct numerical simulation confirms that local linearized models are accurate for small amplitude sinusoidal maneuvers



Large Amplitude Maneuver

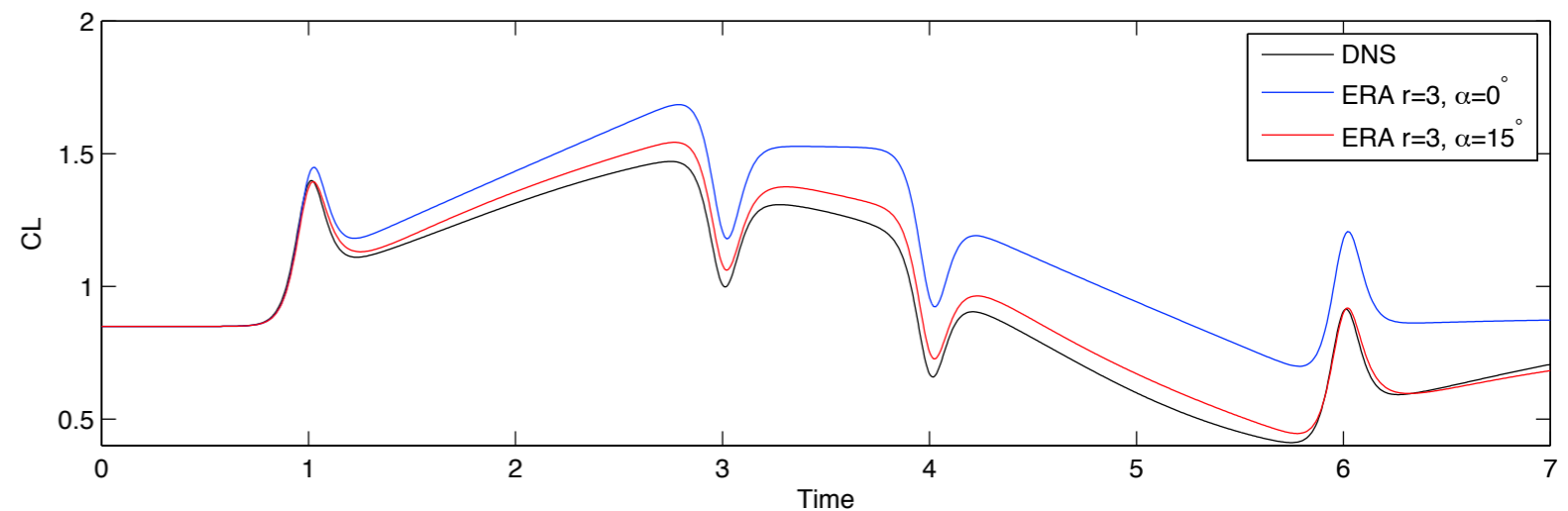


Compare models linearized at

$$\alpha = 0^\circ \quad \text{and} \quad \alpha = 15^\circ$$

For pitching maneuver with

$$\alpha \in [15^\circ, 25^\circ]$$



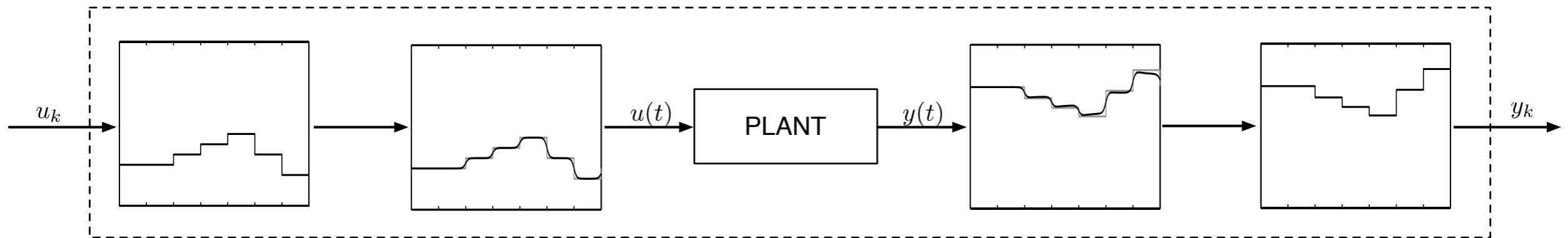
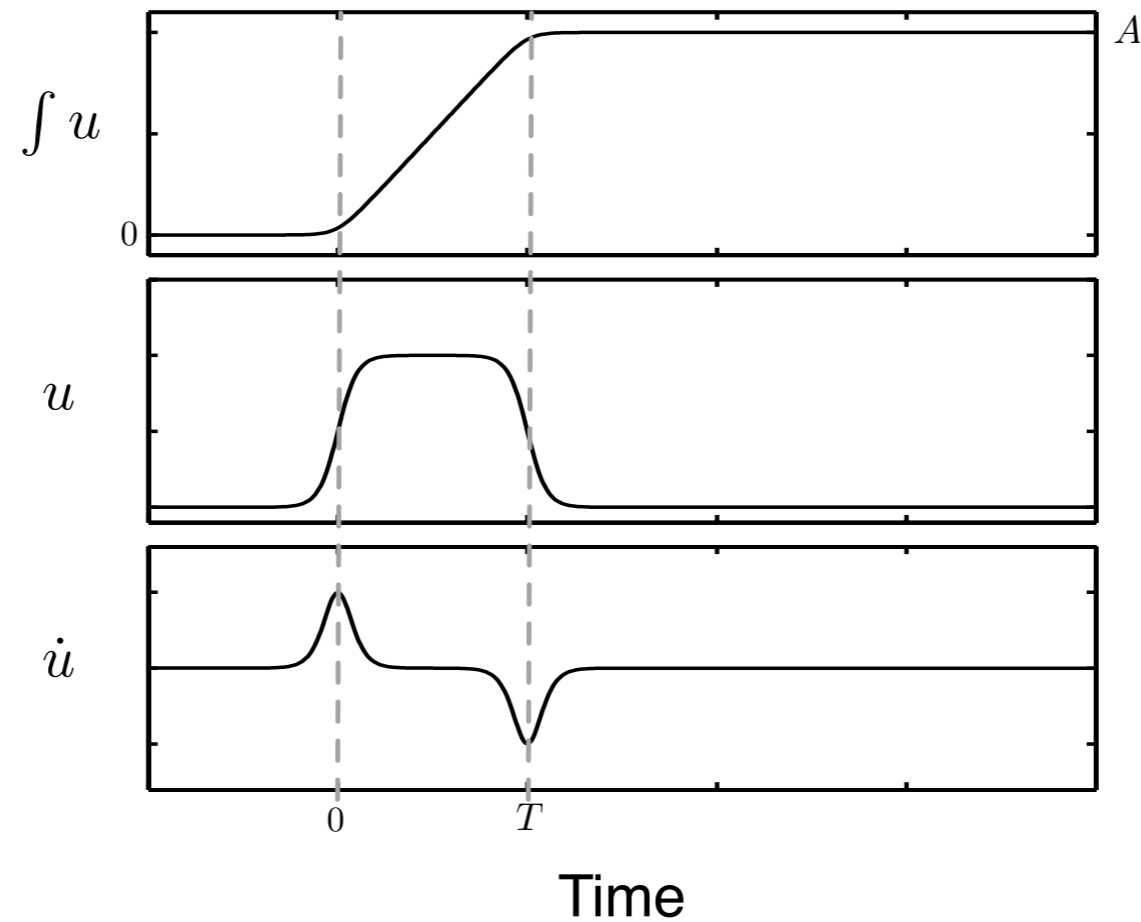
Maneuver:

$$G(t) = \log \left[\frac{\cosh(a(t - t_1)) \cosh(a(t - t_4))}{\cosh(a(t - t_2)) \cosh(a(t - t_3))} \right]$$

$$\alpha(t) = \alpha_0 + \alpha_{\max} \frac{G(t)}{\max(G(t))}$$



(Indicial) Step Response

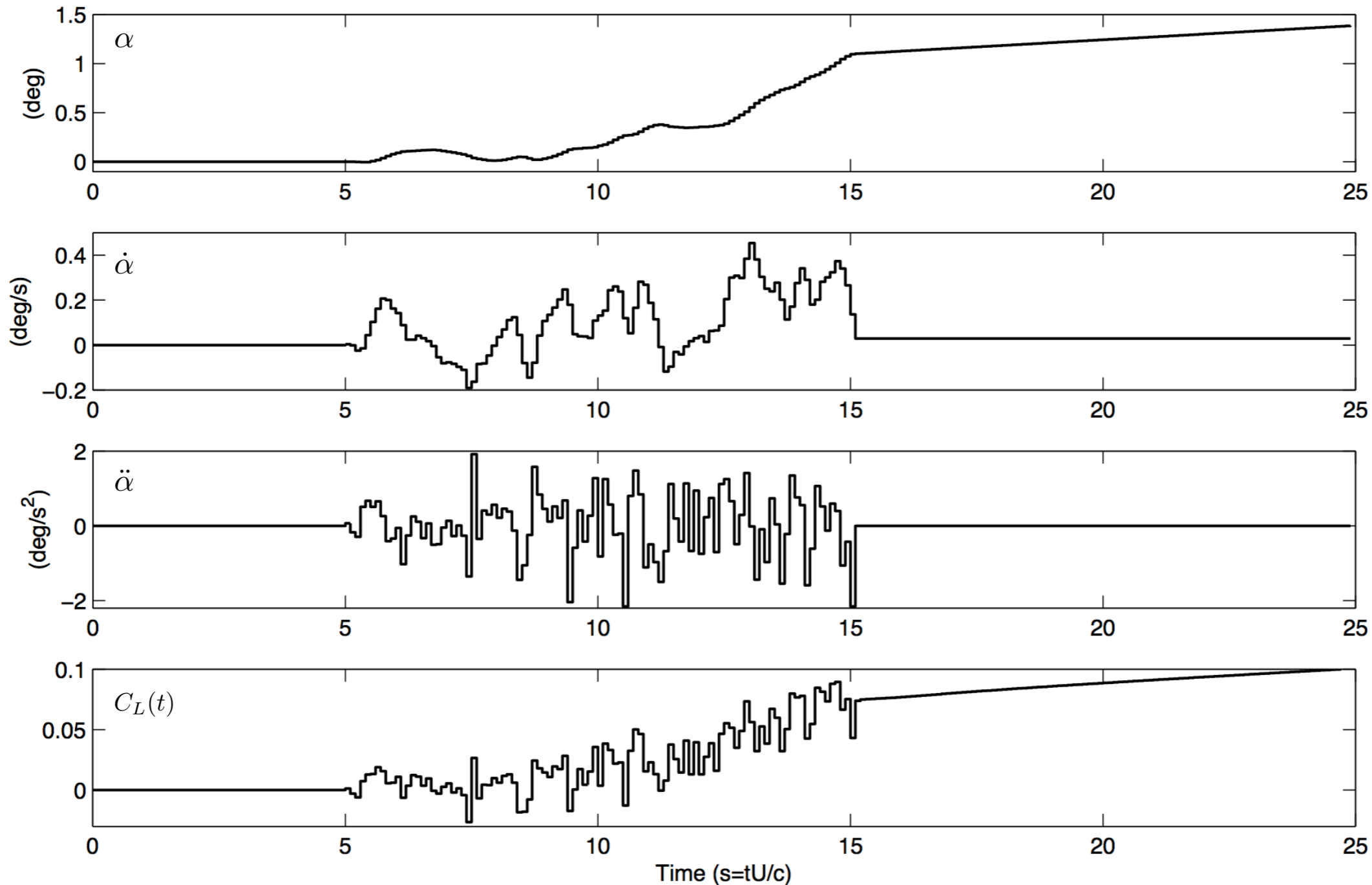


Previously, models are based on aerodynamic step response

Idea: Perform realistic maneuver for some time, back out the Markov parameters, and construct ERA model.



Random Input Maneuver

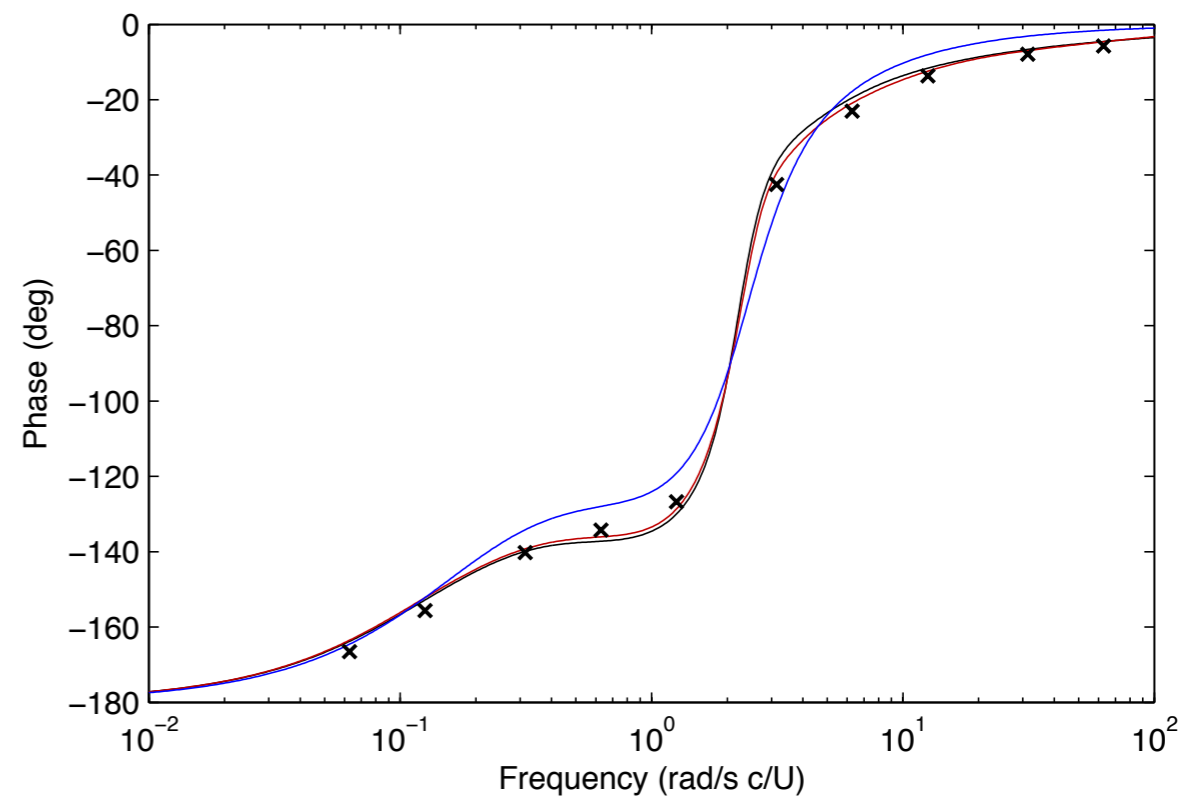
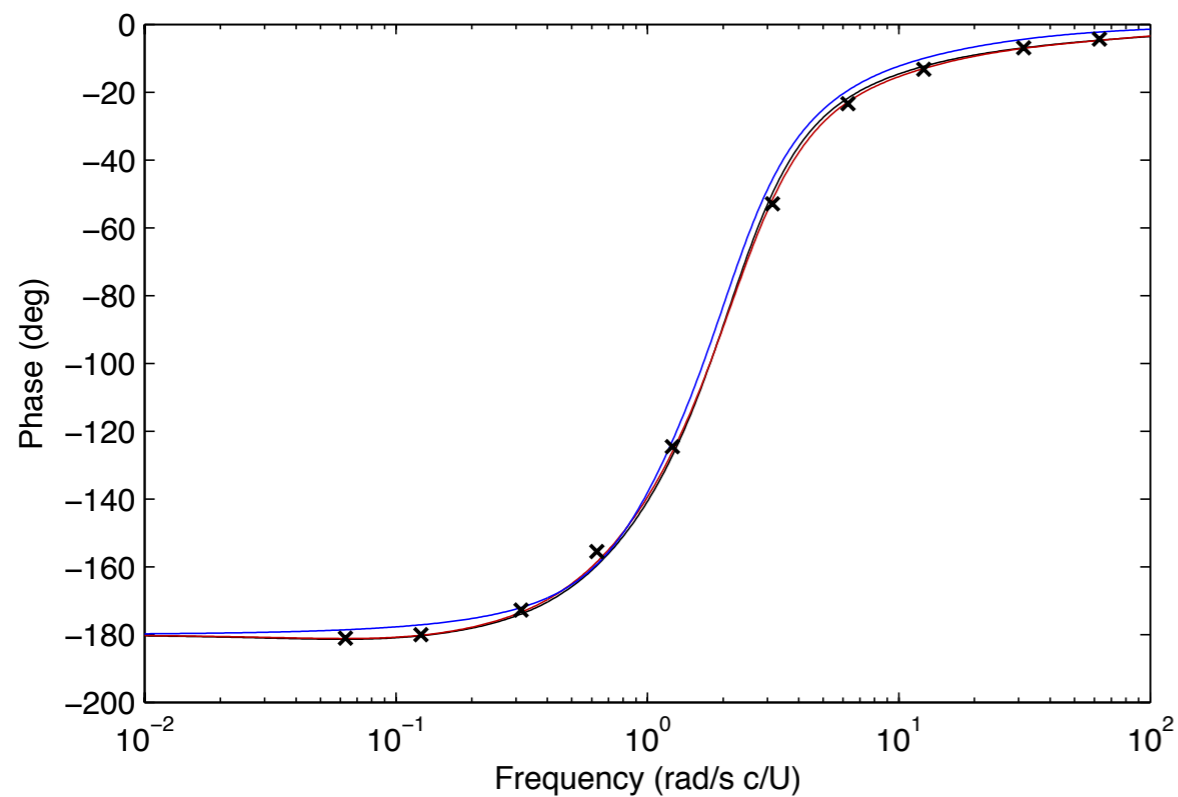
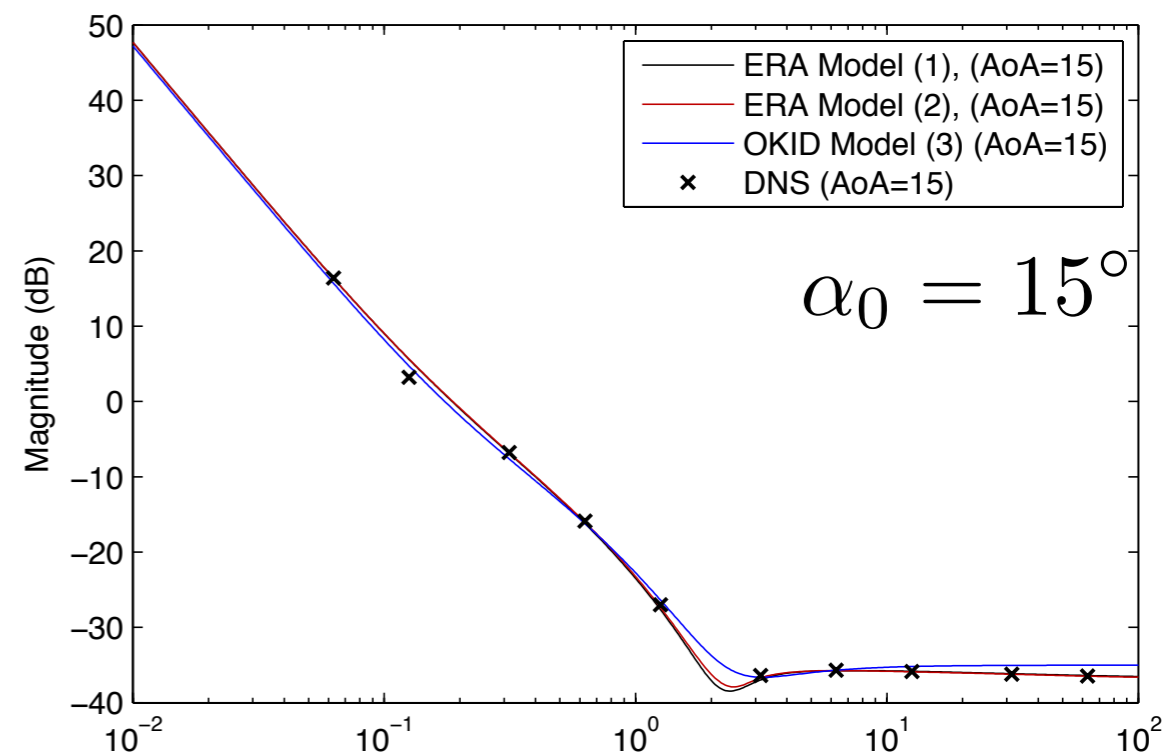
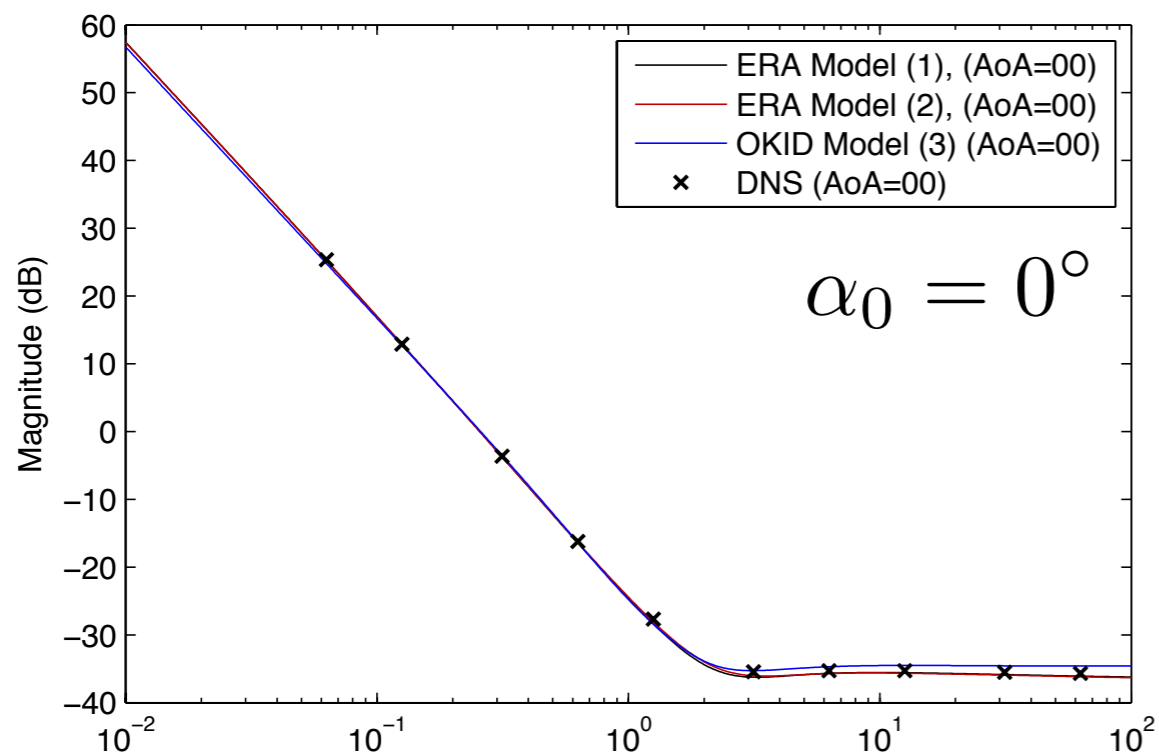


Observer/Kalman filter identification (OKID) works best, so far.

Idea: Perform realistic maneuver for some time, back out the Markov parameters, and construct ERA model.

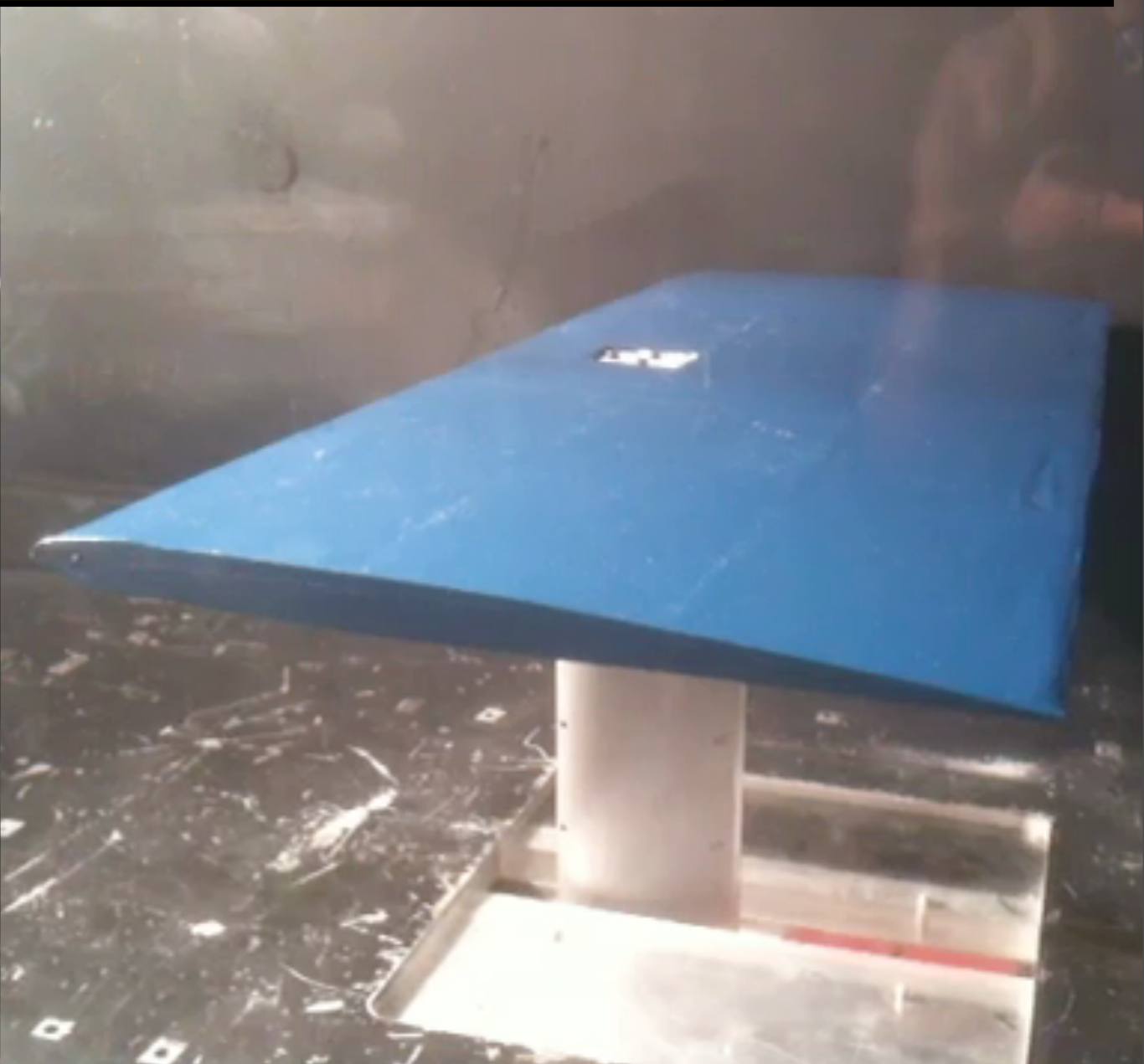


Comparison of Methods





Wind Tunnel Experiments



Andrew Fejer Unsteady Flow Wind Tunnel
Principle Investigator - Dave Williams

NACA 0006 Airfoil

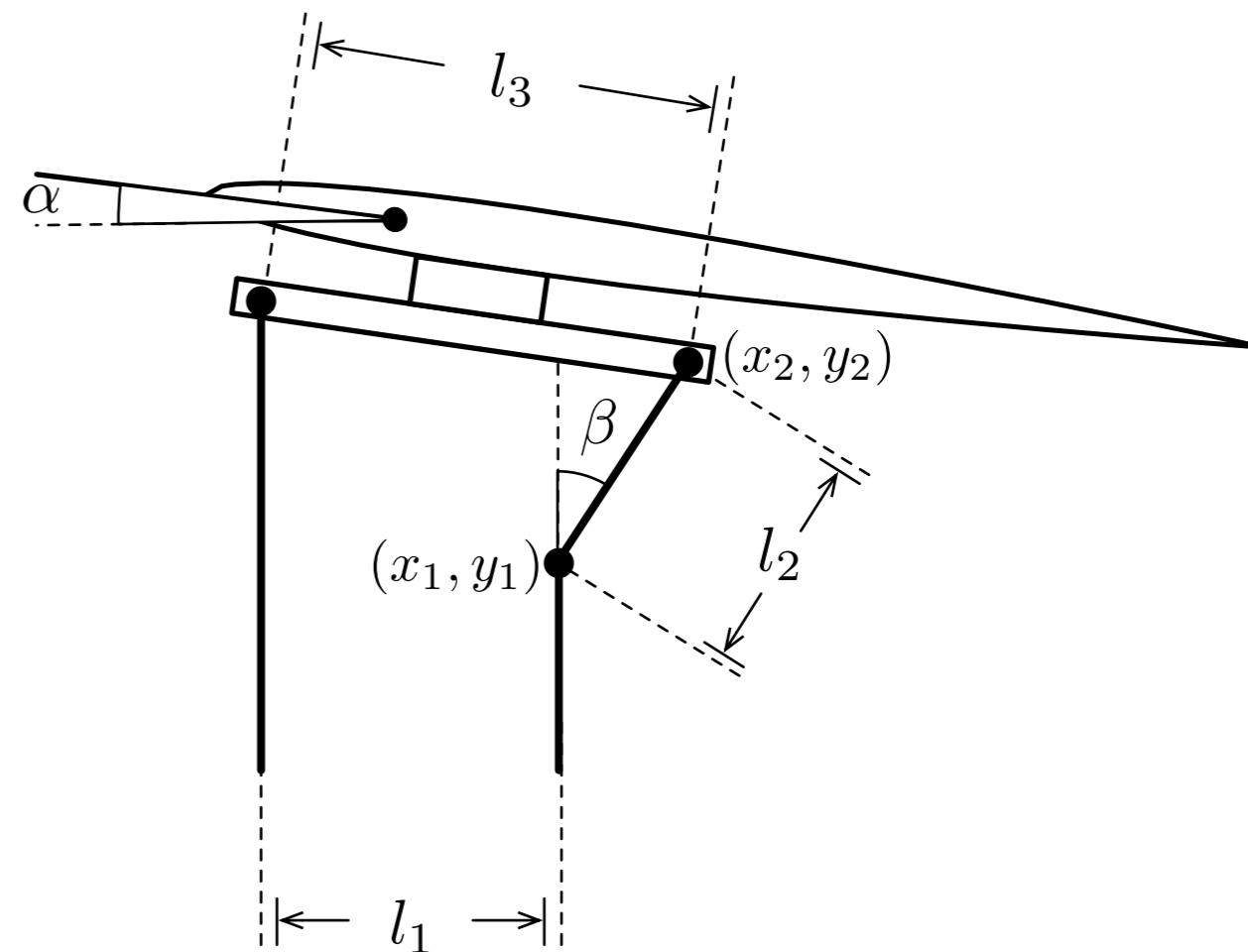
Chord Length: 0.246 m

Free Stream Velocity: 4.00 m/s

Reynolds Number: 65,000



NACA 0006 Model



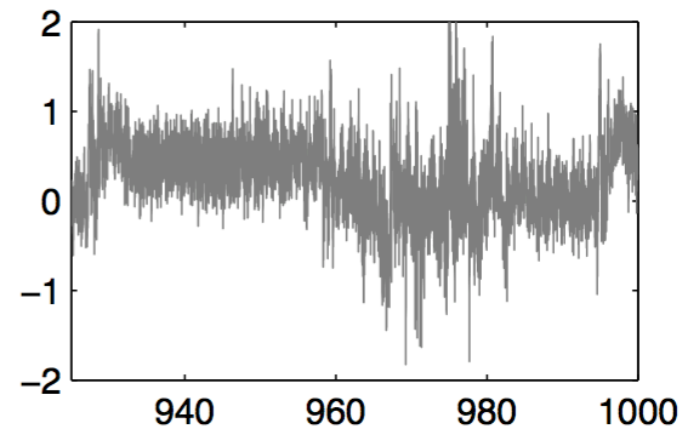
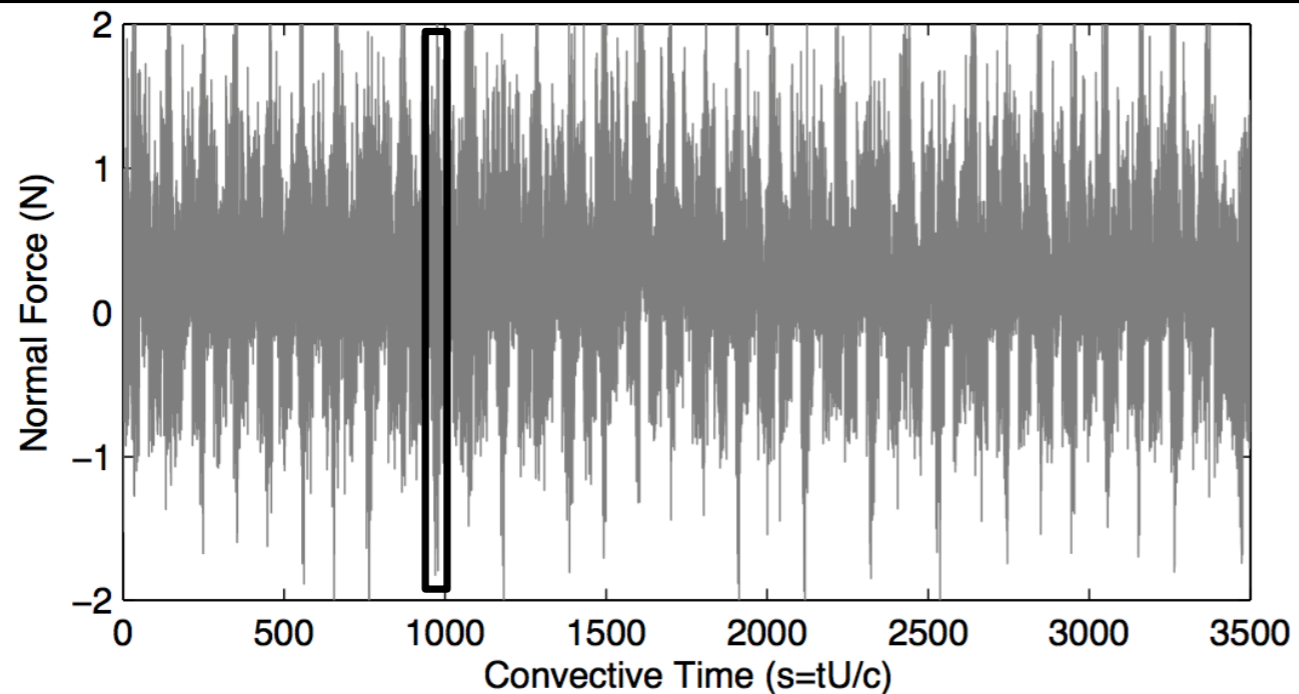
Summary

1. Account for hinge constraint nonlinearity
2. Rotate force vectors to obtain lift force
3. Subtract out point mass effects (mechanical)

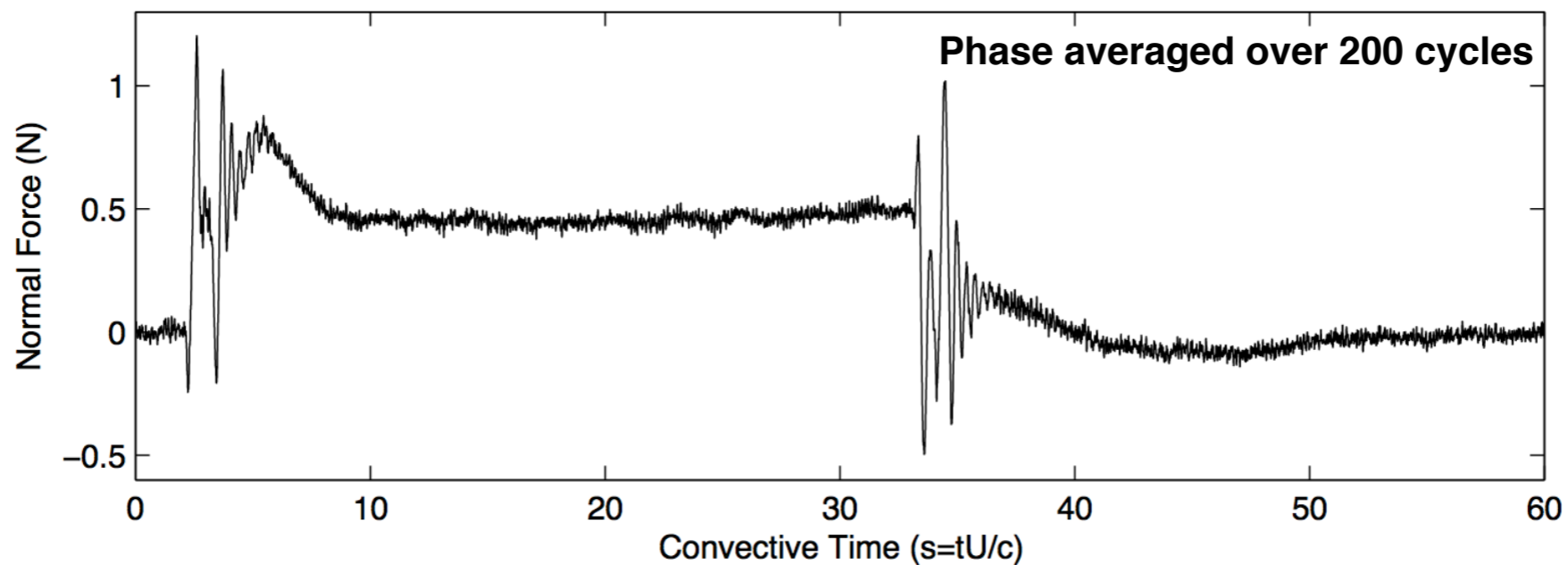
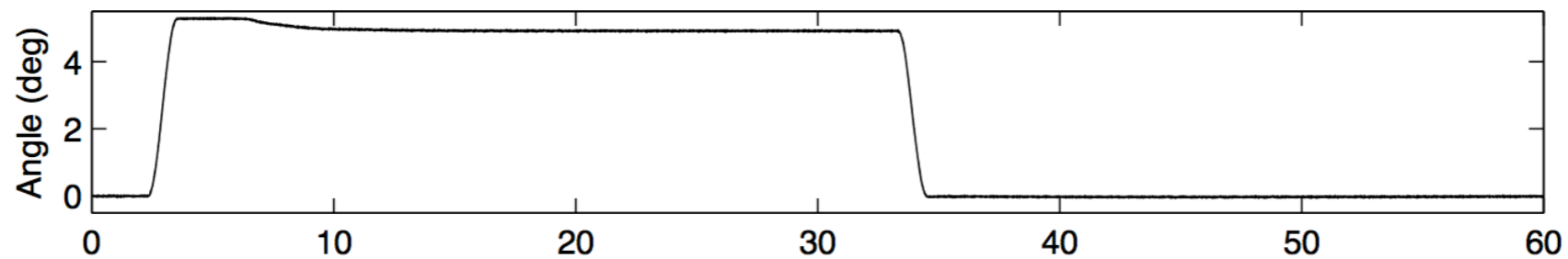
$$\begin{bmatrix} L \\ D \end{bmatrix} = \underbrace{\begin{bmatrix} \cos(\alpha) & -\sin(\alpha) \\ \sin(\alpha) & \cos(\alpha) \end{bmatrix}}_{R_\alpha} \begin{bmatrix} N \\ P \end{bmatrix}$$



Phase Averaged Data

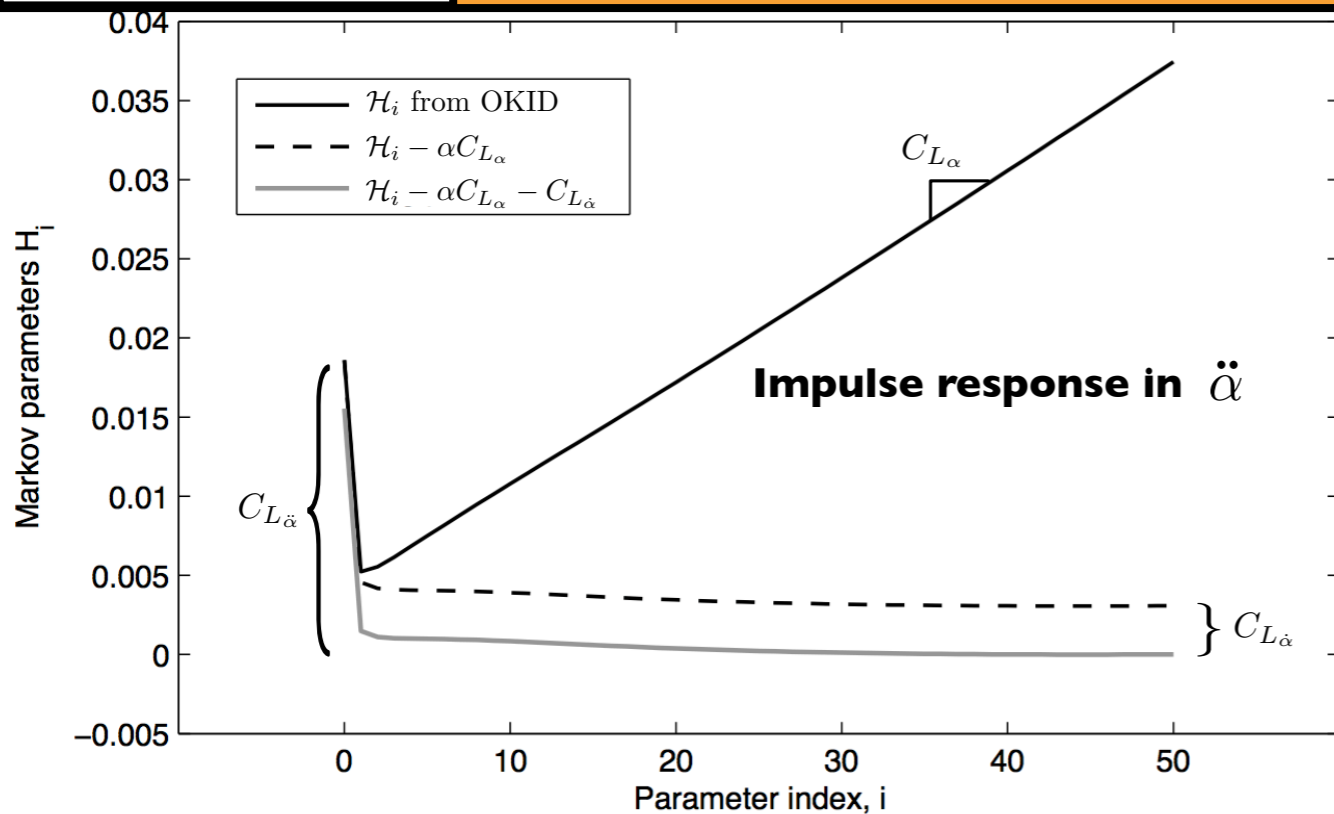


5 degree step-up, step-down maneuver





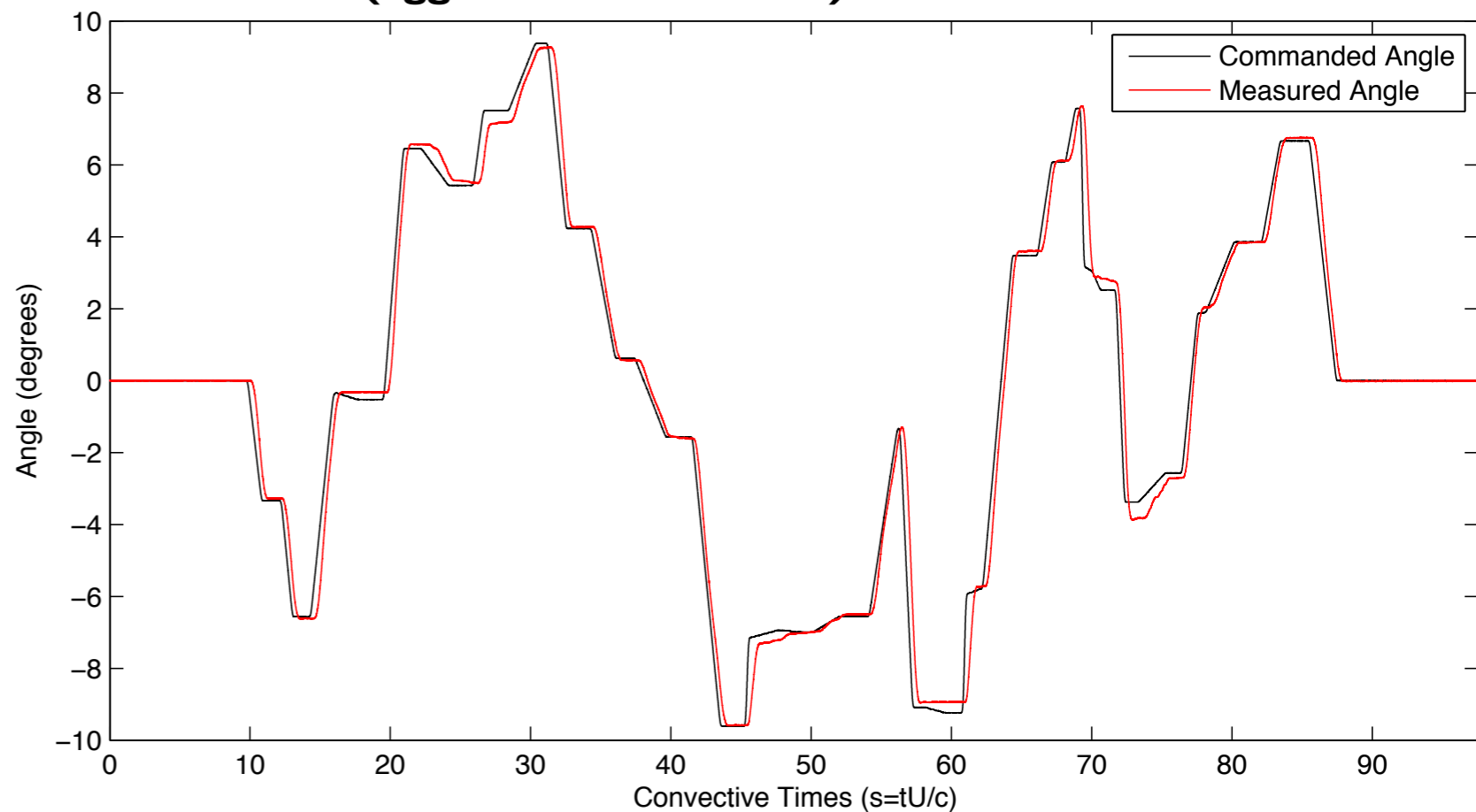
Wing Maneuver



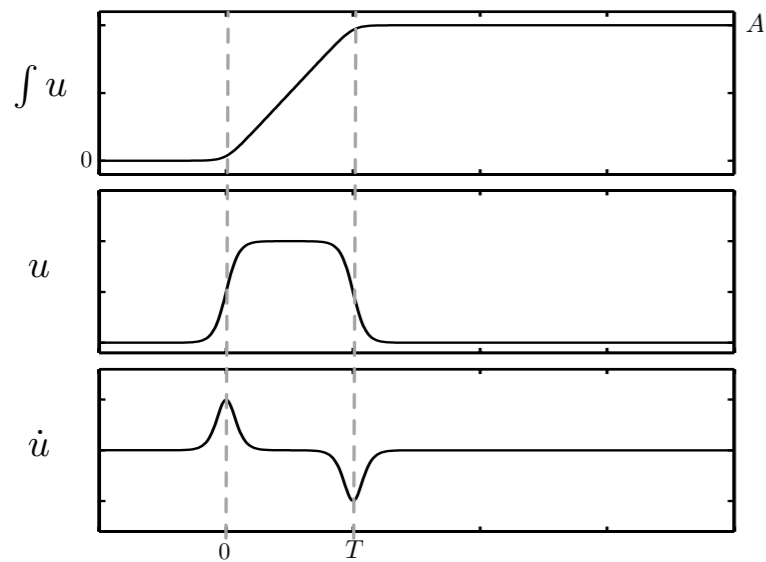
$$\frac{d}{dt} \begin{bmatrix} \mathbf{x} \\ \alpha \\ \dot{\alpha} \end{bmatrix} = \begin{bmatrix} A_r & 0 & 0 \\ 0 & 0 & 1 \\ 0 & 0 & 0 \end{bmatrix} \begin{bmatrix} \mathbf{x} \\ \alpha \\ \dot{\alpha} \end{bmatrix} + \begin{bmatrix} B_r \\ 0 \\ 1 \end{bmatrix} \ddot{\alpha}$$

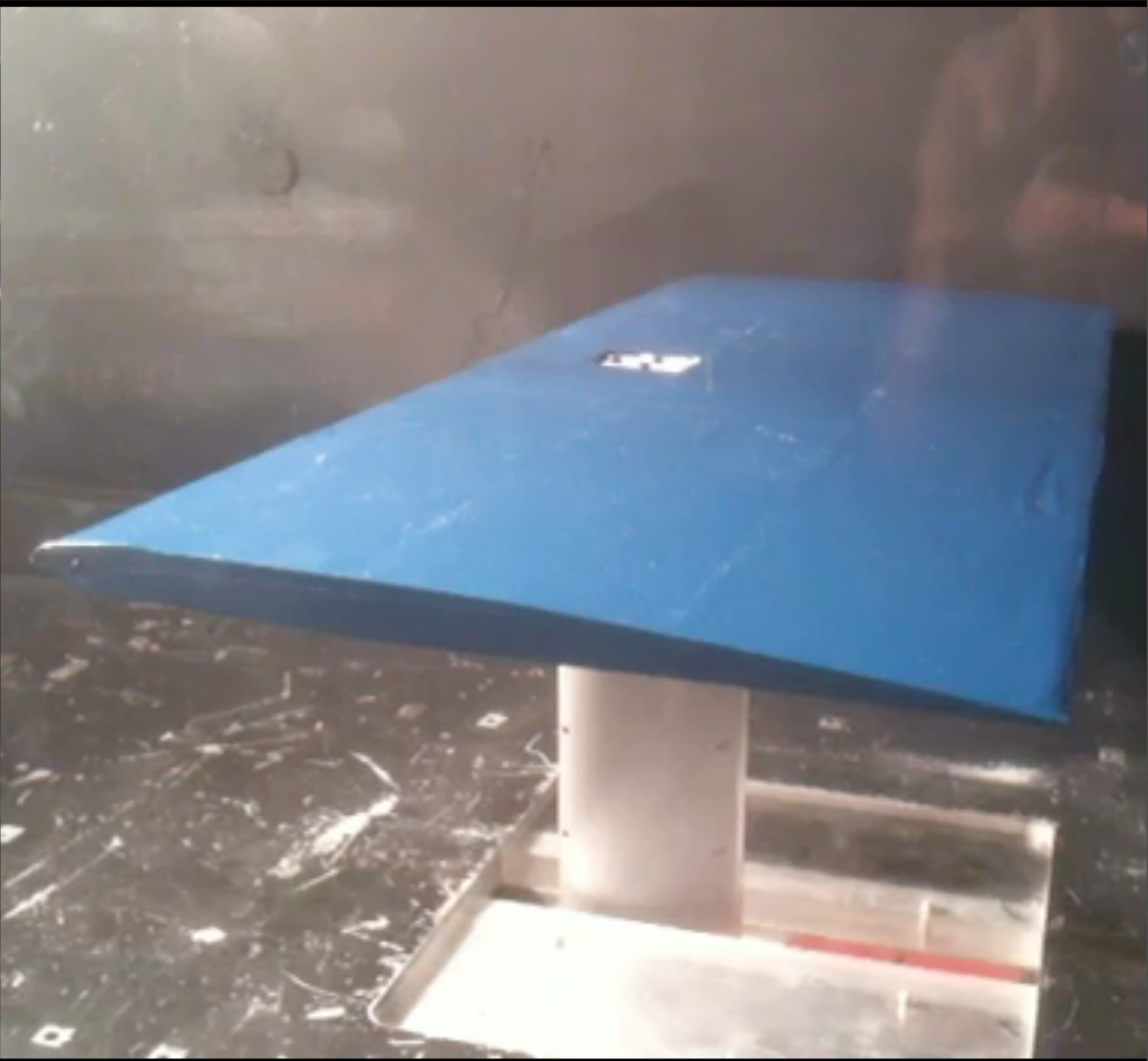
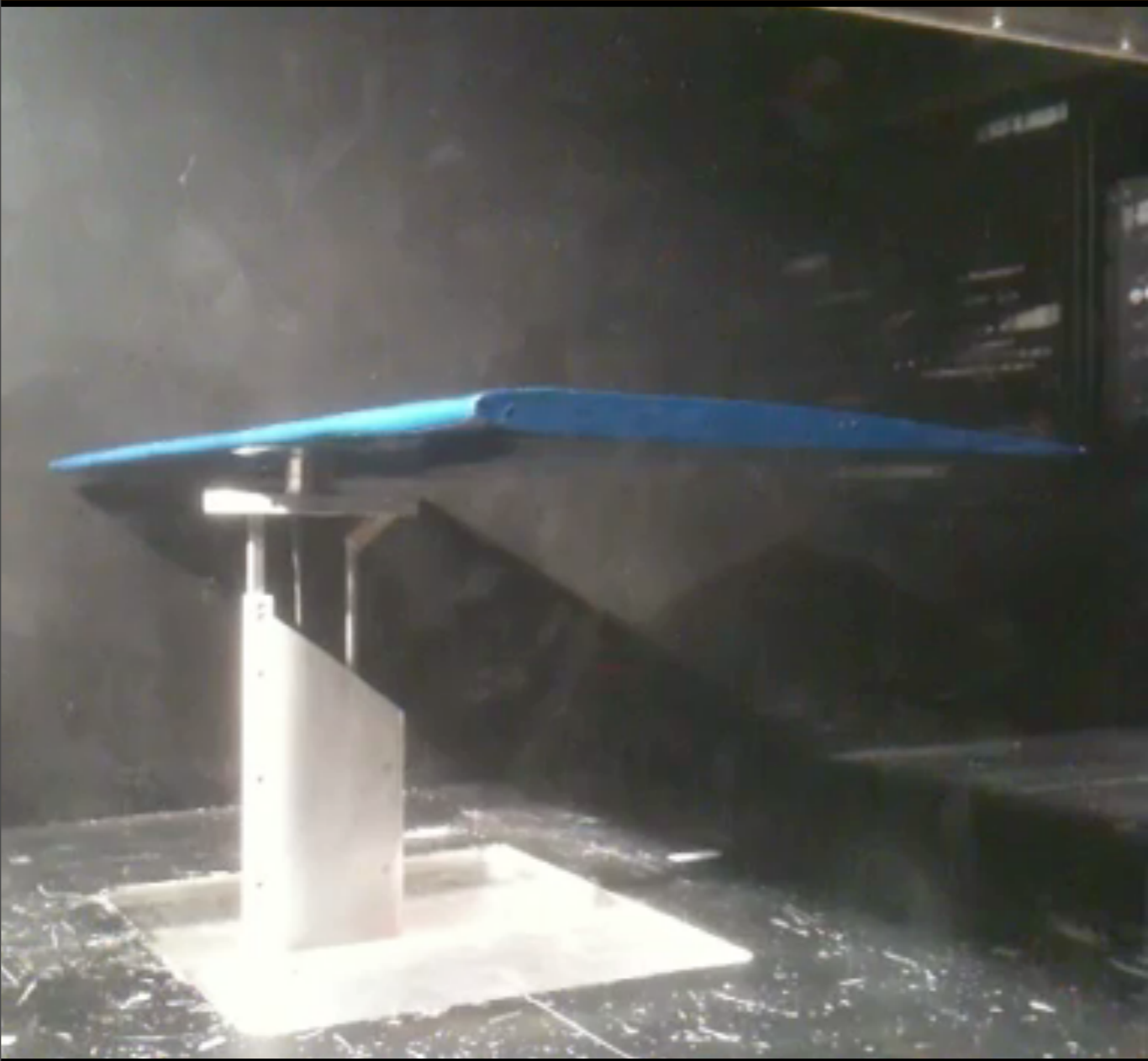
$$C_L = \begin{bmatrix} C_r & C_{L\alpha} & C_{L\dot{\alpha}} \end{bmatrix} \begin{bmatrix} \mathbf{x} \\ \alpha \\ \dot{\alpha} \end{bmatrix} + C_{L\ddot{\alpha}} \ddot{\alpha}$$

Pseudo-random sequence of ramp-hold maneuvers (aggressive maneuver)



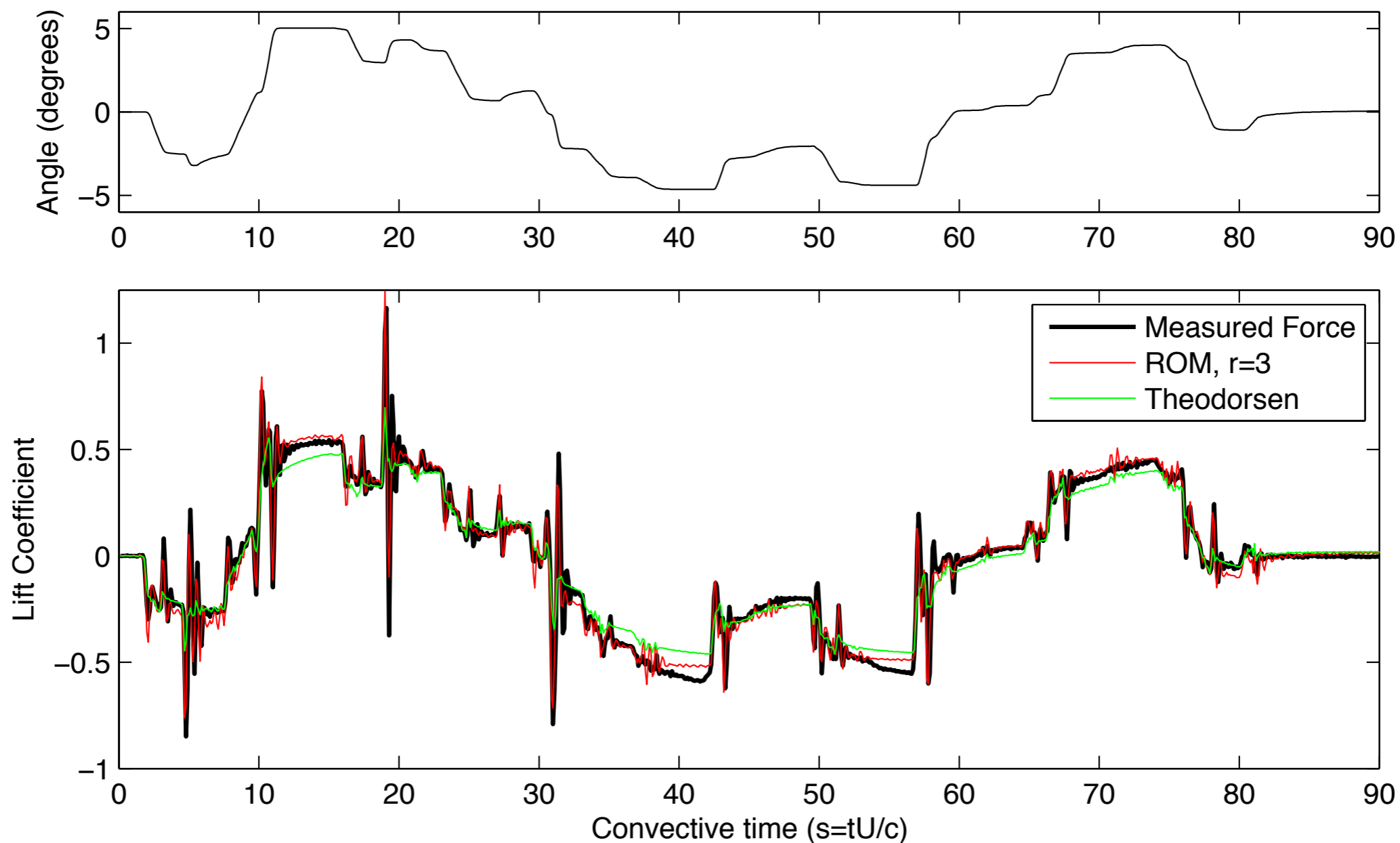
Single ramp-hold maneuver







System ID maneuver



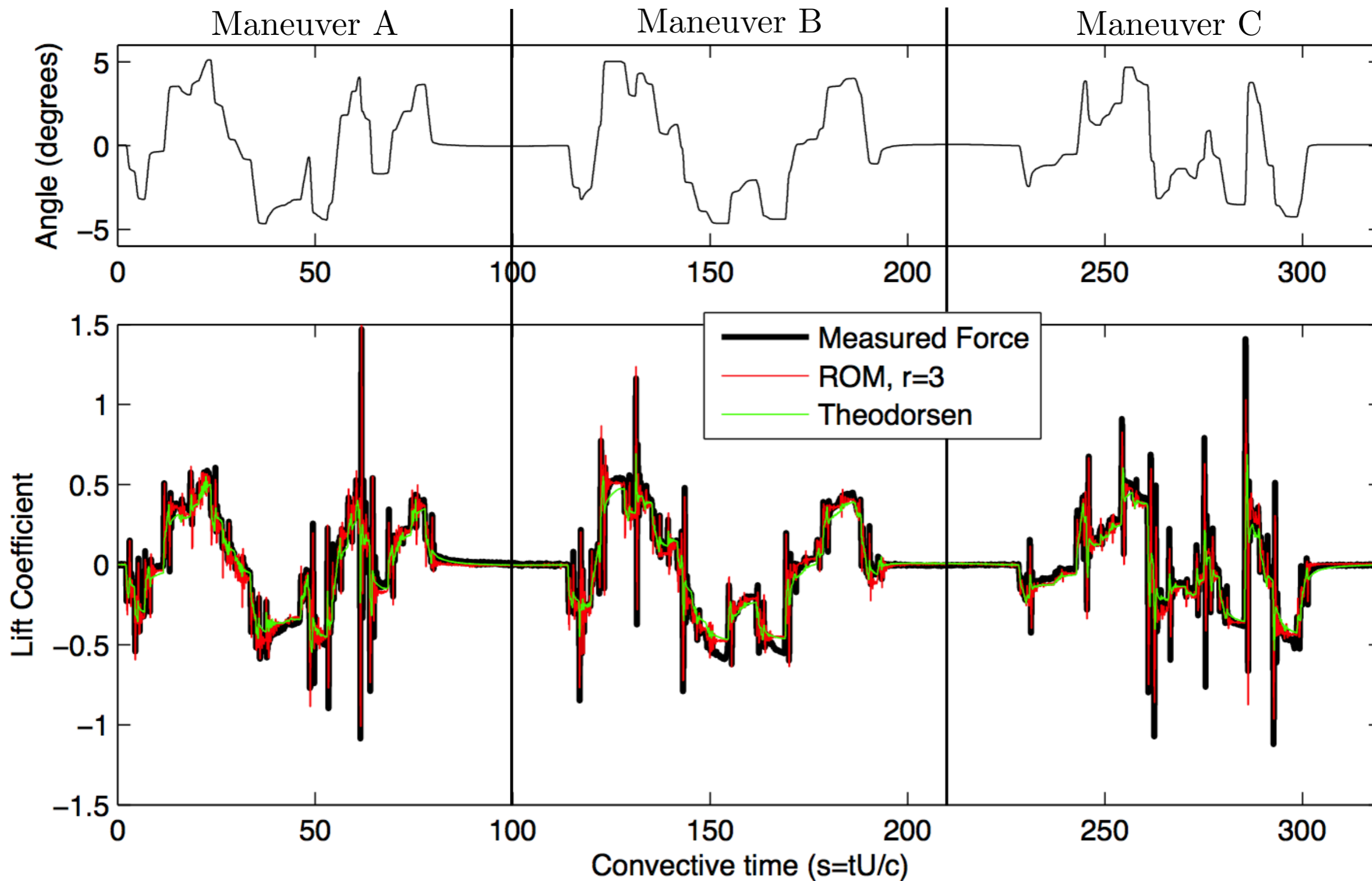
+/- 5 degree maneuver, excites large range of frequencies

Reduced order model outperforms Theodorsen at low and high frequencies

AOA = 0 degrees



Three system ID maneuvers

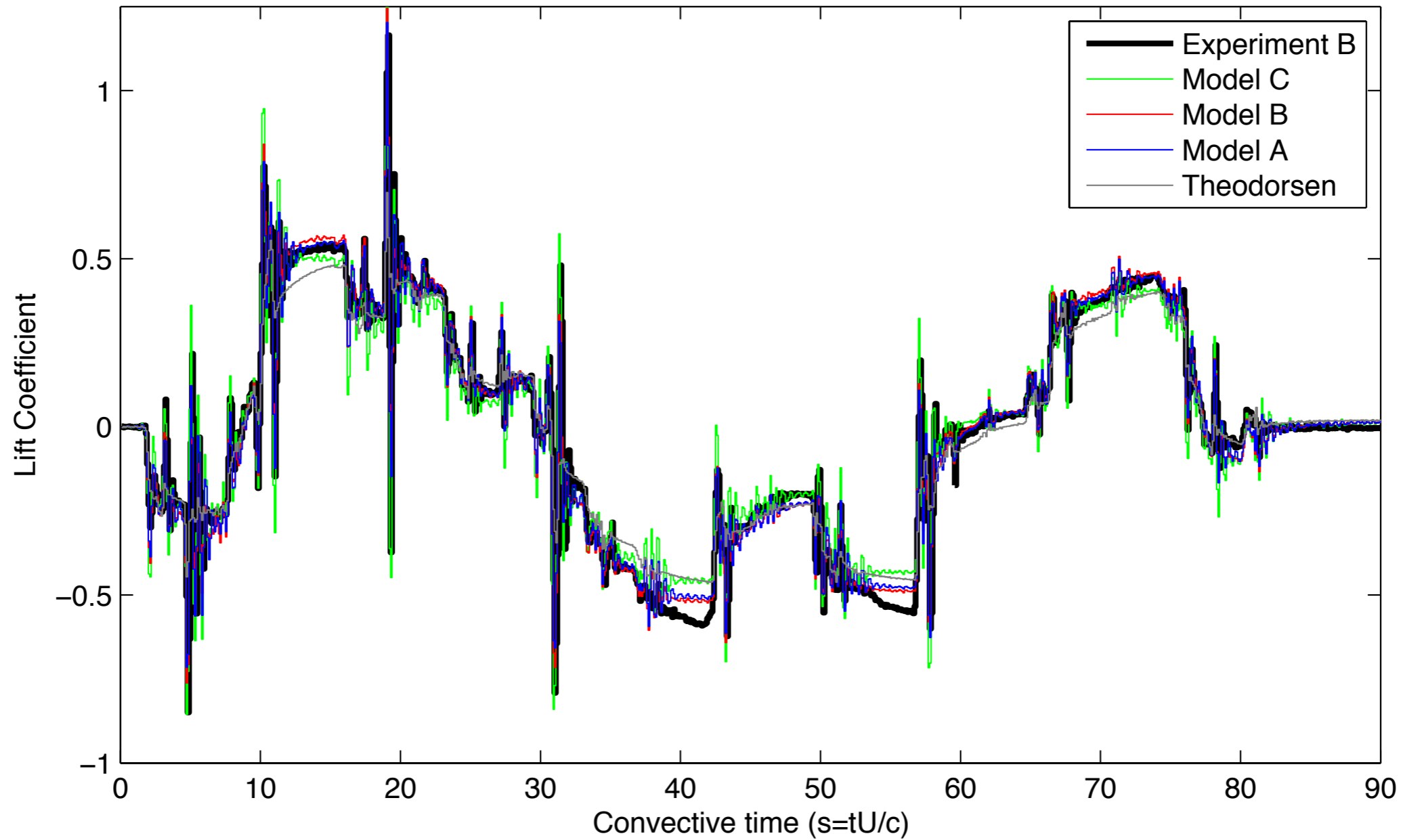


AOA = 0 degrees

We tried three system ID maneuvers: A, B and C.



System ID maneuver



AOA = 0 degrees

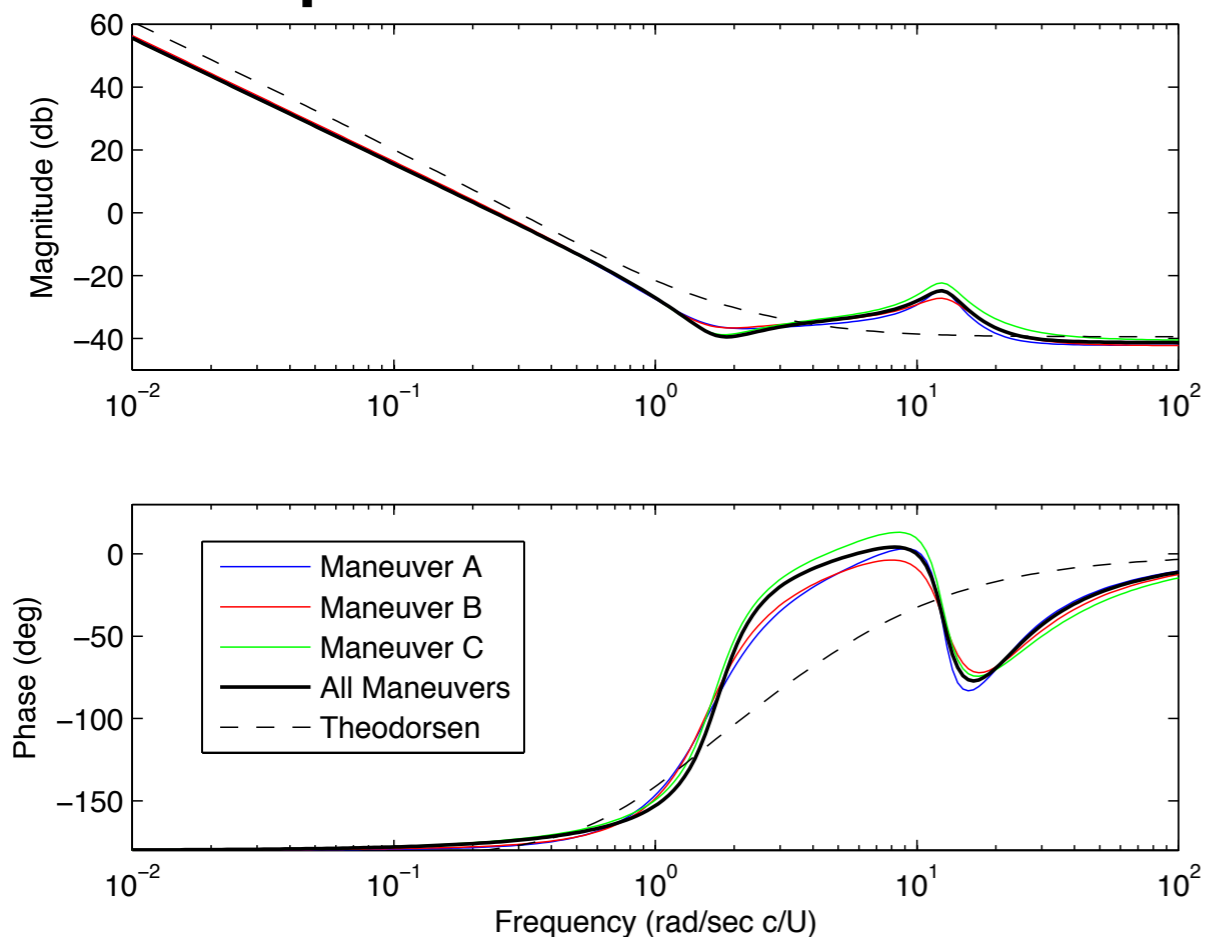
Bootstrap: It is important that models obtained from each ID maneuver accurately reproduce every other maneuver



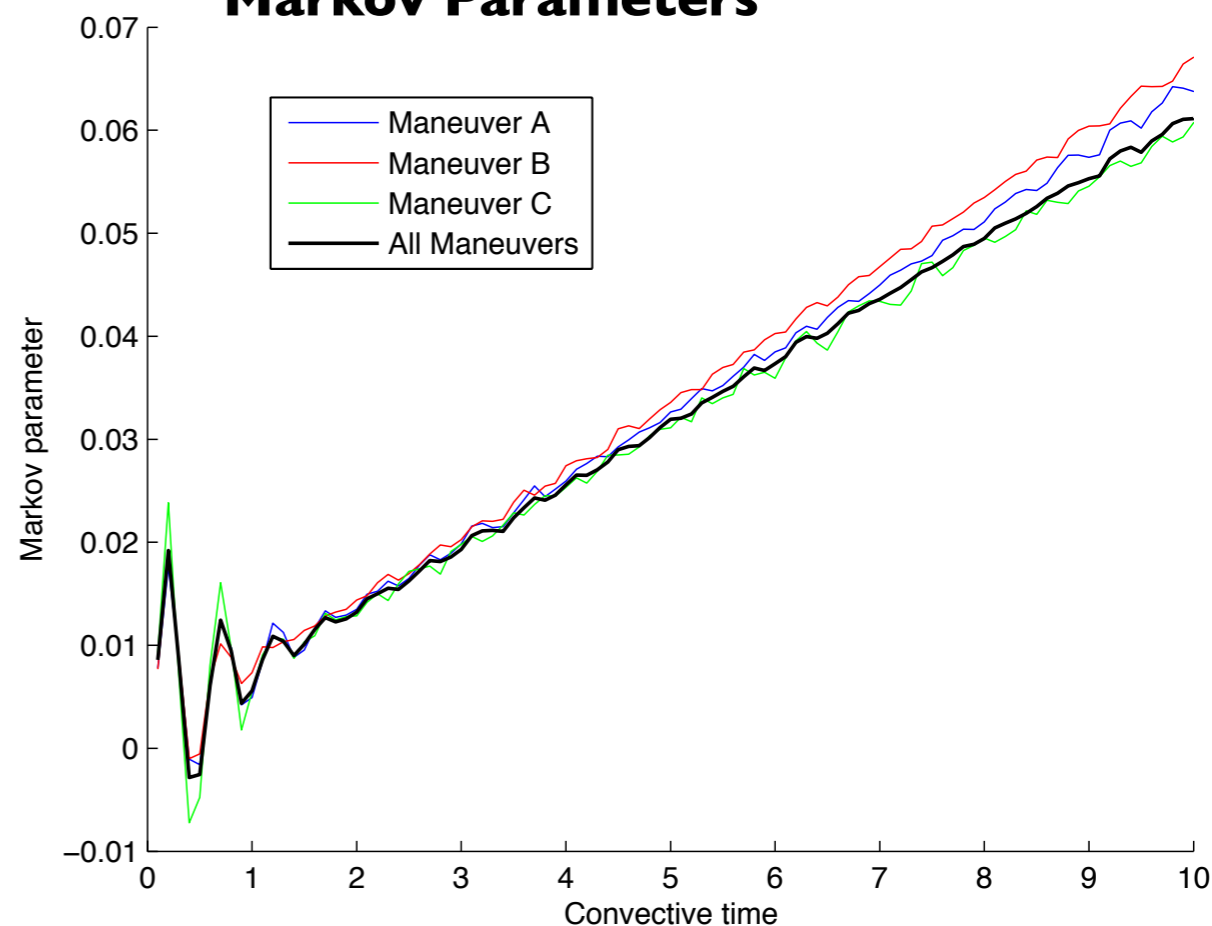
Bode plot and Markov parameters



Bode plot



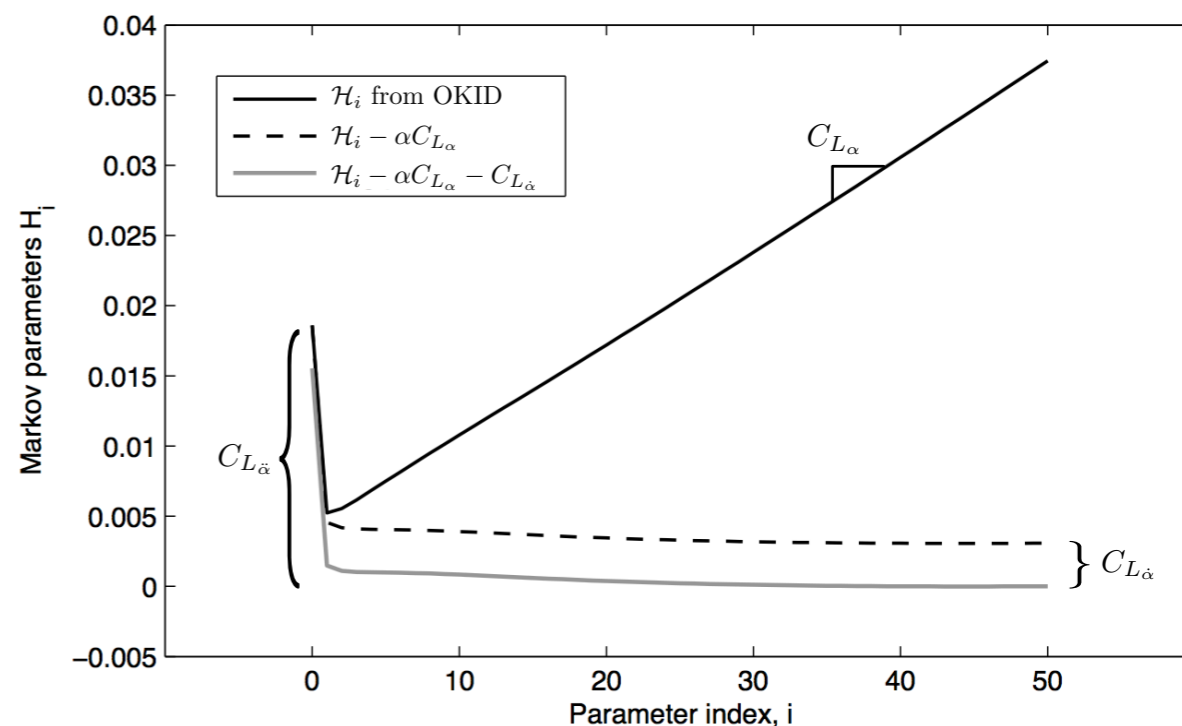
Markov Parameters



Combined maneuver effectively blends each of the three individual maneuvers

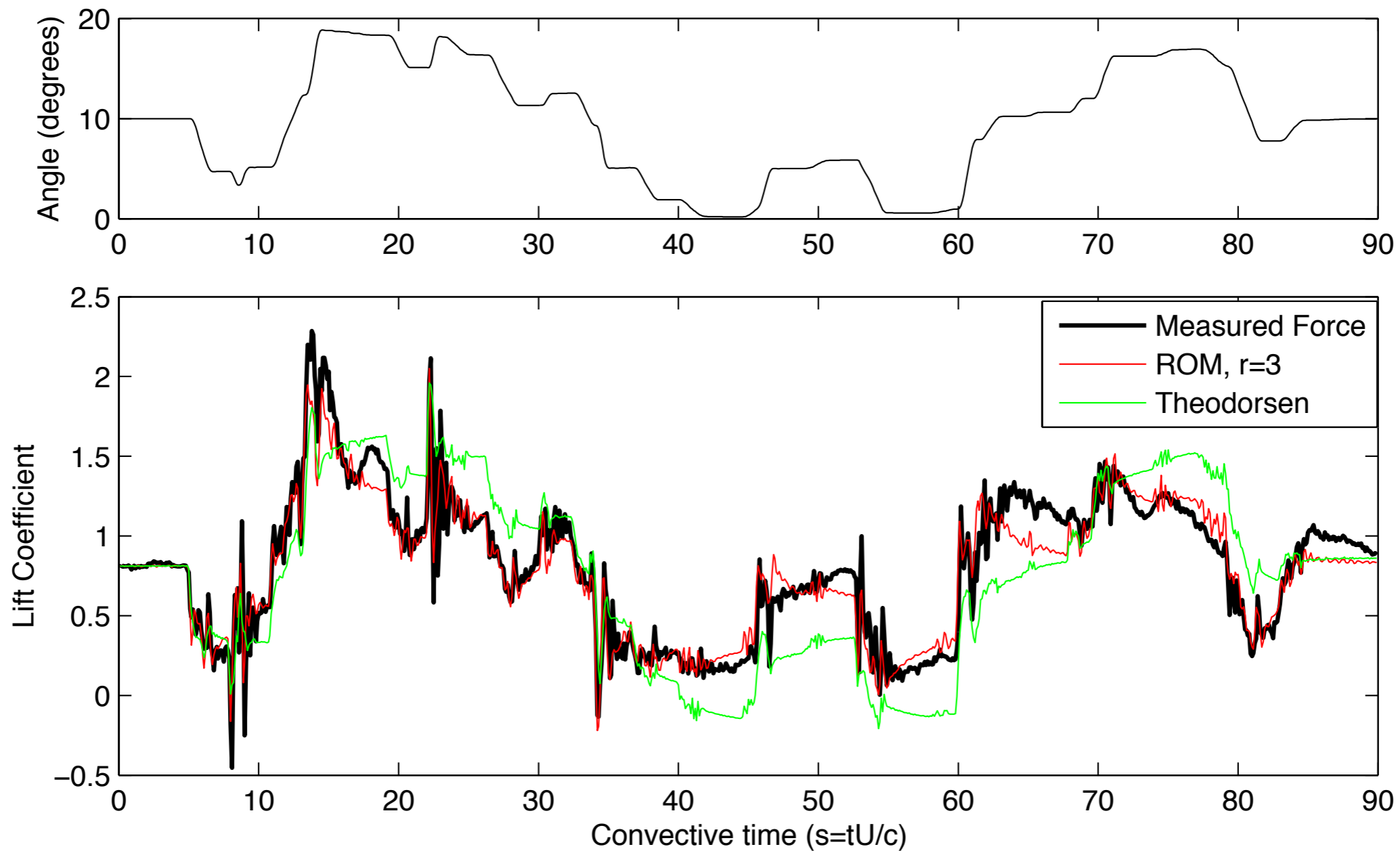
Added-mass is not exclusively in first Markov parameter, but is instead distributed in the first few, contributing to the added-mass “bump”

AOA = 0 degrees





System ID maneuver



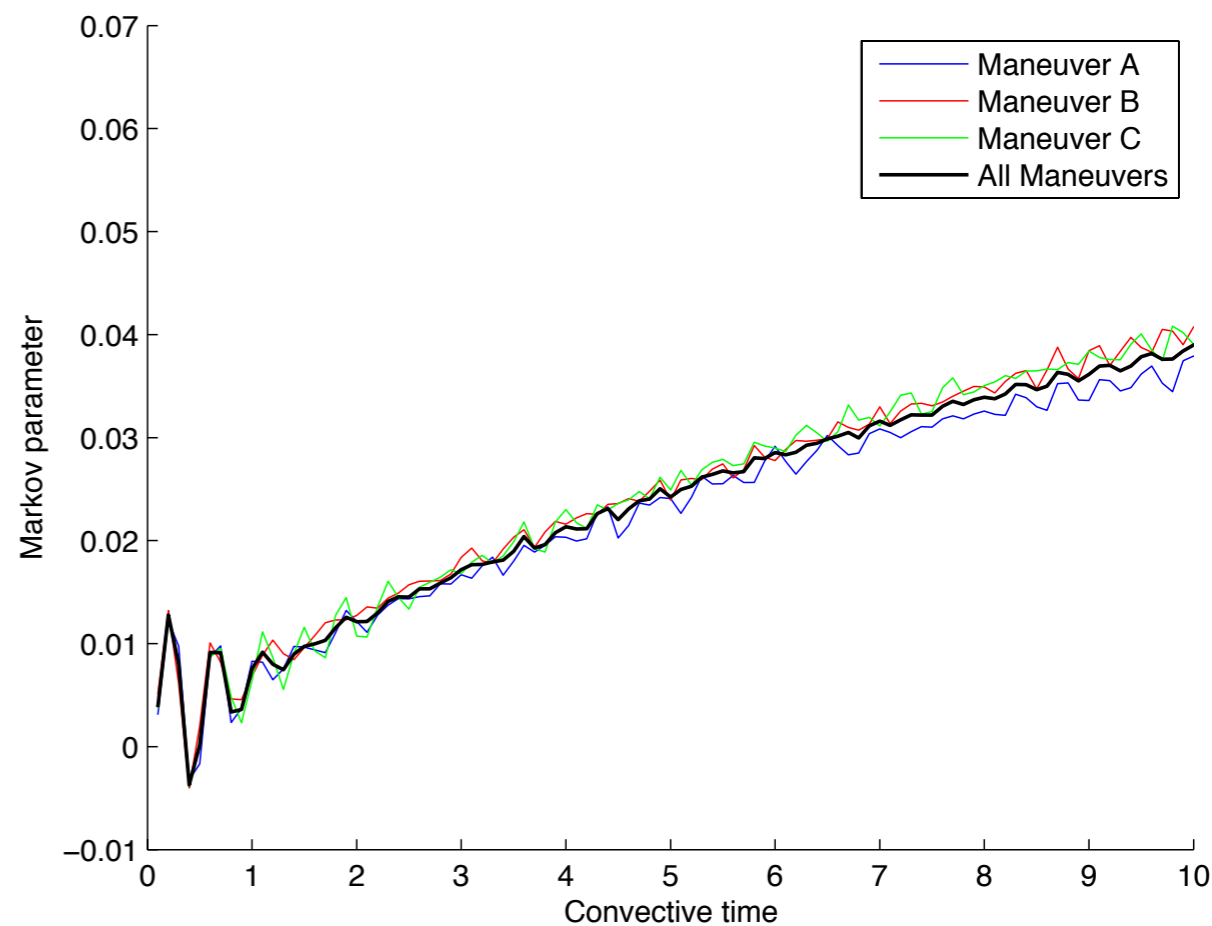
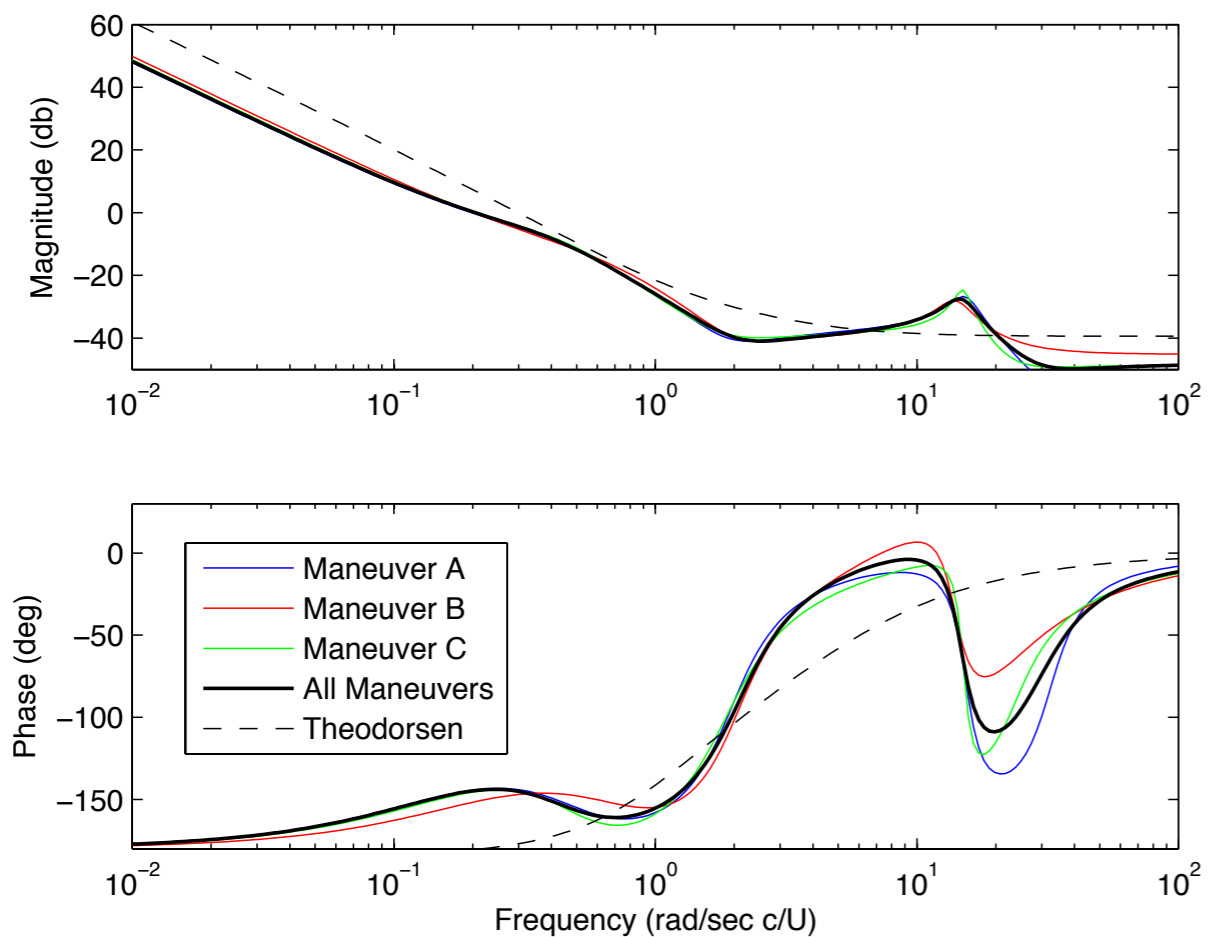
+/- 10 degree maneuver

AOA = 10 degrees

Theodorsen is significantly worse, due to large base angle of attack and flow separation effects.



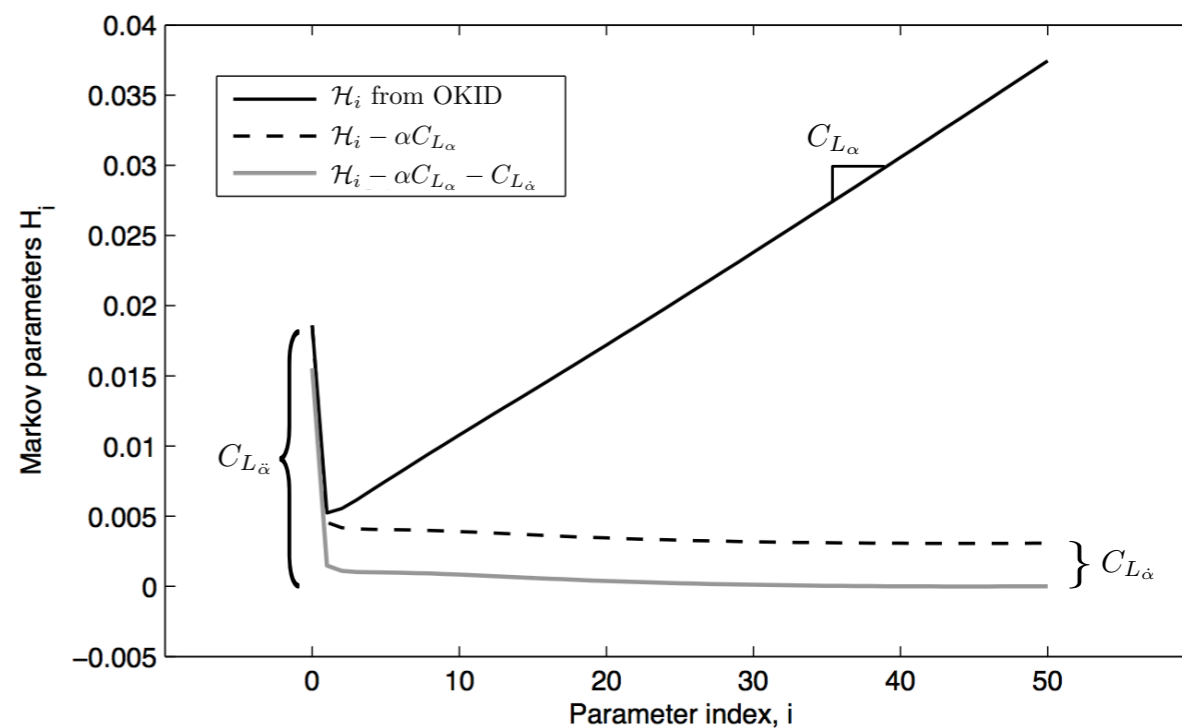
Bode plot and Markov parameters



Flatter Markov parameters indicate smaller lift coefficient slope

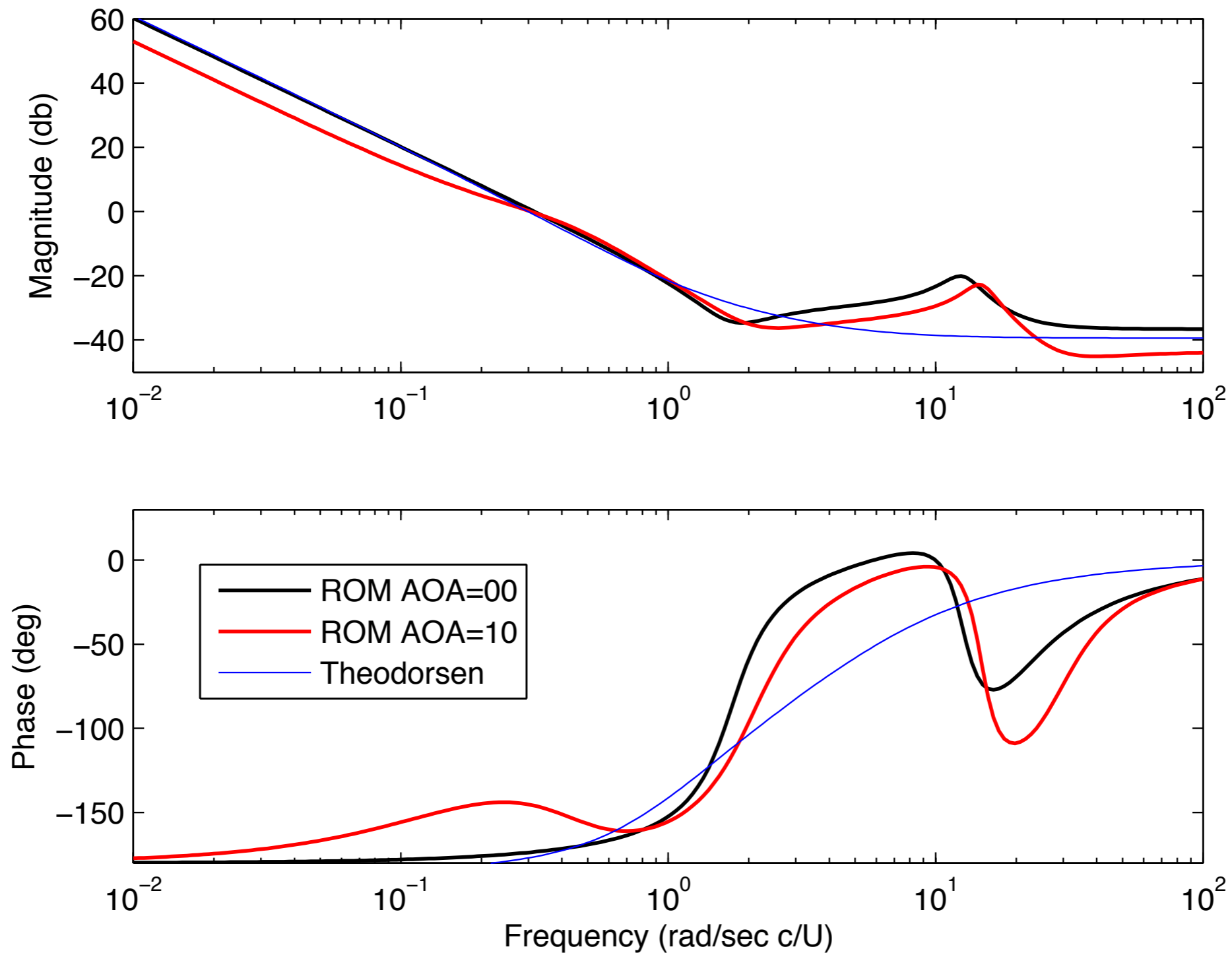
Convergence to asymptote at lower frequency indicate longer transient decay to steady state (more separated flow)

AOA = 10 degrees





AoA=00 vs. AoA=10



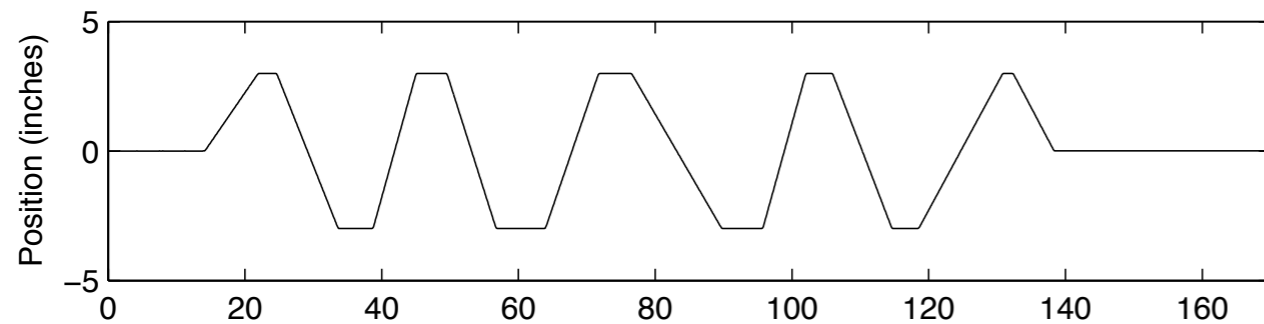
Trend is similar to DNS, where low frequency asymptote converges at lower frequency, for larger angle of attack.



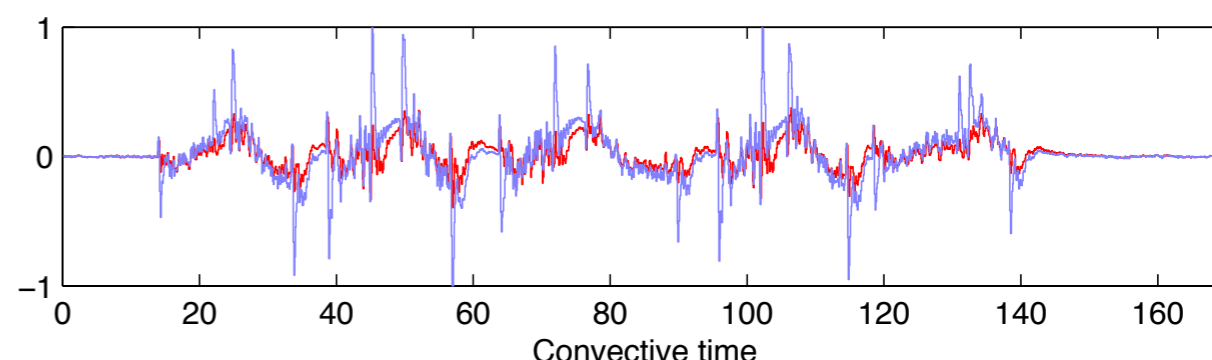
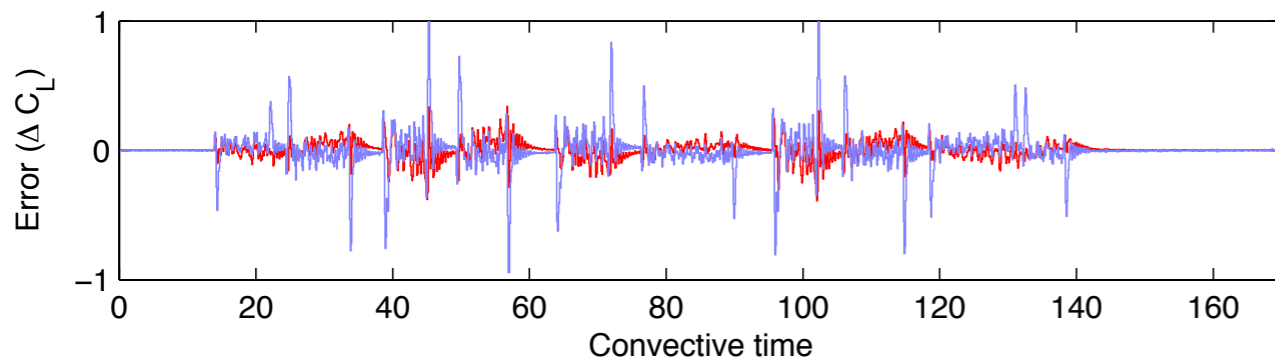
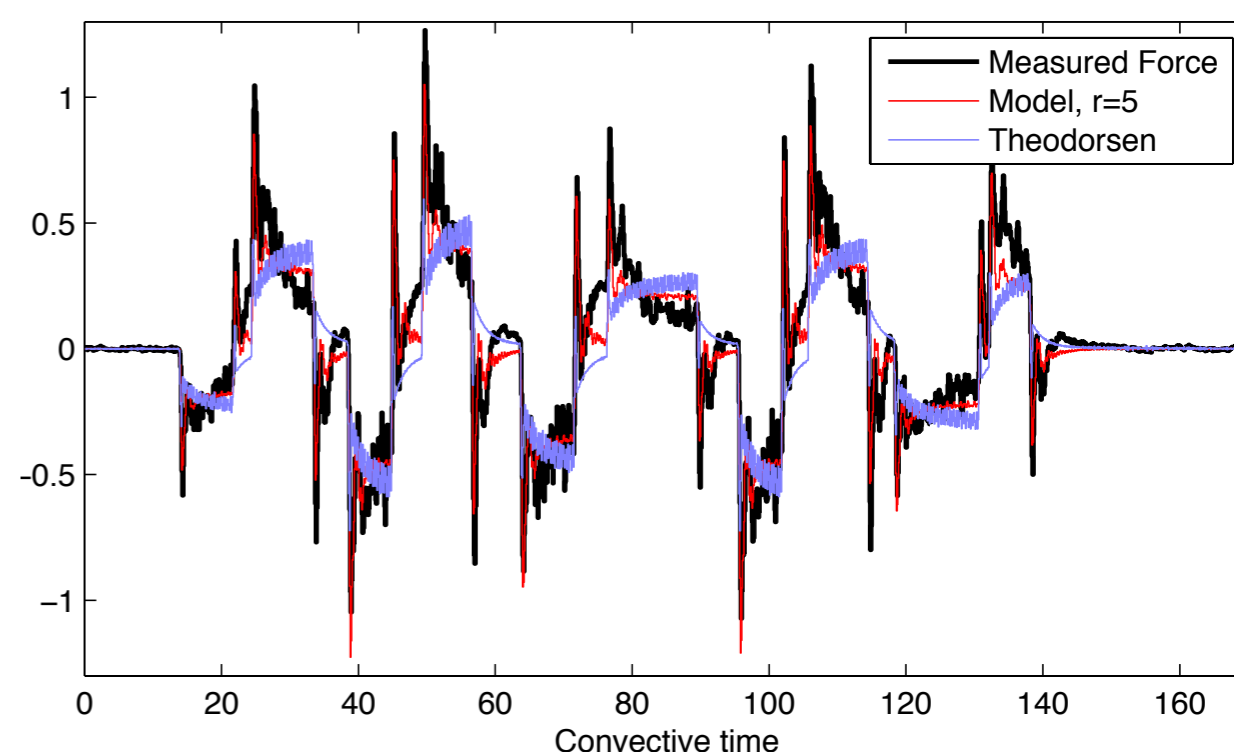
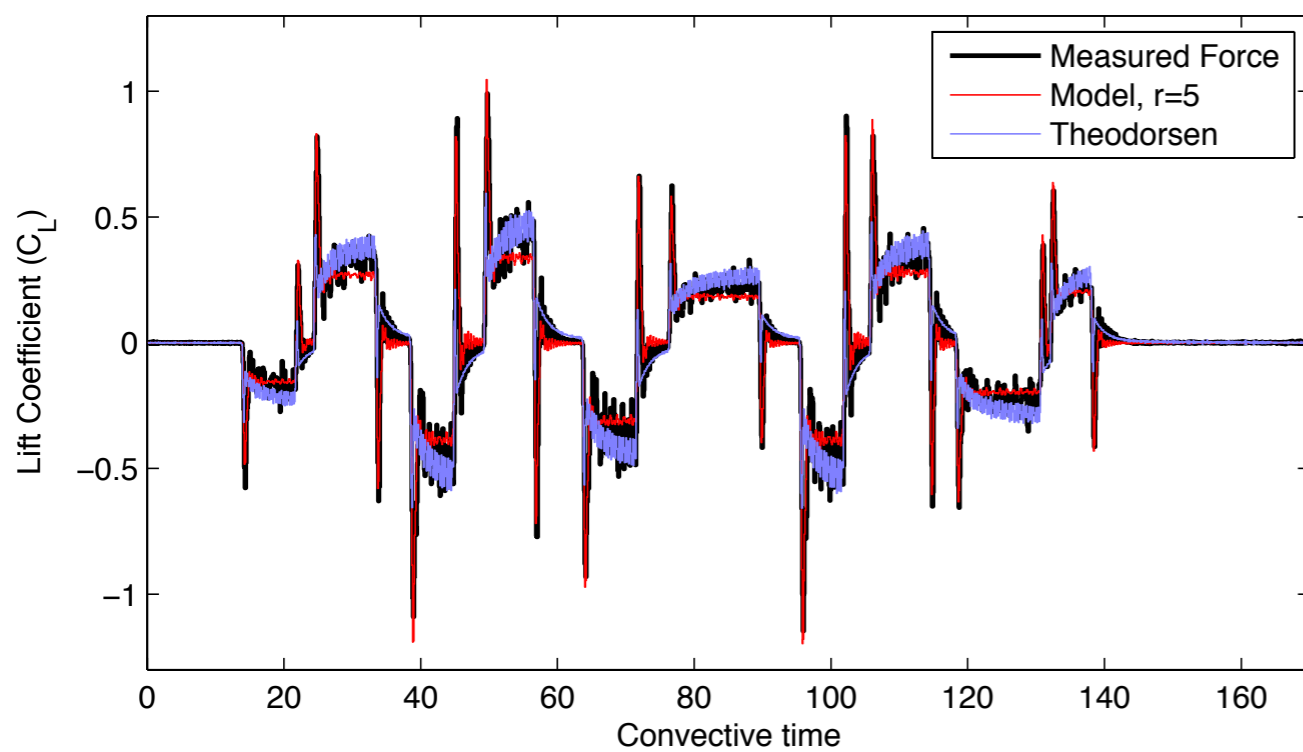
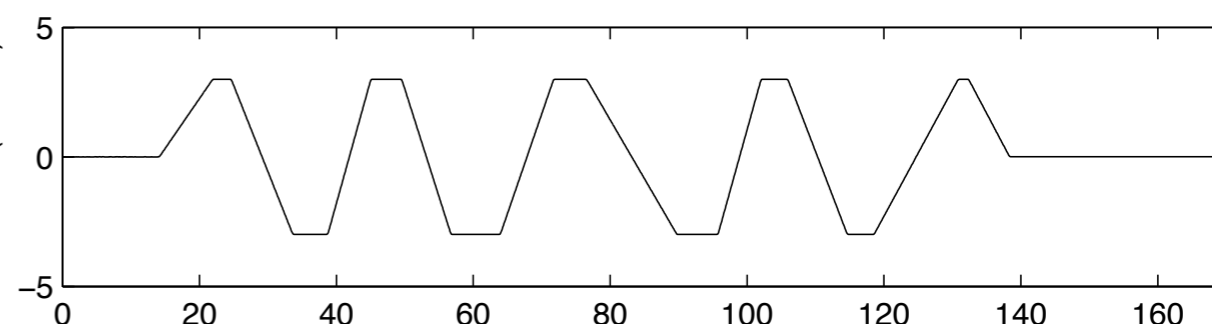
Pure Plunge



AOA = 0 degrees



AOA = 10 degrees



Lift rises to steady state after step-up

Lift relaxes to steady state after step-up



Conclusions & Future Work



1. Improved computational tools

- **Unsteady base flow to solve Navier-Stokes in body fixed frame**
- **Fast computation of Finite-time Lyapunov exponents**
- **About 20X speed-up for both methods**

2. Accurate, efficient reduced order modeling procedure

- **Linear unsteady pitch and plunge models from Navier-Stokes equations**
- **Constructed for specific geometry, Reynolds number**
- **Based on various input maneuvers**
- **Modeling effort is targeted at transient fluid dynamics frequencies**

3. Modeling techniques applied to two test problems

- **Direct numerical simulations of flat plate airfoil, $Re=100$**
- **Wind tunnel experiment with NACA 0006 airfoil, $Re=65,000$**
- **Reduced order model outperforms Theodorsen's model for all cases, especially at large angle of attack**

Future Work:

- **Use pitch/plunge models to develop optimal control laws**
- **Combine into nonlinear model with limit cycle dynamics**
- **Extend models to large parametric study (Re #, Aspect ratio, etc.)**



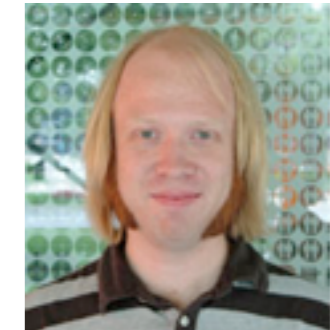
Acknowledgments



Professor Clancy Rowley & Group



Professor Dave Williams & Wes Kerstens



MAE Department Faculty, Students and Staff!

Funding Sources

Air force office of scientific research (AFOSR)

FAA Joint University Program

Gordon Wu Fellowship



Bing and James



QUESTIONS?





Robust Lift Control



Goal: Track reference Lift, while rejecting disturbance and attenuating sensor noise

$$\dot{x} = Ax + Bu + W^{1/2}d \quad d - \text{disturbance}$$

$$y = Cx + Du + V^{1/2}n \quad n - \text{noise}$$

(A,B,C,D) from Theodorsen's pitch model

\mathcal{H}_∞ Loop Shaping

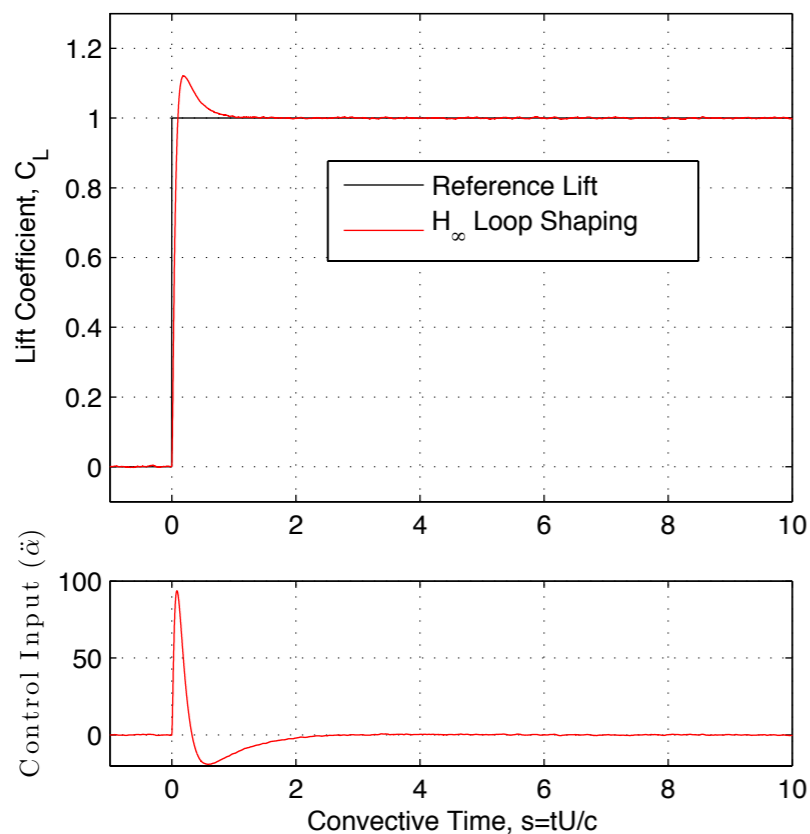
Desired loop shape:

$$G_d = \frac{1500(s-5)}{s^2(s+75)}$$

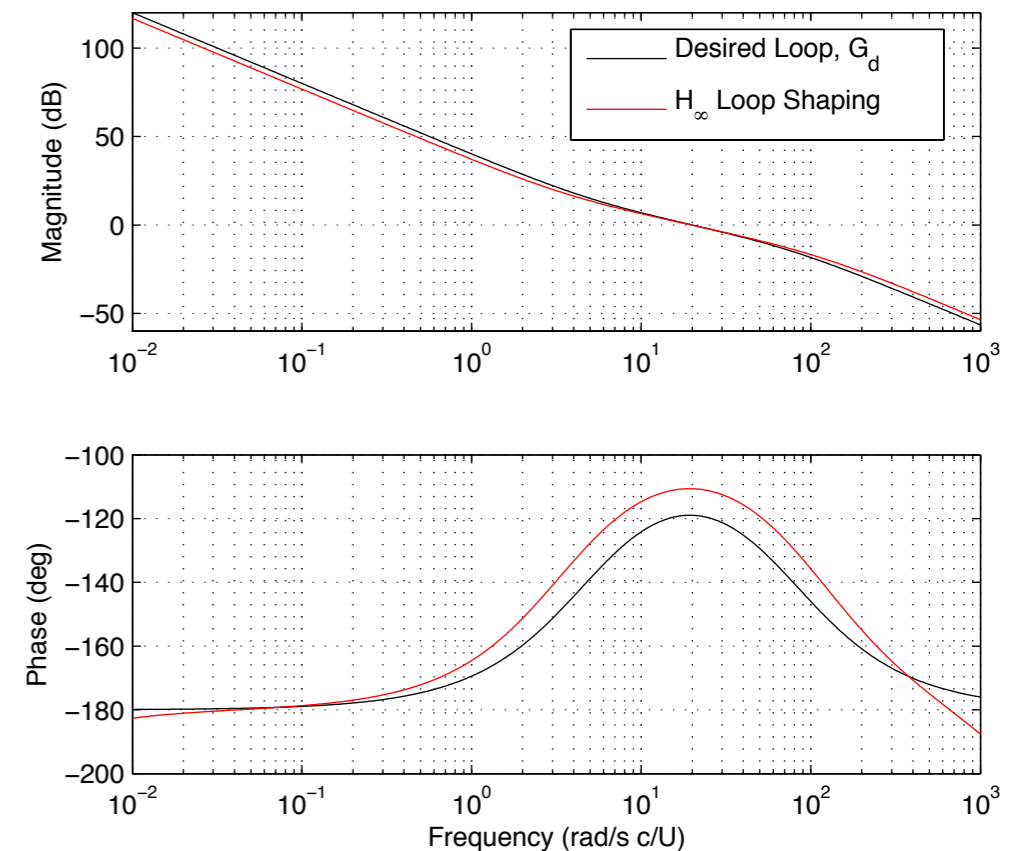
Actuator roll-off:

$$G_a = \frac{300}{(s+500)}$$

Closed-loop step response



Open-loop Bode plot



Brunton and Rowley, in preparation.



Robust Lift Control



Goal: Track reference Lift, while rejecting disturbance and attenuating sensor noise

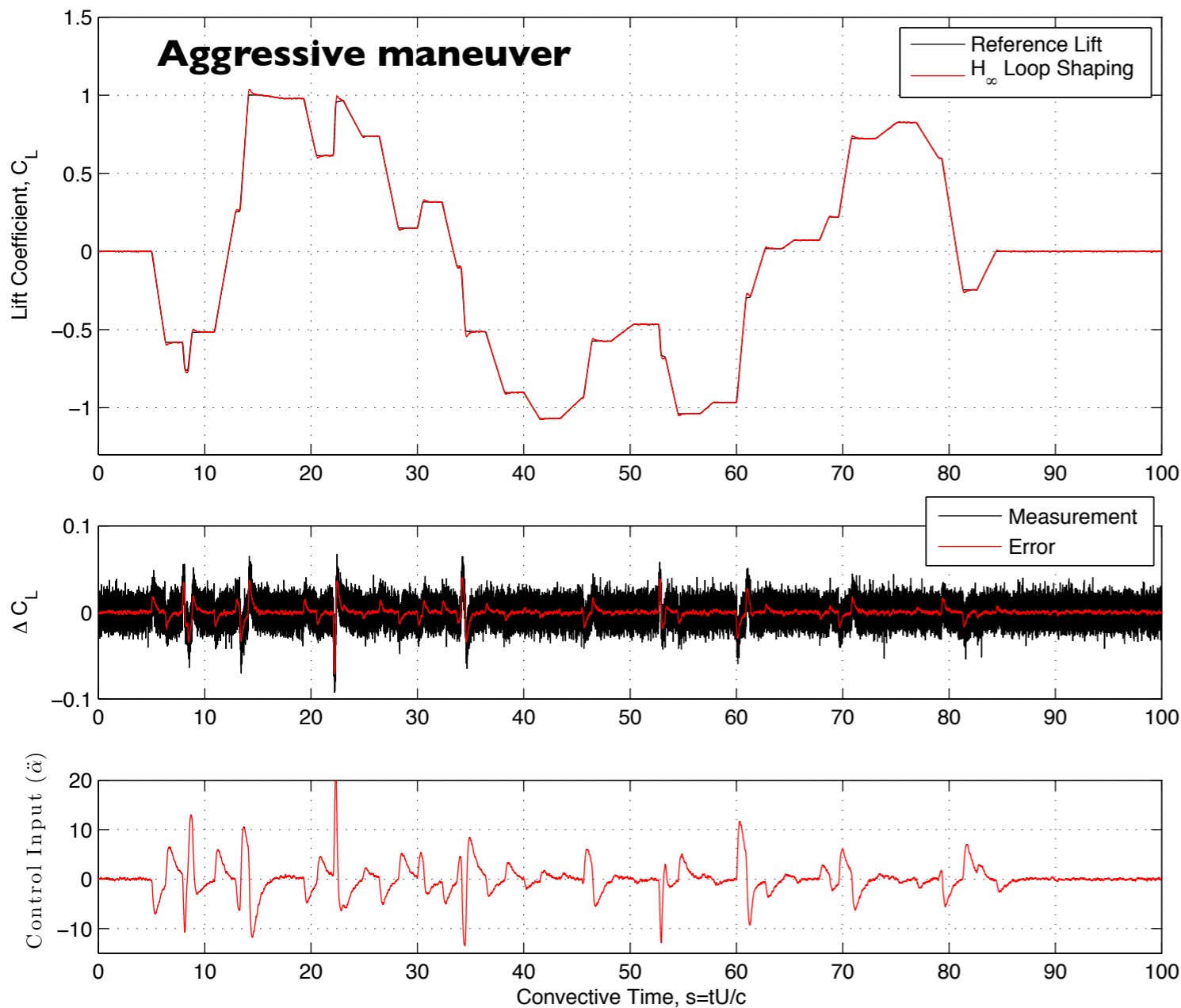
\mathcal{H}_∞ Loop Shaping

Desired loop shape:

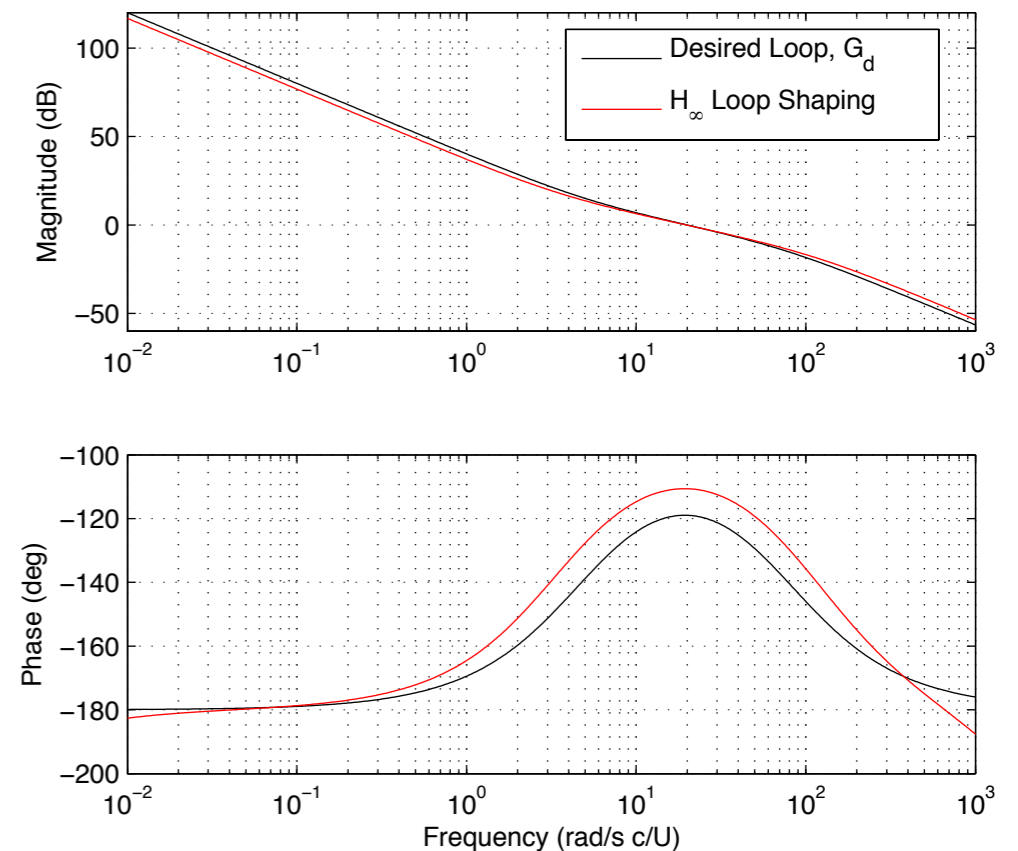
$$G_d = \frac{1500(s-5)}{s^2(s+75)}$$

Actuator roll-off:

$$G_a = \frac{300}{(s+500)}$$



Open-loop Bode plot



Brunton and Rowley, in preparation.



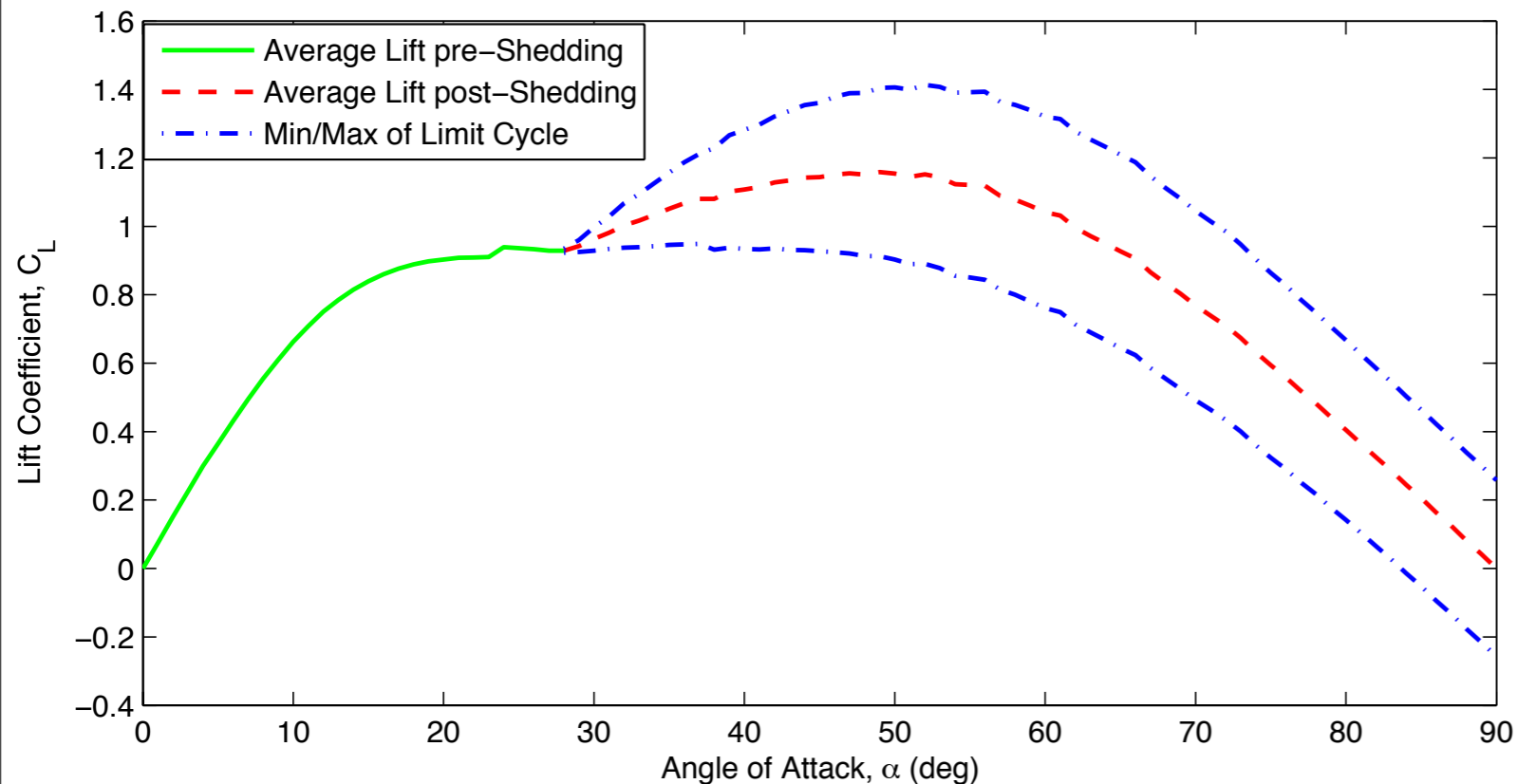
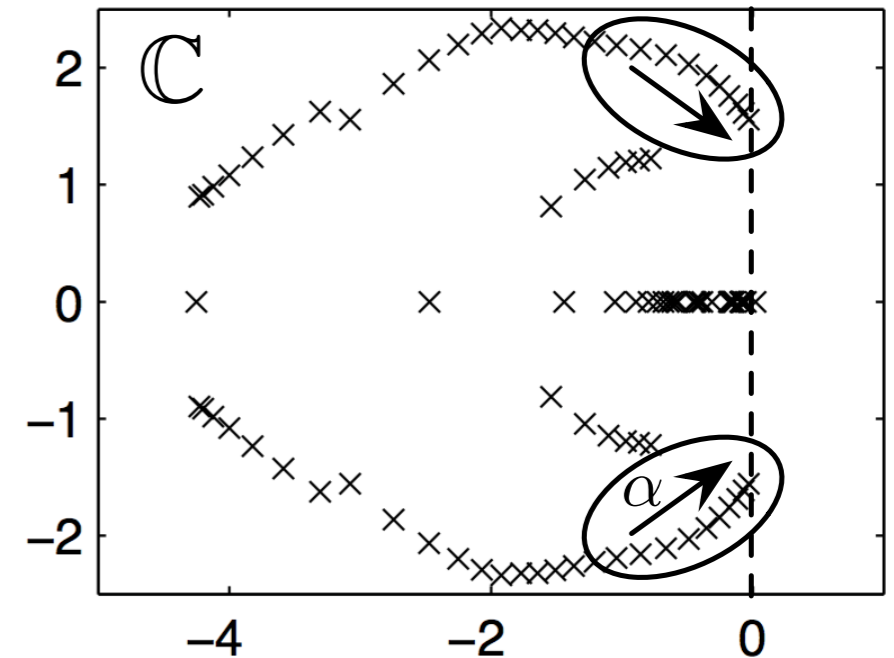
Nonlinear Unsteady Models



What we know

1. Hopf bifurcation at $\alpha = 28^\circ$
2. Linear models capture conjugate pair
3. Linear models based on overarching nonlinear model (Navier-Stokes)

How to construct nonlinear reduced order model?





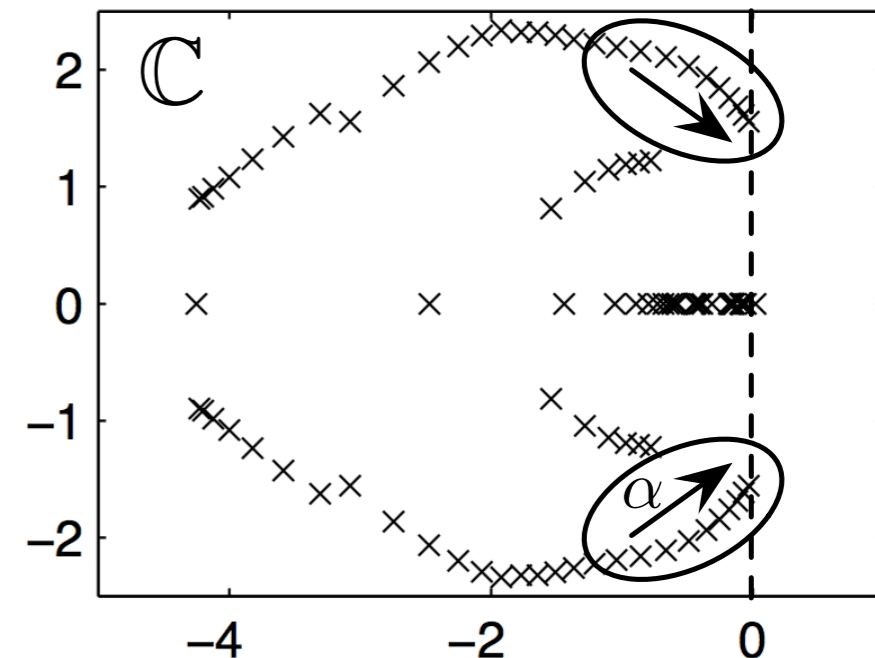
Nonlinear Unsteady Models



What we know

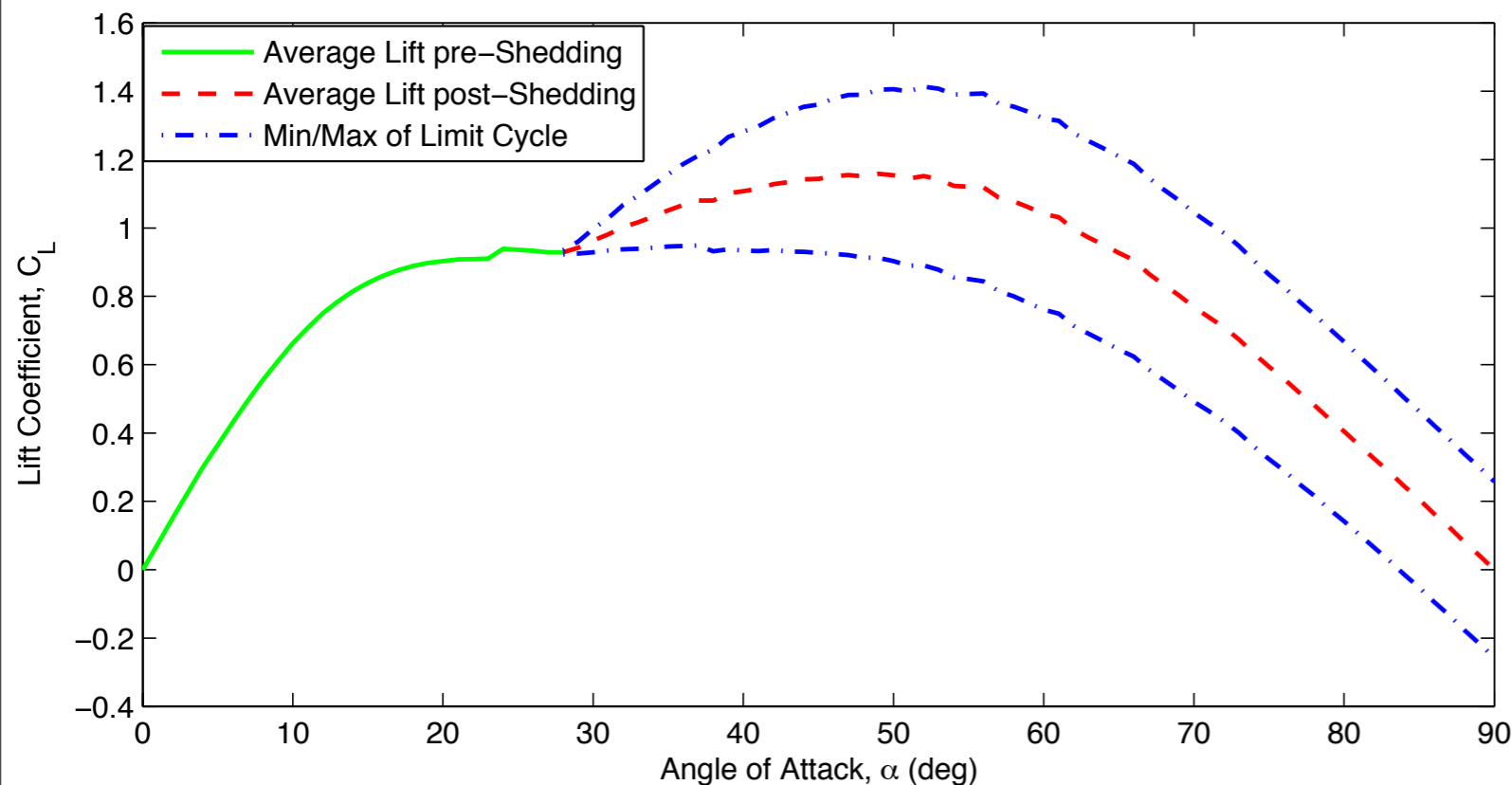
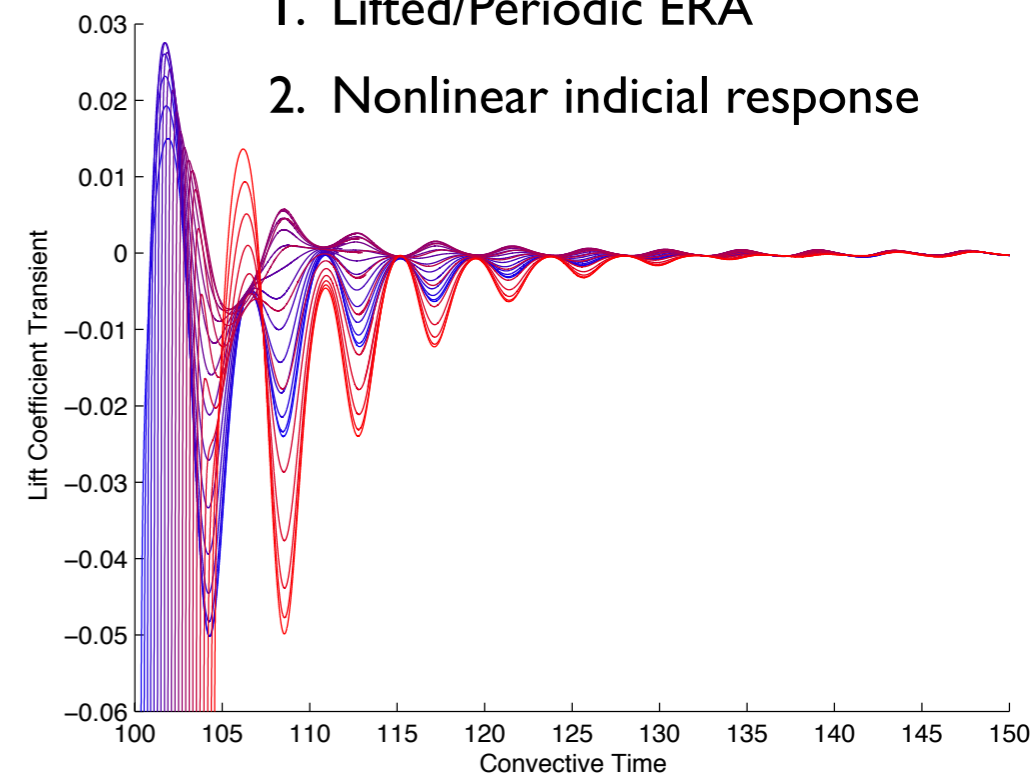
1. Hopf bifurcation at $\alpha = 28^\circ$
2. Linear models capture conjugate pair
3. Linear models based on overarching nonlinear model (Navier-Stokes)

How to construct nonlinear reduced order model?



Transient dynamics from impulse at each phase of limit cycle

1. Lifted/Periodic ERA
2. Nonlinear indicial response





Conclusions



Accurate, efficient reduced order models

- **Models are linearization of full nonlinear model**
- **Constructed for specific geometry, Reynolds number**
- **Based on various input maneuvers**

Modeling techniques applied to two test problems

- **Simulated flat plate airfoil, $Re=100$**
- **Wind tunnel experiment, $Re=65,000$**
- **Pitch and plunge dynamics investigated**
- **Reduced order model outperforms Theodorsen's model for all cases, especially at large angle of attack**

Future Work:

- **Use pitch/plunge models for optimal control (maneuver, lift stabilization)**
- **Combine into nonlinear model with limit cycle dynamics**

Wagner, 1925.

Theodorsen, 1935.

Leishman, 2006.

OL, Altman, Eldredge, Garmann, and Lian, 2010

Brunton and Rowley, AIAA ASM 2009-2011

Juang and Pappa, 1985.

Ma, Ahuja, Rowley, 2010.

Juang, Phan, Horta, Longman, 1991.



Empirical, State-Space Theodorsen



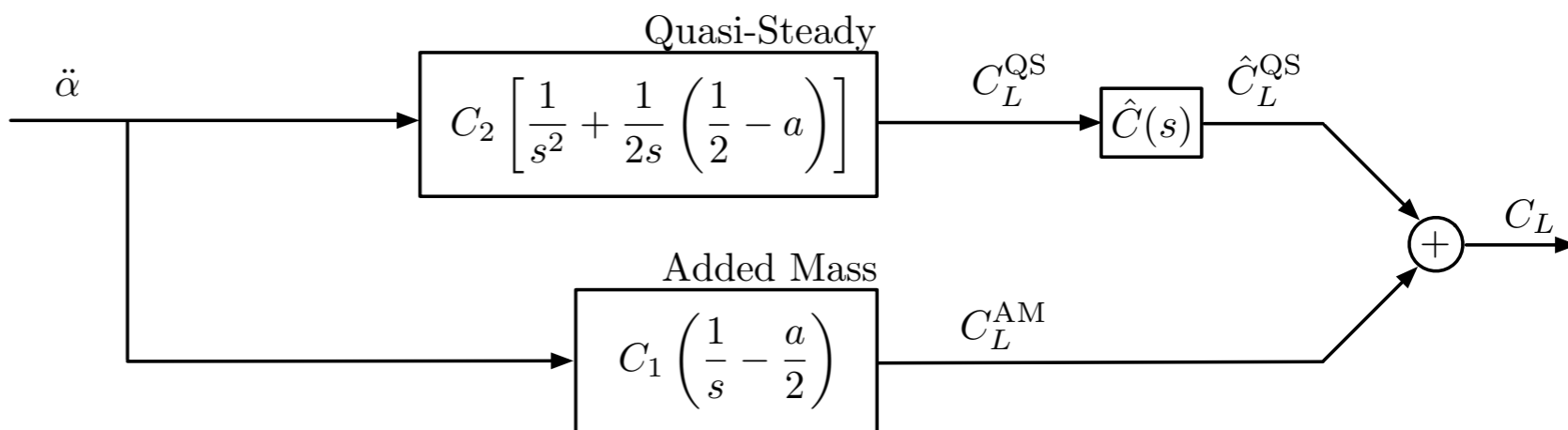
$$C_L = \underbrace{C_1 \left[\frac{\pi}{2} \left(\ddot{h} + \dot{\alpha} - \frac{a}{2} \ddot{\alpha} \right) \right]}_{\text{Added-Mass}} + \underbrace{C_2 \left[\alpha + \dot{h} + \frac{1}{2} \dot{\alpha} \left(\frac{1}{2} - a \right) \right]}_{\text{Circulatory}} \hat{C}(s)$$

Transfer Function

$$\frac{\mathcal{L}[C_L]}{\mathcal{L}[\ddot{\alpha}]} = C_1 \left(\frac{1}{s} - \frac{a}{2} \right) + C_2 \left[\frac{1}{s^2} + \frac{1}{2s} \left(\frac{1}{2} - a \right) \right] C(s)$$

**Approximate C(s),
Breuker et al., 2008**

$$C(s) \approx \frac{.1294s^2 + .1376s + .01576}{.25s^2 + .1707s + .01582}$$



State-space model

$$\frac{d}{dt} \begin{bmatrix} x_1 \\ x_2 \\ \alpha \\ \dot{\alpha} \end{bmatrix} = \begin{bmatrix} -.6828 & -.0633 & C_2 & C_2(1-2a)/4 \\ 1 & 0 & 0 & 0 \\ 0 & 0 & 0 & 1 \\ 0 & 0 & 0 & 0 \end{bmatrix} \begin{bmatrix} x_1 \\ x_2 \\ \alpha \\ \dot{\alpha} \end{bmatrix} + \begin{bmatrix} 0 \\ 0 \\ 0 \\ 1 \end{bmatrix} \ddot{\alpha}$$

$$C_L = [.197 \quad .0303 \quad .5176C_2 \quad C_1 + .5176C_2(1-2a)/4] \begin{bmatrix} x_1 \\ x_2 \\ \alpha \\ \dot{\alpha} \end{bmatrix} - \frac{aC_1}{2} \ddot{\alpha}$$